Derivative Expansion Approximation of Vacuum Polarization Effects

by

Iain William Stewart

A Thesis
Submitted to the Faculty of Graduate Studies
in Partial Fulfillment of the Requirements
for the Degree of

MASTER OF SCIENCE

Department of Physics
University of Manitoba
Winnipeg, Manitoba

TABLE OF CONTENTS

LIST OF FIGURES

LIST OF TABLES

ACKNOWLEDGMENTS

A special thank you to all those who have contributed to this thesis, both directly and indirectly. I would like to express my deepest gratitude to my advisor, Peter Blunden, for his invaluable insight, enthusiasm, and guidance. I would also like to thank him for his tireless effort in helping me to bring the final product together. Thank you also to my thesis committee members, Larry Wilets, and Tom Osborn, for their time and interest in reading the manuscript.

A special thanks to my mother, father, and sister for their love, sacrifice and support throughout my years at the University of Manitoba. Finally, I would like to dedicate this thesis to my wife Susan. Thank you for being my closest friend, sharing in my excitement and my troubles throughout the completion of this thesis.

I would also like to acknowledge the financial support that I received for study through a postgraduate scholarship from the Natural Sciences and Engineering Research Council of Canada.

ABSTRACT

The validity of the derivative expansion (DE) method for calculating one-loop quantum vacuum densities is investigated. Source contributions from fermionic loops in a nonuniform, spherically symmetric background scalar field are considered. The convergence of a derivative expansion for the fermion vacuum scalar density is examined in 3+1 dimensions by means of a partial wave analysis. This is done by comparing the contribution to the density from each partial wave with that of a numerical calculation based on an exact evaluation of the fermionic Green function. For cases where the expansion is not rapidly convergent, a method is introduced that enables us to interpolate between the exact calculation and the full derivative expansion. The procedure combines a derivative expansion for the contributions from large loop energies and high partial waves with the numerical evaluation of the small energy and low partial wave part. It is found that a diminishing sum of correction functions yielding the exact result can be calculated and applied. The effect of including vacuum corrections in self consistent models is then tested. For the quantum hadrodynamics model of finite nuclei, including terms up to second order in the derivatives of the background mean fields gives an accurate evaluation of the one-loop vacuum. It is found that the DE terms have a large effect on the value of the fitted parameters. Small effects are found on physical observables, in accordance with relatively small corrections from the DE terms in a background where the expansion is convergent. The convergence of the derivative expansion is also tested for a soliton solution of fermions coupled to a scalar field for the case of large Yukawa coupling bag model. In this case the derivative expansion does not converge rapidly, and we apply the cor-

rection method to obtain the correct one-loop fermionic vacuum scalar source effect. For a coupling of $g = 10$, we need 4 partial wave corrections to reach convergence. We see a decrease in the scalar field depth of 27%, and the fermion energy levels and scalar field change by 49% and 5%, respectively. However, the total energy of the bag changes by only 0.6%. For a large coupling of $g = 25$, the fourth partial wave correction gives a 103% change in the scalar field depth, while the total energy of the bag changes by 2.6%. A small change in the total energy is important here because for large coupling the energy of the bag is such that it is bound by less than 5%.

Chapter 1

OVERVIEW

1.1 Introduction

In what is known as the standard model, physicists have devised a theory that has the ability to account for a large portion of observable phenomena. The standard model incorporates three of the four known interactions of nature: it includes Quantum Chromodynamics (QCD), the theory accounting for strong interactions, and the Electro-weak model in which the effects due to electromagnetic and weak forces are unified. These interactions take place between quarks and leptons (which are the fundamental matter fields), and are mediated by gauge bosons (the force field quanta). The standard model is a field theory, and therefore quantum fields play the part of the underlying physical degrees of freedom. The accuracy of this model has been repeatedly reaffirmed by experimental findings (such as the recent discovery of the top quark).

Despite its many successes, the standard model is by no means complete or fully understood. In fact there are many reasons that make an extension of the model a necessity, such as unification, the hierarchy problem, reducing the number of input parameters, and explaining phenomena such as the flavor structure and CP violation. Also, many questions remain regarding the tractability of the model itself. A major part of this problem lies in the difficulty of doing calculations in the strong coupling regime, where perturbation theory is not applicable. One of the more important manifestations of this problem is that of solving the bound state problem in QCD.

For QCD at low energies, the dynamical quarks and gluons are strongly coupled with three and four body forces, and large vacuum effects that have so far made direct solution impossible. Even promising lattice gauge techniques have yet to yield an accurate solution. It is in this context that it becomes useful to make solvable approximations to the theory.

In the low energy domain, on the scale of a few fm, the hadronic particles and their interactions are the items of physical observation. This is the realm of so called nuclear interactions. One possible approach is to make use of hadronic field theories — effective field theories which incorporate hadronic particles as the effective degrees of freedom. Here we are really considering interactions mediated by bound states of the exact theory. We attempt to gain an understanding of the bulk properties of the nucleus by solving for interactions between nucleons using meson exchange fields. By gaining an understanding of how far the phenomenology will fit with such a model, we hope to gain a better understanding of the exact theory. Examples of such models include the Walecka model of nucleons and neutral scalar and vector mesons, sometimes called Quantum Hadrodynamics (QHD) [3], and the linear sigma model (with nucleons, pions and neutral scalar mesons) [4]. Other phenomenological theories are often attempts to incorporate the exact QCD theory in a solvable manner. A prototype is the Friedberg-Lee non-topological soliton model, which models confinement in QCD by adding a phenomenological scalar field that mimics the gluon condensate and confines the quarks to color singlet states [5]. This model incorporates both the MIT and SLAC bag models in appropriate limits.

The starting point in dealing with all such phenomenological theories is the Lagrangian density. For example, the QHD Lagrangian density is

$$\begin{aligned}\mathcal{L}_{QHD} &= \bar{\psi}[\gamma_\mu(i\partial^\mu - g_v V^\mu) - (M - g_s\phi)]\psi + \tfrac{1}{2}(\partial_\mu\phi\,\partial^\mu\phi - m_s^2\phi^2) \\ &\quad -\frac{1}{4}F_{\mu\nu}F^{\mu\nu} + \tfrac{1}{2}m_v^2 V_\mu V^\mu + \delta\mathcal{L}, \end{aligned} \tag{1.1}$$

Here ψ is a two component nucleon spinor field (neutrons and protons), ϕ is a scalar

field, $F_{\mu\nu} = \partial_\mu V_\nu - \partial_\nu V_\mu$ is the field tensor for vector field V_μ, and g_v, g_s, m_v, m_s, and M, are coupling and mass parameters. As is customary, $\delta\mathcal{L}$ is taken to represent the terms necessary to renormalize the Lagrangian. Units are chosen so that $\hbar = c = 1$. A further example is furnished by the Lagrangian density of the Friedberg-Lee non-topological soliton model [5]

$$\begin{aligned} \mathcal{L}_{FL} &= \bar{\psi}[i\not{D}^\mu - (M - g_s\phi)]\psi - \frac{1}{4}\beta_e(\phi)F^c_{\mu\nu}F^{\mu\nu}_c \\ &\quad + \tfrac{1}{2}\partial_\mu\phi\,\partial^\mu\phi - \tfrac{1}{2}m_s^2\phi^2 - \frac{\kappa}{3!}\phi^3 - \frac{\lambda}{4!}\phi^4 + \delta\mathcal{L}, \end{aligned} \tag{1.2}$$

where

$$\begin{aligned} D_\mu &= \partial_\mu - \frac{i}{2}g_s\lambda_c A^c_\mu, \\ F^c_{\mu\nu} &= \partial_\mu A^a_\nu - \partial_\nu A^a_\mu + g_s f^a_{bc}A^b_\mu A^c_n u. \end{aligned} \tag{1.3}$$

Here ψ represents the quark spinor fields (flavor indices are suppressed), ϕ is a scalar field, A^a_μ are the gluon fields, $\beta(\phi)$ a dielectric constant, and g_s, κ, λ, m_s are the coupling and mass parameters. In the literature the scalar field may often be found in one the following equivalent forms:

$$g_s\,\sigma(x) = M - g_s\phi(x) = g_s(\phi_0 - \phi(x)). \tag{1.4}$$

A general feature of the theories we consider is the appearance of large couplings so that nonperturbative methods must be used if contributions from the vacuum are to be included. A brief background of the relevant field theory formalism will be given in the next section. In addition, the details of our notational convention can be found in Appendix A.

This thesis investigates the calculation of vacuum effects in the context of including them in self-consistent bound state solutions. In particular, we consider including effects from the one-loop effective action, where our background source may have arbitrary spherically symmetric form. For cases other than a constant background field, the one-loop effective action cannot in general be evaluated analytically. For

this reason it is important to investigate local approximations, such as the derivative expansion, which make analytic methods possible. Often the validity of such an expansion is taken for granted in a particular problem even though its convergence properties have not been well determined. To remedy this, a systematic method is provided for testing the degree of convergence and interpolating to the exact Green function result. The manner in which this is done makes it suitable for inclusion in self-consistent calculations. For simplicity we deal solely with the case of fermionic loops coupled to a background scalar source. It is possible to generalize the method to other background sources (in particular to a vector source). Including boson loops is also a possibility, although the necessity of a self-consistent solution makes it harder to study the density in this case.

1.2 Quantum field theory formalism

The following is a review of the main aspects of quantum field theory which will be needed in the following text. Primary references include [3, 6, 7, 8, 9, 10]. In classical field theory we work with the theory of a Lagrangian of a continuous parameterized variable, where our canonical variables are not a discrete set, but are functions of continuous parameter. The variables in our case are the quantum fields and their conjugate momenta fields, and the parameter is taken as the four vector of position, or spacetime. The Lagrangian here is a density, and the action is defined by

$$S = \int d^4x \, \mathcal{L}(\phi(x), \partial_\mu \phi(x)). \tag{1.5}$$

For illustration we limit ourselves here to the case of a Lagrangian depending on a real scalar field $\phi(x)$. The dynamics are determined through Hamilton's principle, $\delta S = 0$, with suitable boundary conditions, and lead to the Euler-Lagrange equations for the case of continuous media

$$\frac{\partial \mathcal{L}}{\partial \phi} - \frac{\partial}{\partial x_\mu} \frac{\partial \mathcal{L}}{\partial(\partial\phi/\partial x_\mu)} = 0. \tag{1.6}$$

The quantum nature of the field theory can be introduced by making our fields into Heisenberg picture operators that obey equal time commutation relations. This method is known as canonical quantization. For spin-0 and spin-$\frac{1}{2}$ fields, we have [7]

$$\text{Bosonic Field:} \qquad [\phi(\vec{x}\,,t), \dot{\phi}(\vec{x}\,',t)] = i\delta^{(3)}(\vec{x} - \vec{x}\,'), \tag{1.7}$$

$$\text{Spinor Field:} \qquad \{\psi(\vec{x}\,,t), \psi^{\dagger}(\vec{x}\,',t)\} = i\delta^{(3)}(\vec{x} - \vec{x}\,'). \tag{1.8}$$

The quantum states here are elements of a Hilbert space known as Fock Space [11], and are multiparticle states representing particle occupation. The ground state is chosen to be the vacuum state with no real particles, and is written $|0\rangle$. However, interactions with this state are nontrivial, as it must be interpreted as representing an infinite product of oscillator ground states which are self interacting through excitations. Observables are then expressed as matrix elements of the field operators between these particle states.

Another important concept for understanding the structure of quantum field theory is that of the Feynman diagram expansion. By expressing an interaction diagrammatically we not only have a way of defining the interaction but also a method of calculating the corresponding amplitude by applying the appropriate Feynman rules. One important quantity to know when dealing with diagrams and calculating observables are the n-point Green functions

$$G^{(n)}(x_1, \ldots, x_n). \tag{1.9}$$

These are defined so they represent the sum of all Feynman diagrams with n external legs [12]. In a free field theory, the two-point Green functions are simply the free field propagators, and can be written in several equivalent forms [7]:
Free scalar theory propagator:

$$\begin{aligned} iD(x-y) &= [\phi(x), \phi(y)] = \langle 0|T\left(\phi(x)\phi(y)\right)|0\rangle \\ &= i\int_C \frac{d^4k}{(2\pi)^4}\,\frac{e^{-ik\cdot(x-y)}}{k^2 - m_s^2} = i\int_{-\infty}^{\infty} \frac{d^4k}{(2\pi)^4}\,\frac{e^{-ik\cdot(x-y)}}{k^2 - m^2 + i\epsilon}\,, \end{aligned} \tag{1.10}$$

Free fermionic theory propagator:

$$\begin{aligned} iS(x-y) &= \{\psi(x), \bar{\psi}(y)\} = \langle 0|T\left(\psi(x)\bar{\psi}(y)\right)|0\rangle \\ &= (i\partial\!\!\!/ + M)iD(x-y) = i\int_{-\infty}^{\infty} \frac{d^4p}{(2\pi)^4}\,\frac{e^{-ip\cdot(x-y)}}{p\!\!\!/ - M + i\epsilon}\,. \end{aligned} \tag{1.11}$$

T here is the time-ordering operator. The limits on the integrals are for p_0, the energy of the corresponding four-momentum. The curve C represents a closed path encompassing the poles of the integrand for this variable. This path is more simply dealt with by introducing the $i\epsilon$ shift in the pole, where ϵ is a positive infinitesimal, so that the energy can run over real values. When dealing with bound states, the propagators will no longer be free, as interactions with other fields are taken into account. The bound state propagator may be calculated by including diagrams representing the interactions to the prescribed order.

The following manipulations will show us how to deal with the n-point Green functions in general, and will enable us to remove contributions from undesirable disconnected diagrams. First of all we define the generating functional in the presence of an interaction governed by an external source $j(x)$. In the interaction picture this contributes a term to the Hamiltonian density with the form $\mathcal{H} = \phi(x)j(x)$, and the generating functional may be written

$$W[j] = \langle 0|T\,\exp\, i\int d^4x\,\phi(x)j(x)|0\rangle \tag{1.12}$$

$$= \sum_{n=0}^{\infty}\frac{i^n}{n!}\int d^4x_1\,\cdots d^4x_n\,j(x_1)\cdots j(x_n)\,G^{(n)}(x_1,\ldots,x_n). \tag{1.13}$$

This expression allows us to determine the n-point Green functions by simple functional differentiation

$$G^{(n)}(x_1,\ldots,x_n) = \langle 0|T\left(\phi(x_1)\cdots\phi(x_n)\right)|0\rangle \tag{1.14}$$

$$= (-i)^n\frac{1}{W[0]}\frac{\delta^n}{\delta j(x_1)\ldots\delta j(x_n)}W[j]\bigg|_{j=0}. \tag{1.15}$$

To eliminate disconnected diagrams, we note that each is composed of a finite number of connected diagrams which, when counted properly, can be removed by

defining the generating functional for connected Green functions, $G_c^{(n)}$, as

$$\begin{aligned} iZ[j] &= \ln W[j] \\ &= \sum_{n=1}^{\infty} \frac{i^n}{n!} \int d^4x_1 \cdots d^4x_n \, j(x_1) \cdots j(x_n) \, G_c^{(n)}(x_1, \ldots, x_n). \end{aligned} \tag{1.16}$$

A further reduction can then be made by considering truncated diagrams which essentially have their external lines removed. These diagrams can then be further refined to one-particle irreducible (denoted 1PI, and also called proper) diagrams by taking the truncated diagrams which remain connected when an arbitrary internal line is cut [6]. The importance of these one particle irreducible diagrams can be seen as follows [12]. Let $-i\Pi(p^2)$ be the sum of *all* such 1PI diagrams that have had two external legs removed. If we wish to consider the full propagator of a theory, this can be obtained by adding up a sum of contributions from these 1PI diagrams with free particle external legs (a so called ring sum) to give

$$\frac{i}{p^2 - m^2 - \Pi(p^2) + i\epsilon} \tag{1.17}$$

as the exact propagator.

The generating functional Γ for these proper diagrams is found by taking the Legendre transformation of $Z[j]$. Defining

$$\phi_c(x) = \frac{\delta}{i\delta j(x)} G_c(j), \tag{1.18}$$

$$i\Gamma[\phi_c] = \left(Z[j] - i \int d^4x \, j(x)\phi_c(x) \right)_{j(x)=j_c(x,\phi)} , \tag{1.19}$$

we find that

$$j_c(x, \phi) = -\frac{\delta}{\delta \phi_c(x)} \Gamma[\phi_c]. \tag{1.20}$$

It can then be shown that

$$\Gamma[\phi_c] = \sum_{n=1}^{\infty} \frac{1}{n!} \int d^4x_1 \cdots d^4x_n \, \Gamma^{(n)}(x_1, \ldots, x_n) \, \phi_c(x_1) \cdots \phi_c(x_n) \tag{1.21}$$

is the generating functional for the proper Green functions $\Gamma^{(n)}(x_1, \ldots x_n)$, which are the sum of 1PI diagrams with n legs. For instance, in momentum space the two point

function is found to be

$$\Gamma^{(2)}(p,-p) = p^2 - m^2 - \Sigma(p^2), \tag{1.22}$$

which contains the contribution $\Sigma(p^2)$ from all two-point irreducible graphs.

Another useful formalism of quantum field theory can be made in terms of the path integral approach. Here the fields remain complex-valued functions, but the theory is formulated in terms of functional integration over all possible configurations of the field. The generating functional here can be written

$$W[j] = N \int [d\phi] \, \exp\left\{ i \int d^4x \, \left[\mathcal{L}(\phi, \partial\phi) + j(x)\phi(x) \right] \right\}, \tag{1.23}$$

where N is a normalization constant. In this approach, we define $Z[j]$ and $\Gamma[j]$ as was done above, but use expression (1.23) for $W[j]$. This formalism is useful for variational calculations such as the one-loop expansion, which we now consider.

1.3 The loop expansion for the quantum vacuum

Our objective in this section is to derive the form of the well known loop expansion [3, 4, 6]. The expansion in this case is with respect to the number of loops appearing in the irreducible Feynman graphs. Therefore it remains exact to all orders in the coupling to external fields at each level of the expansion. This will allows us to perturbatively include vacuum corrections to the classical equations of motion. We will deviate slightly from our system of units here by leaving in the factors of $\hbar$. This is done because consideration of the following simple argument [4] reveals that $\hbar$ is the natural bookkeeping parameter.

As we are considering one particle irreducible diagrams, only internal factors are relevant, and we have the following relation:

$$(\#Loops) = (\#internal\ lines) - (\#internal\ vertices) + 1 \tag{1.24}$$

(where a line occurs between two vertices). In the Feynman rules, each propagator has a factor $\hbar$ and each vertex a factor $\hbar^{-1}$, plus an overall factor $\hbar$ for each diagram. Thus, for each additional loop we gain an additional power of $\hbar$.

To illustrate the method of expansion, we consider a self interacting scalar theory with the Lagrangian

$$\mathcal{L} = \tfrac{1}{2}(\partial_\mu\phi\partial^\mu\phi - m_s^2\phi^2) + j\phi - V(\phi). \tag{1.25}$$

Here j is an external source and $V(\phi)$ is the self interaction potential. Taking ϕ_0 to be the solution to the classical equation of motion

$$(\partial^2 + m_s^2)\ \phi_0 + V'(\phi_0) = j, \tag{1.26}$$

where the prime denotes a functional derivative with respect to ϕ, we use the path integral formalism and expand the action about ϕ_0. We set $\phi = \phi_0 + \tilde{\phi}$, and make a Taylor series expansion of $V(\phi)$ about ϕ_0. The action functional is therefore

$$\begin{aligned}
S[\phi] &= \int d^4x\ \left[\tfrac{1}{2}(\partial_\mu\phi\partial^\mu\phi - m_s^2\phi^2) + j\phi - V(\phi)\right] \\
&= \int d^4x \left[\tfrac{1}{2}(\partial_\mu\phi_0\partial^\mu\phi_0 - m_s^2\phi_0^2) + j\phi_0 - V(\phi_0) + \mathcal{O}(\tilde{\phi})\right. \\
&\qquad \left. +\tfrac{1}{2}(\partial_\mu\tilde{\phi}\partial^\mu\tilde{\phi} - m_s^2\tilde{\phi}^2) - \frac{V''(\phi_0)}{2!}\tilde{\phi}^2 - \sum_{q>2}\frac{V^{(q)}(\phi_0)}{q!}\tilde{\phi}^q\right] \\
&= S[\phi_0] + \int d^4x \left[\tfrac{1}{2}\left(\partial_\mu\tilde{\phi}\partial^\mu\tilde{\phi} - (m_s^2 + V''(\phi_0))\tilde{\phi}^2\right)\right. \\
&\qquad \left. - \sum_{q>2}\frac{V^{(q)}(\phi_0)}{q!}\tilde{\phi}^q\right].
\end{aligned} \tag{1.27}$$

The order $\mathcal{O}(\tilde{\phi})$ term vanishes because ϕ_0 was defined to leave the action stationary. Using Wick's Theorem [6], contributions from odd powers of $\tilde{\phi}$ in the action will vanish when we calculate the generating functional. Omitting the normalization for now, we have

$$W[j] = \int [d\phi]\ \exp\left\{\frac{i}{\hbar}S[\phi]\right\}$$

$$= e^{\frac{i}{\hbar}S[\phi_0]} \int [d\tilde{\phi}] \exp\Big\{ \frac{i}{\hbar} \int d^4x \left[\tfrac{1}{2} \left(\partial_\mu \tilde{\phi} \partial^\mu \tilde{\phi} - (m_s^2 + V''(\phi_0)) \tilde{\phi}^2 \right) - \sum_{q>1} \frac{V^{(2q)}(\phi_0)}{(2q)!} \tilde{\phi}^{2q} \right] \Big\}. \tag{1.28}$$

The scalar field has $\hbar$ dependence $\tilde{\phi} \sim \hbar^{1/2}$. By rescaling the field to $\hbar^{1/2}\tilde{\phi}$ we can display this dependence explicitly:

$$W[j] = e^{\frac{i}{\hbar}S[\phi_0]} \int [d\tilde{\phi}] \exp\Big\{ i \int d^4x \left[\tfrac{1}{2} \left(\partial_\mu \tilde{\phi} \partial^\mu \tilde{\phi} - (m_s^2 + V''(\phi_0)) \tilde{\phi}^2 \right) - \sum_{q>1} \hbar^{q-1} \frac{V^{(2q)}(\phi_0)}{(2q)!} \tilde{\phi}^{2q} \right] \Big\}. \tag{1.29}$$

We see explicitly that our expansion is in powers of $\hbar$. Keeping terms up to those quadratic in the fluctuation from the classical field yields values valid to one-loop order. After an integration by parts, we have

$$W[j] = e^{\frac{i}{\hbar}S[\phi_0]} \int [d\tilde{\phi}] \exp\left\{ i \int d^4x \, \tfrac{1}{2} \tilde{\phi} D^{-1} \tilde{\phi} \right\}. \tag{1.30}$$

The interacting and free scalar propagators, D and D_0, satisfy

$$(\partial_x^2 + m_s^2 + V''(\phi_0)) \; D(x, x') = -\delta^{(4)}(x - x'), \tag{1.31}$$

$$(\partial_x^2 + m_s^2) \; D_0(x, x') = -\delta^{(4)}(x - x'). \tag{1.32}$$

The path integral in (1.30) may be normalized by dividing out the free field result, which is obtained by letting $D^{-1} \to D_0^{-1}$. The path integral of the quadratic part can then be performed, giving the normalized result

$$W[j] = e^{\frac{i}{\hbar}S[\phi_0]} \; \Big(\mathrm{Det}(D_0 D^{-1}) \Big)^{-1/2} + \ldots \tag{1.33}$$

Making use of the identity

$$\mathrm{Det}\, A = e^{\mathrm{Tr}\, \ln A} \tag{1.34}$$

we can evaluate the generating functional for connected Green functions, $Z[j]$, where

$$W[j] = \exp\left\{ \frac{i}{\hbar} Z[j] \right\}, \tag{1.35}$$

as

$$Z[j] = S[\phi_0] + \frac{i}{2}\hbar \,\mathrm{Tr}\, \ln(D_0 D^{-1}) + \mathcal{O}(\hbar^2). \tag{1.36}$$

To obtain the effective action from this connected generating functional, we make the Legendre transformation

$$\begin{aligned} \phi(x,j) &= \frac{\delta Z[j]}{\delta j(x)}, & (1.37)\\ \Gamma[\phi] &= Z[j] - \int d^4x\, j(x)\phi(x). & (1.38) \end{aligned}$$

Note that as we are expanding about the stationary point $S(\phi) = S(\phi_0) + \mathcal{O}(\hbar^2)$, and $\phi = \phi_0 + \mathcal{O}(\hbar)$. Hence

$$\begin{aligned} \Gamma[\phi] &= \int d^4x \left[\tfrac{1}{2}(\partial_\mu\phi\partial^\mu\phi - (m_s^2 + V''(\phi))\phi^2\right] \\ &\quad + \frac{i}{2}\hbar \mathrm{Tr}\, \ln(D_0 D^{-1}) + \mathcal{O}(\hbar^2), \end{aligned} \tag{1.39}$$

where the interacting scalar propagator $D(x,x')$ now satisfies

$$(\partial_x^2 + m_s^2 + V''(\phi))\; D(x,x') = -\delta^{(4)}(x-x'). \tag{1.40}$$

As this expression does not explicitly contain the field ϕ_0, we have the freedom of choosing the ground state of our theory to include the one-loop vacuum effects. The one-loop effective action contribution from scalar loops is therefore

$$\begin{aligned} \Gamma_{vac}[\phi] &= \frac{i}{2}\hbar \,\mathrm{Tr}\, \ln(D_0 D^{-1}) \\ &= \frac{i}{2}\hbar \left(\mathrm{Tr}\, \ln(D^{-1}) - \mathrm{Tr}\, \ln(D_0^{-1})\right). \end{aligned} \tag{1.41}$$

To see that this contribution includes one-loop diagrams with an arbitrary number of external vertices, we may write [4]

$$\begin{aligned} \mathrm{Tr}\, \ln(D_0 D^{-1}) &= \mathrm{Tr}\, \ln(1 - D_0 V''(\phi_0)) \\ &= -\mathrm{Tr} \sum_{n=1}^{\infty} \frac{1}{n} (D_0 V''(\phi_0))^n \\ &= -\int d^4x\, D_0(x,x) V''(\phi_0(x)) \\ &\quad - \int d^4x \int d^4x'\, D_0(x,x') V''(\phi_0(x')) D_0(x',x) V''(\phi_0(x)) \\ &\quad - \ldots \end{aligned} \tag{1.42}$$

The fermionic contribution at the one-loop level can be evaluated in a manner analogous to the boson case given above. One important difference is that here the fields of our internal loop lines have a different background source field. To derive an equation similar to (1.41), an assumption must be made about this source. In general the path integral is over all the independent fields in the Lagrangian. In the Relativistic Hartree Approximation (RHA) we treat the background fields that appear as classical. Then the only difference in the derivation is that because of the spin-$\frac{1}{2}$ nature of the fermions, the fields in the path integrals are Grassman valued [3]. This leads to a quadratic path integral which evaluates to $(\mathrm{Det}(M))$ rather than $(\mathrm{Det}(M))^{-1/2}$. The final result for the effective action in a background of scalar and vector fields is [3],

$$\Gamma_{vac}[\psi] = -i\hbar(\mathrm{Tr}\ \ln(S^{-1}) - \mathrm{Tr}\ \ln(S_0^{-1})), \tag{1.43}$$

where the interacting and free fermion Green functions, S and S_0, obey

$$(i\partial\!\!\!/ - (M - g_s\phi) - g_v V\!\!\!/)S(x,x') = \delta^4(x-x'), \tag{1.44}$$

$$(i\partial\!\!\!/ - (M - g_s\phi_0) - g_v V\!\!\!/_0)S_0(x,x') = \delta^4(x-x'). \tag{1.45}$$

The effective actions given in (1.41) and (1.43) will be applicable to any Yukawa coupled scalar-fermion field theory. However, these expressions still require renormalization. The relevant counterterms will be discussed when we use the actions to calculate physical quantities. To go beyond one-loop methods similar to those developed by Jackiw [13] may be employed. For instance, Coppens and Verchelde have applied functional methods to calculate the 3-loop effective potential for scalar ϕ^4 theory in $3+1$ dimensions [14] .

When we attempt to solve a model with effective fields the question arises whether we should include interactions that occur beyond tree level. Should we include loop effects if the field in question is not fundamental? Proponents [15] argue that their inclusion makes the theory physically complete. It seems hard to justify the case for

formulating a relativistically covariant model while ignoring some of the dynamics which the model predicts. In any case, it is interesting to include the loop terms to see what effect they have on the dynamics of the effective phenomenological theory. This will be our ideology when we examine loop effects in QHD for finite nuclei.

1.4 Bound state calculations with interacting fields

For the calculation of scattering processes where the interaction occurs for a limited time with a small coupling, a valid assumption is to use the analytically known free wave functions for the external lines of the various diagrams contributing to a particular amplitude. This is the usual Feynman perturbation expansion, and in the case of small couplings calculations can be extended to many orders perturbatively. However, when the problem we are dealing with has the form of a bound state we must use wave functions that are solved with source terms from the other fields. The calculations are in general no longer possible analytically. When vacuum corrections are included they must also be calculated with respect to the interacting wave function, yet these corrections will in turn affect the wave function solution, so they must be included in a self-consistent manner. Also, for cases where the coupling is large, expansions with respect to the coupling are no longer valid and methods such as the one-loop approximation must be employed. This expansion is still, however, perturbative in the number of loops. Below some methods that are used to deal with bound state problems are outlined.

To attempt a steady state solution of an effective field theory model we begin by working at tree level. Writing down the Euler-Lagrange equations from the appropriate Lagrangian gives us equations which are quantum in nature and represent the interactions of many body states. As an example, we consider the Walecka model Lagrangian (1.1). The field equations here are:

$$(\partial^2 + m_s^2)\phi \;=\; g_s\bar{\psi}\psi, \tag{1.46}$$

$$\partial_\nu F^{\nu\mu} + m_v^2 V^\mu \;=\; g_v \bar{\psi}\gamma^\mu\psi, \tag{1.47}$$

$$[\gamma^\mu(i\partial_\mu - g_v V_\mu) - (M - g_s\phi)]\psi \;=\; 0. \tag{1.48}$$

The first approximation we consider in solving these equations is the Mean Field Approximation (MFA). Here the scalar and vector field equations are evaluated at their classical expectation values [3]. Our dependent variables are

$$\phi \to \langle\phi\rangle = \phi_0, \qquad V_\mu \to \langle\, V_\mu\rangle = \delta_{\mu 0} V_0. \tag{1.49}$$

It is simplest to begin by considering the case of a spatially uniform system. The spacelike component of the vector field vanishes due to rotational invariance. The field equations then become

$$\phi_0 \;=\; \frac{g_s}{m_s^2}\langle\bar{\psi}\psi\rangle \equiv \frac{g_s}{m_s^2}\rho^s, \tag{1.50}$$

$$V_0 \;=\; \frac{g_v}{m_v^2}\langle\bar{\psi}\gamma_0\psi\rangle \equiv \frac{g_v}{m_v^2}\rho^v, \tag{1.51}$$

$$[i\partial\!\!\!/ - g_v\gamma^0 V_0 - (M - g_s\phi_0)]\psi \;=\; 0. \tag{1.52}$$

Equation (1.52) for the nucleon fields is the only remaining quantum equation. Because of the classical nature of the potentials, the fermionic operator can be expanded in a normal mode sum. This reduces the equation to a single particle equation for the mode wave functions, which can be identified as the Dirac equation with shifted mass and energy. The solutions are therefore known analytic functions. The scalar and vector fields are fixed by the fermion source expectation values, which define the scalar and vector fermion densities ρ^s and ρ^v, respectively.

In a uniform system the conservation of baryon number density fixes the value of V_0. However, the equation (1.50) for the scalar field must be solved self-consistently with the nucleon equation (1.52). This approximation is physically valid for the case of media with an infinite extent, such as infinite nuclear or neutron matter. The ground state is obtained by filling states of the MFA Hamiltonian up to the Fermi momentum k_F. In terms of diagrammatic techniques the MFT involves modifying the

free propagators by adding the effect of tadpole diagrams self-consistently. However, only contributions from nucleons in the levels filled up to k_F are included, and effects from the negative energy sea are neglected.

The MFA can be extended to apply to systems that are nonuniform in space such as finite nuclei. If the scalar and vector fields are allowed spherically symmetric spatial dependence, their field equations become Poisson like equations with source terms from the fermionic densities:

$$\nabla^2\phi(r) - m_s^2\phi(r) \;=\; -g_s\rho^s(r), \tag{1.53}$$

$$\nabla^2 V_0(r) - m_v^2 V_0(r) \;=\; -g_v\rho^v(r), \tag{1.54}$$

$$[i\partial\!\!\!/ - g_v\gamma^0 V_0(r) - (M - g_s\phi(r))]\psi \;=\; 0. \tag{1.55}$$

The densities are derived in the same way as in the uniform MFA — from the expectation value of the appropriate fermionic fields with respect to the corresponding state. The nucleon equation can again be reduced because the field equation allows normal mode solutions. The angular momentum dependence in the equation for the mode wave functions can be factored out in the standard manner [16], leaving a radial Dirac equation. Because the potential terms are now radially dependent, we have three coupled equations to solve for a self-consistent solution.

To include the vacuum contributions in a self-consistent calculation we desire an analytic form for the contributions that can be included in the field equations. To do this we make use of the effective action formalism and one-loop approximation given in section 1.3. Extending the MFT by including contributions from this approximation is known in nuclear physics as the Relativistic Hartree Approximation (RHA). Note that the expression for the one-loop fermion action (1.43) is derived under the assumption of the fields interacting at tree level. When the scalar field is constant, the one-loop contributions can be evaluated exactly. We will see how to do this calculation in section 2.3. When the scalar field is radially dependent, the zero-point corrections can be calculated under the Local Density Approximation (LDA), which

simply replaces the constant potential in the MFA vacuum result with the radially dependent potential. This essentially evaluates the one-loop level contribution under the assumption of a locally uniform source field configuration.

To improve on the Local Density Approximation, we consider adding in one-loop level terms that depend on derivatives of the field. This gives the so called Derivative Expansion (DE) approximation. The exact one-loop quantity is expanded in a series of derivatives of the source field, which is also an expansion in inverse powers of the effective mass (i.e. the local scalar field value). This follows in a straightforward manner from dimensional considerations [17]. These two expansions are not identical as essentially the choice of the expansion parameter defines what terms are included at each order. Here we consider the order of the derivatives as they will be the important factor in determining a solution self-consistently, and seem to have better convergence properties [17]. The termwise convergence of this series will give some indication as to the validity of the expansion, although a much better method is through comparison with the exact "brute force" result.

The convergence has been studied by several authors. In 1+1 dimensions, Li, Perry and Wilets [18] utilized the numerical Green function method to study the DE convergence of the vacuum energy in soliton theories for both fermionic and bosonic loops in a background scalar field. Blunden [19] has studied the convergence of fermionic scalar and vector densities at the one-loop level for both scalar and vector background fields in 1+1 dimensions by also comparing the results with exact Green function calculations. To improve the speed of convergence of the exact calculation, Wasson and Koonin [20] considered using the DE and WKB methods to account for the high energy loops. Wasson [21] has devised a method of interpolating the 1+1 dimension loop results in a background scalar potential by incorporating the exact calculation up to a cutoff. In 3+1 dimensions, DE results for the energy have been tested by Perry through partial wave analysis of fermionic loops in a background scalar theory [22]. These calculations have been extended to both fermionic and

bosonic loops with an improved numerical method by Li, Wilets and Perry [2, 23].

In this work these results are extended to include a calculation in 3+1 dimensions of the fermionic vacuum scalar density in a background scalar field. This derivative expansion is then tested for each partial wave. The advantage here is that using the vacuum density allows the one-loop contribution to be included directly in the equations of motion. This is an improvement over the method used by Li [24] who attempts to gain self-consistency by minimizing the energy of the system with respect to parameters in a postulated background field. Also, when we examine the convergence of the derivative expansion energy, some of the information may be lost in the spatial integration. Using the density, we can naturally examine the convergence at different spatial locations. When the density is not convergent, methods devised along a similar line to those of Wasson [21] can be implemented to interpolate the DE to the exact result. The result will be a derivative expansion improved exact calculation of the dynamic vacuum density in 3+1 dimensions.

Chapter 2

DERIVATIVE EXPANSIONS

2.1 Methods of derivation

The idea of a derivative expansion consists of writing the one-loop contribution to the effective action as a series in an increasing order of spacetime derivatives of the background field. Consider a theory with Yukawa interactions between fermions and scalar and vector bosons as well as three and four body scalar self interactions. We write the Lagrangian as

$$\begin{aligned}\mathcal{L} &= \bar{\psi}[\gamma_\mu(i\partial^\mu - g_v V^\mu) - (M - g_s\phi)]\psi + \tfrac{1}{2}\partial_\mu\,\phi\partial^\mu\phi - U(\phi) \\ &\quad -\frac{1}{4}F_{\mu\nu}F^{\mu\nu} + \tfrac{1}{2}m_v^2 V_\mu V^\mu + \delta\mathcal{L},\end{aligned} \tag{2.1}$$

where

$$U(\phi) = \frac{m_s^2}{2}\phi^2 + \frac{\kappa}{3!}\phi^3 + \frac{\lambda}{4!}\phi^4. \tag{2.2}$$

The vacuum contributions arise from fermion loops in a background of scalar and vector fields, as well as boson loops from the scalar self interactions. We therefore have contributions to the effective action under the one-loop approximation from both equations (1.41) and (1.43). The general form of the derivative expansion of the effective action follows from Lorentz covariance, and to fourth order is:

$$\begin{aligned}\Gamma_{vac} &= \int d^4x\Big[-U_s(\phi) + \tfrac{1}{2}Z_{1s}(\phi)\,\partial_\mu\phi\,\partial^\mu\phi + \tfrac{1}{2}Z_{2s}(\phi)(\partial^2\phi)^2 \\ &\qquad + \tfrac{1}{2}Z_{3s}(\phi)(\partial_\mu\phi)^2(\partial^2\phi) + \tfrac{1}{2}Z_{4s}(\phi)(\partial_\mu\phi)^4 + \ldots \\ &\qquad + \tfrac{1}{4}Z_{1v}(\phi)F_{\mu\nu}F^{\mu\nu} + \tfrac{1}{2}Z_{2v}(\phi)(\partial_\alpha F^{\alpha\mu})(\partial^\beta F_{\beta\mu}) + \ldots \\ &\qquad - U_b(\phi) + \tfrac{1}{2}Z_{1b}(\phi)\,\partial_\mu\phi\,\partial^\mu\phi + \tfrac{1}{2}Z_{2b}(\phi)(\partial^2\phi)^2\end{aligned}$$

$$+\tfrac{1}{2}Z_{3b}(\phi)(\partial_\mu\phi)^2(\partial^2\phi)+\tfrac{1}{2}Z_{4b}(\phi)(\partial_\mu\phi)^4+\quad\ldots\quad\Big]. \qquad (2.3)$$

Some effort is required to find the expansion coefficients. For the effective action they have been evaluated by many authors. For most applications, considering the effects of terms of up to fourth order is sufficient, although terms up to sixth order have appeared in the literature [25]. In practical self-consistent calculations the expansion is found to be useful only when the second order terms dominate higher order terms, because including the fourth order derivatives tends to make the self-consistent solution numerically unstable [26].

We define

$$g_s\sigma(x)\to\sigma(x)=M-g_s\phi(x), \qquad g_s\sigma_0\to\sigma_0=M. \qquad (2.4)$$

The coupling has been absorbed into the definition of the effective scalar field $\sigma(x)$ to simplify the form of the following equations. This convention will be followed until the end of section 2.2. Results for the expansion in $3+1$ dimensions with derivatives up to 4th order of the scalar field, and 2nd order in the vector field are given below (some terms can be found in [15, 23, 24, 27, 28, 29], a general method is discussed in Appendix B):

Fermion Loops:

$$U_s = -\frac{\lambda}{16\pi^2}\left\{\sigma^4(x)\,\ln\left(\frac{\sigma^2(x)}{\sigma_0^2}\right)+\sum_{k=0}^{4}f_n\sigma_0^{4-k}(\sigma_0-\sigma(x))^k\right\}, \qquad (2.5)$$

$$Z_{1s} = -\frac{\lambda}{8\pi^2}\left\{\ln\left(\frac{\sigma^2(x)}{\sigma_0^2}\right)+z_{1s}\right\}, \qquad (2.6)$$

$$Z_{2s} = \frac{\lambda}{80\pi^2}\left\{\frac{1}{\sigma^2(x)}+\frac{z_{2s}}{\sigma_0^2}\right\}, \qquad (2.7)$$

$$Z_{3s} = -\frac{11\lambda}{720\pi^2}\left\{\frac{1}{\sigma^3(x)}\right\}, \qquad (2.8)$$

$$Z_{4s} = \frac{11\lambda}{1440\pi^2}\left\{\frac{1}{\sigma^4(x)}\right\}, \qquad (2.9)$$

$$Z_{1v} = \frac{\lambda}{12\pi^2}\left\{\ln\left(\frac{\sigma^2(x)}{\sigma_0^2}\right) + z_{1v}\right\}, \tag{2.10}$$

$$Z_{2v} = -\frac{\lambda}{60\pi^2}\left\{\frac{1}{\sigma^2(x)} + \frac{z_{2v}}{\sigma_0^2}\right\}, \tag{2.11}$$

Boson Loops:

$$U_b = \frac{1}{64\pi^2}\Big\{W^2(x)\,\ln\left(\frac{W(x)}{W_0}\right) - \frac{1}{2}(W(x)-W_0)(3W(x)-W_0) + f_b(\phi)\Big\}, \tag{2.12}$$

$$Z_{1b} = \frac{1}{192\pi^2}\left\{\frac{(W')^2}{W}\right\}, \tag{2.13}$$

$$Z_{2b} = \frac{1}{1920\pi^2}\left\{\frac{(W')^2}{W^2}\right\}, \tag{2.14}$$

$$Z_{3b} = -\frac{1}{480\pi^2}\left\{\frac{(W')^3}{3W^3} - \frac{(W')(W'')}{2W^2}\right\}, \tag{2.15}$$

$$Z_{4b} = \frac{1}{480\pi^2}\left\{\frac{(W')^4}{8W^4} + -\frac{(W')^2(W'')}{3W^3} + \frac{(W'')^2}{4W^2}\right\}, \tag{2.16}$$

where $W(x) = U_s''(\phi)$, primes denote differentiation with respect to ϕ, and λ is the degeneracy parameter of the field ψ. The parameters $f_n, z_{1s}, z_{2s}, z_{1v}, z_{2v}$, and the function $f_b(\phi)$, are fixed by the choice of renormalization, and are written to facilitate the different models we consider. In this expansion the terms with no field derivatives, $U_s(\phi)$ and $U_b(\phi)$, give the local density approximation. The LDA is therefore the first term in the derivative expansion. The next orders in the expansion are given by the $Z_1(\phi)$ and $Z_2(\phi)$ terms respectively. The analogous results in $1+1$ dimensions can be found in [18].

There are several variations of the methods by which the above expansion(s) can be derived that have grown from early work on the subject [27, 30, 31, 32, 33]. One method by which we can quickly arrive at the expansion is that based on the knowledge of the polarization insertion ($\Pi(p^2)$) calculated for the appropriate Feynman diagrams [22, 34]. Often in a problem the form of the polarization insertions for a particular diagrams or set of diagrams has been calculated. In this case it becomes a

straight forward exercise to calculate vacuum contributions to the effective potential by simply expanding the momentum space polarization about zero momenta. For example, Furnstahl and Horowitz [35] give a scalar polarization function due to fermion loops whose momentum dependent terms are

$$\Pi_s(q) = \frac{3\lambda g_s^2}{4\pi^2}\left(-\frac{q^2}{6} - \int_0^1 dz\,(\sigma(x)^2 - z(1-z)q^2)\,\ln\left(\frac{\sigma(x)^2 - z(1-z)q^2}{\sigma_0^2}\right)\right). \tag{2.17}$$

The derivative coefficients can then be determined using

$$Z_1 = -\frac{\partial\,\Pi_s(q^2)}{\partial(q^2)}\bigg|_{q^2=0} \qquad Z_2 = -\frac{1}{2}\frac{\partial^2\,\Pi_s(q^2)}{\partial(q^2)^2}\bigg|_{q^2=0}. \tag{2.18}$$

As the expression (2.17) has previously been renormalized, the effective action with these coefficients will obey the same normalization conditions.

An alternative approach to the derivation starts directly from the equation for the one-loop effective action. In this method we work in momentum space and expand the log of the inverse Green function in various derivative orders. Often, some simplifying manipulations are made depending on the exact form of the quantity being calculated. Some authors [24, 29, 32], for instance, find it useful to introduce additional parameters into the expansion. This involves making use of identities such as

$$\mathrm{Tr}\,\ln(X+Y) = \mathrm{Tr}\,\ln X + \int_0^1 dz\,\frac{1}{A+zB}B, \tag{2.19}$$

where X and Y are operators. A rather elegant derivation [25] makes use of the identity

$$\mathrm{Tr}\,\ln(XY) = \mathrm{Tr}\,(\ln X + \ln Y)\,. \tag{2.20}$$

which follows from the Campbell-Hausdorff relation and contains no additional parameters. Special attention is made to the gauge invariance and symmetries in this derivation, allowing the authors to obtain results for the bosonic expansion to 6th order in the the derivatives. At this order 28 terms were found. In a later section of this thesis a similar calculation will be made for the fermionic fields. However,

we choose to expand the Green function directly instead of using either of the above identities.

Before doing this we consider how the effective action expansion can be used to give us the quantities of interest. The full effective quantum action is given by

$$\begin{aligned}\Gamma &= \int d^4x\, \mathcal{L} + \Gamma_{vac} \\ &= \int d^4x\, (\mathcal{L} + \mathcal{L}_{vac}) \\ &= \int d^4x\, \mathcal{L}_{eff}. \end{aligned} \tag{2.21}$$

This defines the effective Lagrangian $\mathcal{L}_{eff}$ (where the renormalization still needs to be defined). The energy functional is related to the effective action by

$$E[\Phi] = -\frac{\Gamma[\Phi]}{\int dt}, \tag{2.22}$$

where Φ is a general source field. The ground state of the system Φ_c is then defined at the minimum of $E[\Phi]$, where

$$\left.\frac{\delta E[\Phi]}{\delta \Phi}\right|_{\Phi=\Phi_c} = 0\ . \tag{2.23}$$

In this expression we see how the nature of the one-loop expansion allows us the freedom of choosing the true ground state about which we are expanding *after* the expansion has been made.

The expression (2.23) is essentially equivalent to applying the Euler-Lagrange equation to the effective Lagrangian. However, the effective Lagrangian depends on higher order derivatives of the field so we reapply Hamilton's principle to generalize equation (1.6) to

$$\frac{\partial \mathcal{L}}{\partial \Phi} - \partial_\mu \left(\frac{\partial \mathcal{L}}{\partial(\partial_\mu \Phi)}\right) + \partial^2 \left(\frac{\partial \mathcal{L}}{\partial(\partial^2 \Phi)}\right) + \ldots = 0, \tag{2.24}$$

where $\mathcal{L} = \mathcal{L}(\Phi, \partial_\mu \Phi, \partial^2 \Phi, ...)$. Recall that terms beyond the first two only have contributions from the vacuum part of the effective Lagrangian. To group the vacuum

contributions together in the Euler-Lagrange equations we may define

$$\rho_{vac} = \frac{\partial \mathcal{L}_{vac}}{\partial \Phi} - \partial_\mu \left(\frac{\partial \mathcal{L}_{vac}}{\partial(\partial_\mu \Phi)} \right) + \partial^2 \left(\frac{\partial \mathcal{L}_{vac}}{\partial(\partial^2 \Phi)} \right) + \dots \tag{2.25}$$

This is one way in which the vacuum density can be defined. As a result the vacuum density can be represented in the field equations as a source term. We see that the derivative expansions for the energy and the density can thus be derived from the effective action derivative expansion using a combination of equations (2.21), (2.22), and (2.25).

2.2 QED vacuum polarization

As a simple example of the effective Lagrangian formalism and the validity of the derivative expansion we consider the vacuum polarization process in Quantum Electrodynamics (QED). Abundant evidence exists that supports the idea that QED is the fundamental theory of electromagnetic interactions below 100 GeV. As well, it is usually considered to be the most well understood physical field theory. The simplest form is that of a theory of spin-$\frac{1}{2}$ charged fermions with field ψ, mass M, and charge e, with interactions mediated by the spin-1 massless gauge field for photons, A_μ. The QED Lagrangian in the Feynman gauge is

$$\mathcal{L}_{QED} \;=\; \bar{\psi}[\gamma_\mu(i\partial^\mu - eA^\mu) - M]\psi - \frac{1}{4}F_{\mu\nu}F^{\mu\nu} - \tfrac{1}{2}(\partial_\mu A^\mu)^2 + \delta\mathcal{L}, \tag{2.26}$$

where $F_{\mu\nu} = \partial_\mu A_\nu - \partial_\nu A_\mu$. We treat a case which may be evaluated perturbatively about the free particle solution. In this setting we will clearly be able to see the effects of the shape of the source density in a calculation that has the same flavor as the DE approximation. The analysis is simplified here by treating the interaction perturbatively in the coupling and comparing quantities only to $\mathcal{O}(\alpha)$, where $\alpha = e^2/4\pi$ is the usual fine structure constant. This is accomplished by considering the modification of the free photon propagator by the $\mathcal{O}(\alpha)$ vacuum polarization insertion.

In momentum space the propagator $iD_{\alpha\beta}(q)$ then becomes

$$iD_{\alpha\beta}(q) = iD_{0\alpha\beta}(q) + iD_{0\alpha\mu}(q)\, i\Pi^{\mu\nu}(q)\, iD_{0\nu\beta}(q). \tag{2.27}$$

Note that from gauge invariance $q^\mu\, \Pi_{\mu\nu}(q) = 0$, which dictates the Lorentz invariant form

$$\Pi^{\mu\nu} = (g^{\mu\nu} - \frac{q^\mu q^\nu}{q^2})\, \Pi(q^2), \tag{2.28}$$

so that

$$iD_{\alpha\beta}(q) = -\frac{ig_{\alpha\beta}}{q^2 + i\epsilon} - \frac{ig_{\alpha\beta}}{(q^2 + i\epsilon)^2}\, \Pi(q^2). \tag{2.29}$$

From the well known Feynman rules of QED with the usual charge renormalization, the propagator's polarization insertion is found to be [8]

$$\Pi(q^2) = \frac{2\alpha}{\pi} q^2 \int_0^1 dz\, z(1-z)\, \ln\left(1 - z(1-z)\frac{q^2}{M^2}\right). \tag{2.30}$$

This integral can be evaluated, and for the case of a stationary source the momentum is spacelike, $q^2 = -\vec{q}^{\,2}$, and

$$\Pi_R(-\vec{q}^{\,2}) = -\frac{\alpha\vec{q}^{\,2}}{3\pi}\, \left(-\frac{5}{3} + \frac{4M^2}{\vec{q}^{\,2}} + (1 - \frac{2M^2}{\vec{q}^{\,2}})\sqrt{1 + \frac{4M^2}{\vec{q}^{\,2}}}\, \ln\left(\frac{\sqrt{1 + \frac{4M^2}{\vec{q}^{\,2}}} + 1}{\sqrt{1 + \frac{4M^2}{\vec{q}^{\,2}}} - 1}\right)\right). \tag{2.31}$$

To write an expression for the vacuum polarization potential we fold a background spherically symmetric charge charge density source, $\rho_{ch}(r)$, over the new part of the propagator. This is most easily done in momentum space, where for a time independent source

$$V^E_{vac}(\vec{x}\,) = \int \frac{d^3q}{(2\pi)^3}\, e^{i\vec{q}\cdot\vec{x}}\, \frac{\Pi_R(-\vec{q}^{\,2})}{|\vec{q}\,|^4} \rho_{ch}(\vec{q}). \tag{2.32}$$

The angular part may be integrated, leaving

$$V^E_{vac}(r) = \frac{2\alpha}{\pi} \int_0^\infty dq\, \frac{\sin(qr)}{qr}\, \frac{\Pi_R(-q^2)}{q^2}\, \rho_{ch}(q), \tag{2.33}$$

where

$$\rho_{ch}(q) = \int d^3x\, e^{-i\vec{q}\cdot\vec{x}} \rho_{ch}(\vec{x}\,) = 4\pi \int_0^\infty dr\, r^2\, \frac{\sin(qr)}{qr} \rho_{ch}(r). \tag{2.34}$$

This expression gives the "exact" effect of vacuum polarization in our theory (to $\mathcal{O}(\alpha)$).

For comparison, the derivative expansion coefficients can be evaluated using equation (2.18) and the integral form (2.30), giving

$$Z_1 = 0, \qquad Z_2 = \frac{\alpha}{15\pi M^2}. \tag{2.35}$$

The result $Z_1 = 0$ is a manifestation of charge conservation, which implies that corrections to the charge density are total derivatives that vanish under a spatial integration. This allows us to write an effective Lagrangian for low energy photons that takes into account the vacuum polarization loop in an additional derivative term. The full effective one-loop Lagrangian will contain contributions for the photon-electron vertex correction that are of order α^2. It is referred to as the Euler and Heisenberg Effective Lagrangian [4]. Here we are interested in the order α part (only the vacuum polarization)

$$\mathcal{L}_{eff} = -\frac{1}{4}F_{\mu\nu}F^{\mu\nu} - \frac{\alpha}{30\pi M^2}(\partial_\mu F^{\mu\lambda})(\partial^\nu F_{\nu\lambda}) - j^\mu A_\mu. \tag{2.36}$$

The fermion part of the Lagrangian has been dropped here, and an external source current j^μ is included. The gauge fixing term can be dropped because we will restrict ourselves to the time like part of the vector potential in the case where it is independent of time. The suitable form for the Euler-Lagrange equations are

$$\frac{\partial\mathcal{L}}{\partial A_\mu} - \partial_\lambda\left(\frac{\partial\mathcal{L}}{\partial\left(\partial_\lambda A_\mu\right)}\right) + \partial^2\left(\frac{\partial\mathcal{L}}{\partial\left(\partial^2 A_\mu\right)}\right) = 0. \tag{2.37}$$

Considering the time-like part of the potential A_0 and a source current $j^\mu = \delta^{\mu 0} j_0$, we obtain a modified form of Maxwell's equation

$$\partial^2 A_0 = j_0 + \frac{\alpha}{15\pi M^2}\partial^4 A_0, \tag{2.38}$$

which for a time independent potential becomes

$$\nabla^2 A_0 = -j_0 - \frac{\alpha}{15\pi M^2}\nabla^4 A_0. \tag{2.39}$$

Making use of the identity $\nabla^2 1/|\vec{x}\,| = -4\pi\delta(\vec{x}\,)$ this can be written as an integro-differential equation:

$$\begin{aligned} A_0(\vec{x}\,) &= \frac{1}{4\pi}\int d^3x' \,\frac{1}{|\vec{x}\,' - \vec{x}\,|}\left(j_0(\vec{x}\,') + \frac{\alpha}{15\pi M^2}\nabla^4 A_0(\vec{x}\,')\right) \\ &= \frac{1}{4\pi}\int d^3x' \,\frac{1}{|\vec{x}\,' - \vec{x}\,|} j_0(\vec{x}\,') + \frac{\alpha}{60\pi^2 M^2}\int d^3x' \,\left(\nabla^2 \frac{1}{|\vec{x}\,' - \vec{x}\,|}\right)\nabla^2 A_0(\vec{x}\,') \\ &= \frac{1}{4\pi}\int d^3x' \,\frac{1}{|\vec{x}\,' - \vec{x}\,|} j_0(\vec{x}\,') - \frac{\alpha}{15\pi M^2}\nabla^2 A_0(\vec{x}\,). \end{aligned} \tag{2.40}$$

As the electromagnetic coupling α is small, we can solve this equation iteratively by substituting for the RHS A_0 with the LHS A_0 in an iterative manner. For example, with a point-like source with charge $-Ze$ we have $j_0(\vec{x}\,) = -Ze\,\delta^{(3)}(\vec{x}\,)$, so

$$\begin{aligned} A_0(\vec{x}\,) &= -\frac{Ze^2}{4\pi|\vec{x}\,|} - \frac{\alpha}{15\pi M^2}\nabla^2 A_0(\vec{x}\,) \\ &= -\frac{Z\alpha}{|\vec{x}\,|} - \alpha Z\alpha\frac{4\delta^{(3)}(\vec{x}\,)}{15M^2}. \end{aligned} \tag{2.41}$$

This is the familiar term which contributes to the Lamb shift in hydrogen [8].

To understand how useful the effective Lagrangian is here we consider the spherically symmetric charge density, $j_0 = \rho_{ch}(r)$. Solving (2.40) iteratively we have for the vacuum polarization contribution to the potential

$$V^D_{vac}(r) = \frac{4\alpha^2}{15M^2}\rho_{ch}(r). \tag{2.42}$$

This expression can be compared to the exact result which we also calculated to $\mathcal{O}(\alpha^2)$ (2.33). For simplicity, we choose a Gaussian source density

$$\rho_{ch}(r) = \frac{1}{\pi^{3/2}a^3}\;\; e^{-(r/a)^2}, \qquad \rho_{ch}(q) = e^{-a^2q^2/4}, \tag{2.43}$$

where the parameter a controls the shape of the potential. (This potential has a height of $\pi^{-3/2}a^{-3}$, a width at half max of $a\sqrt{\ln 2}$, and is normalized to unity). Equations (2.33) and (2.42) can then be compared for different values of a, as seen in figures 2.1 and 2.2.

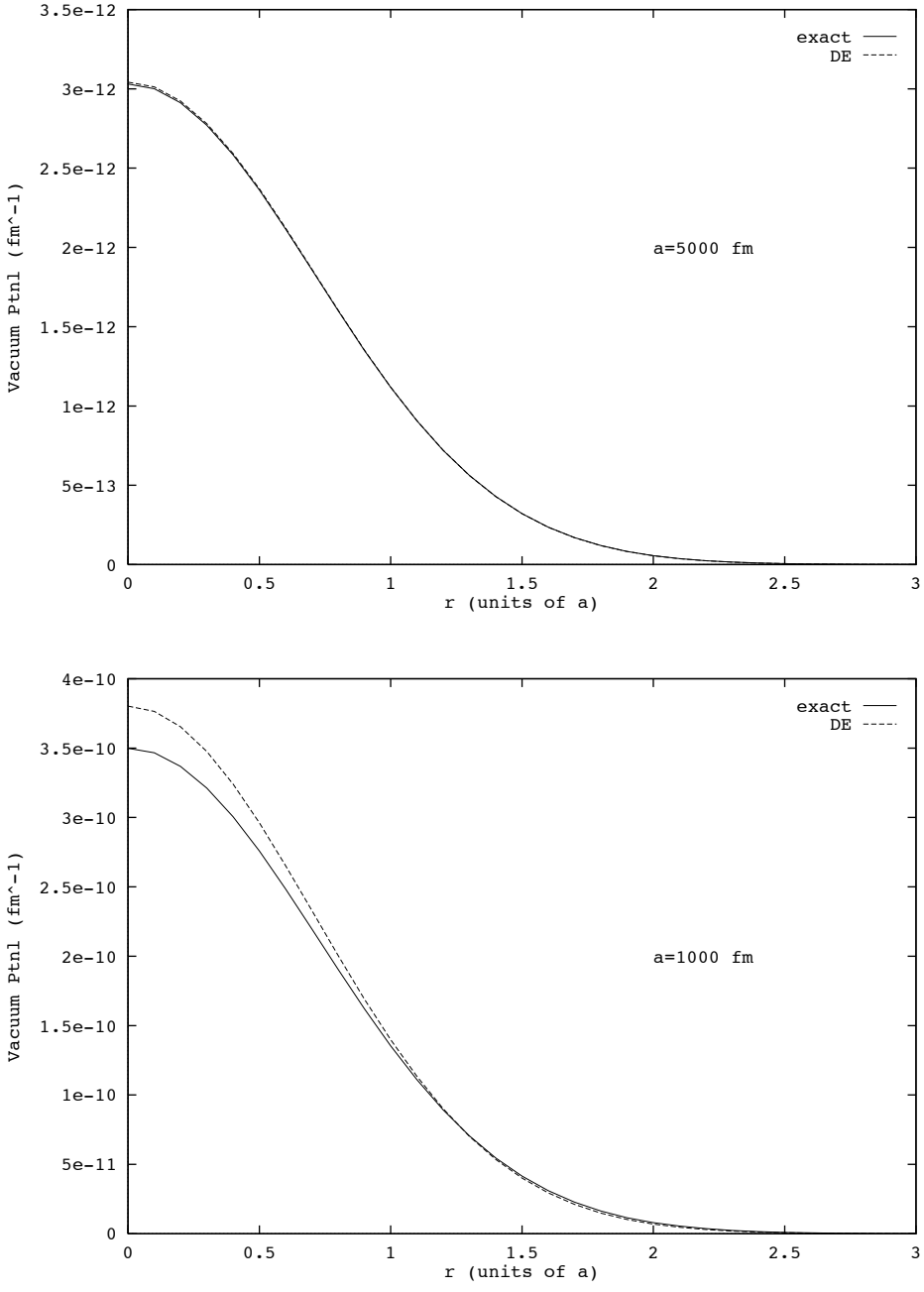

Figure 2.1: Validity of the DE level QED vacuum potential for large a.

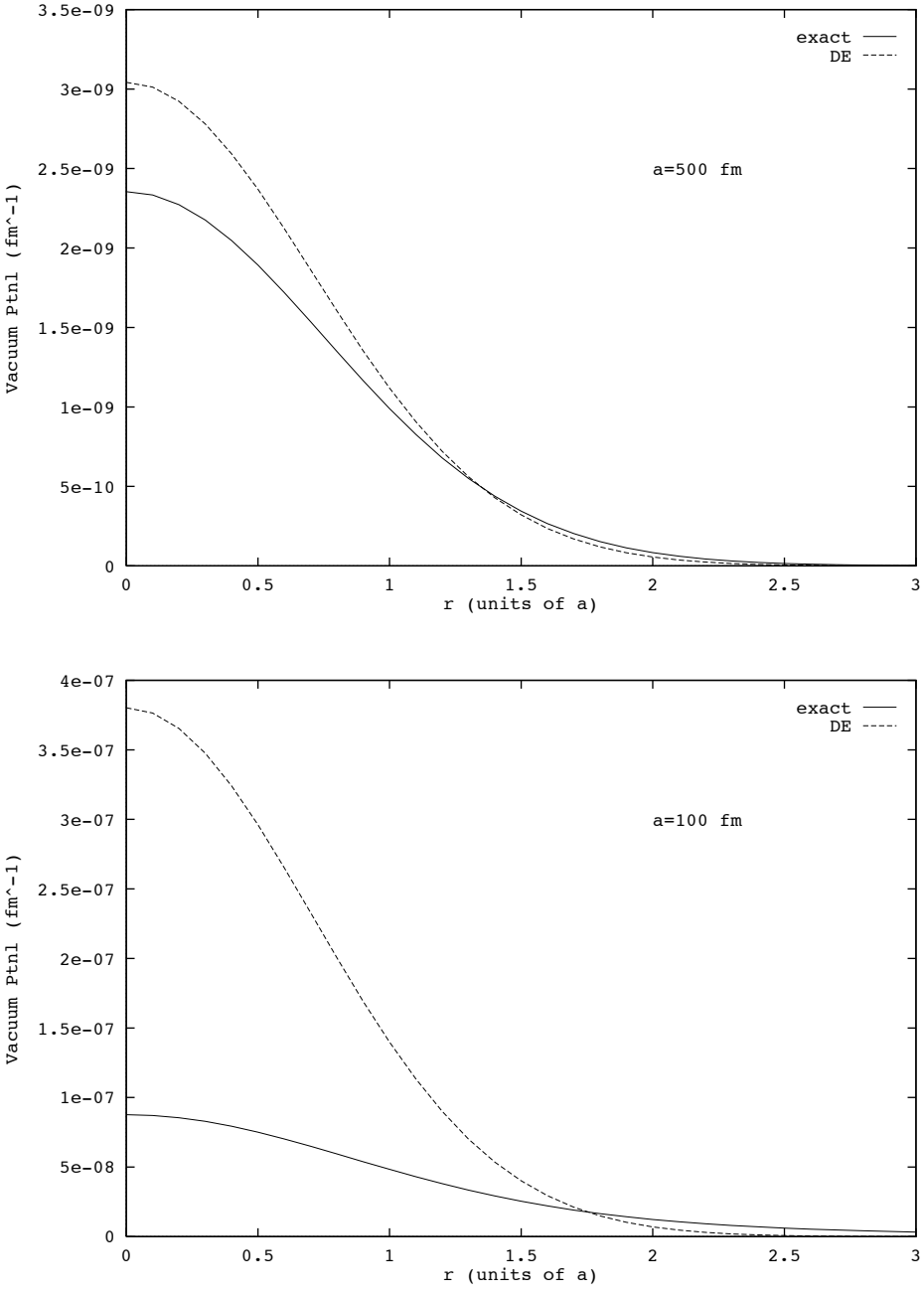

Figure 2.2: Validity of the DE level QED vacuum potential for small a.

We see that for large a (small height, big width) the derivative procedure gives a valid description of the vacuum. For smaller a, the height increases and depth decreases, and the approximation loses its validity. It is important to remember that a is large or small compared with the length scale $1/M$. In other words, we expect the derivative expansion to be valid for fields that fall off slowly compared with a length scale determined by the inverse of the fermion mass. Here we have used the mass of the electron, with $m_e^{-1} = 386$ fm, and observe that the derivative expansion breaks down for a comparable or small than this value. For muon loops, we would expect the derivative expansion to be valid down to length scales of $m_\mu^{-1} = 1.88$ fm.

2.3 Direct expansion

2.3.1 Expressions for the energy and density

As an alternative method to deriving the derivative expansion for the effective action, we can derive equations for the energy and density in terms of the Green function and expand the Green function directly. To see how this is done, consider the one-loop fermionic contribution to the effective action for a scalar background:

$$\begin{aligned} \Gamma_{vac} &= -i \,\mathrm{Tr}_x^{int} \left(\ln S^{-1}(\phi_c) - \ln S_0^{-1}(\phi_c) \right) \\ &= -i \int d^4x \,\mathrm{tr}\, \langle x | \left(\ln S^{-1}(\phi_c(x)) - \ln S_0^{-1}(\phi_c(x)) \right) | x \rangle. \end{aligned} \tag{2.44}$$

Here Tr_x^{int} denotes a trace taken over spacetime as well as the internal degrees of freedom (such as spin, isospin etc.) whereas tr denotes simply the trace over the internal degrees of freedom. This action has not yet been renormalized and is technically an infinite quantity. To deal with the renormalization we consider all four dimensional integrals in D dimensions. This is the method of Dimensional Regularization which allows us to consider finite quantities in our intermediate steps and take care of the renormalization at the end. As an even further simplification we drop the contribution from the free Green function S_0, and will pick it up again when performing the

renormalization, so that

$$\Gamma_{vac} = -i\,\mathrm{Tr}_x^{int}\,\left(\ln S^{-1}(\phi_c)\right). \tag{2.45}$$

The fermion Green function $S(\phi_c)$ can be written symbolically as

$$S(\phi_c) = \frac{1}{i\partial\!\!\!/ - \sigma_c(x) + i\epsilon}, \tag{2.46}$$

where $\sigma_c(x) = M - g_s\,\phi_c(x)$. Because the scalar field is independent of time we can equivalently use the Fourier transformed Green function

$$S(p_0) = \int dt\, S(\phi_c) e^{-ip_0 t}. \tag{2.47}$$

Also, the energy functional $E(\phi_c) = -\Gamma/\int dt$, so we have

$$E_{vac} = -\frac{i}{2\pi}\int dp_0\,\mathrm{Tr}_{\vec{x}}^{int}\ln S^{-1}(p_0). \tag{2.48}$$

A Wick rotation of the p_0 contour integral to the imaginary axis can be made by the replacement $p_0 \to i\omega$, where ω is taken to be real. This alleviates the necessity of the $i\epsilon$ prescription for getting the path right, so

$$S(i\omega) = \frac{1}{i\gamma_0\omega + i\vec{\gamma}\cdot\nabla - \sigma_c(x)}. \tag{2.49}$$

Using this expression in (2.48) and an integration by parts of the resulting line integral, we obtain the following result for the energy in terms of the fermion Green function

$$E_{vac} = -\frac{i}{2\pi}\int d\omega\,\omega\,\mathrm{Tr}_{\vec{x}}^{int}\,(\gamma_0 S(i\omega)). \tag{2.50}$$

The scalar vacuum density can be obtained from the energy by taking the functional derivative

$$\rho_{vac}^s(x) = \frac{\delta E_{vac}}{\delta g\phi_c(x)} = -\frac{\delta E_{vac}}{\delta\sigma_c(x)}. \tag{2.51}$$

When this result is used in the expression for E_{vac}, the spatial integral part of the trace is removed, leaving simply the diagonal spatial matrix element, denoted $S(x,x;i\omega)$. The result can be further simplified by making using of the identity [21]

$$\mathrm{tr}\;\gamma_0\frac{\partial}{\partial\sigma_c}S(i\omega) = -\mathrm{tr}\;i\frac{\partial}{\partial\omega}S(i\omega). \tag{2.52}$$

This expression can easily be derived from the form of the Green function (2.46). An integration by parts will then give the result for the scalar density,

$$\rho^s_{vac}(x) = -\frac{1}{2\pi}\int d\omega\, \mathrm{tr}(S(x,x;i\omega)). \tag{2.53}$$

One possible advantage of using equations (2.50) and (2.53) is that from a derivative expansion of the Green function we obtain the expansion directly in terms of physical quantities we are interested in. The importance of this will become clear when we consider numerical calculations. Although formally the vacuum density as given in equation (2.53) is equivalent to that derived from the vacuum Lagrangian or energy functional using (2.25) or (2.51), these expressions will differ when a finite numerical cutoff is imposed on the ω integral. This cutoff is in no way related to our method of renormalization but is simply imposed by a numerical solution. Essentially the formalisms will differ by a total derivative under the ω integral, which will not vanish when a finite cutoff is imposed. Therefore, the convergence versus the cutoff becomes an important issue. In $1+1$ dimensions the connection between the two methods is cited by Wasson [21]. However, no attempt is made to compare the the difference of the two methods for cutoff convergence. A comparison of the convergence versus the form of the expansion will be given in section 3.1. Similar things happen in $3+1$ dimensions. When a partial wave decomposition is made, we find that the value of a particular partial wave term may differ if a total momentum divergence is added before the decomposition is made. The calculation of each of the partial wave terms involves imposing a cutoff which is again another dependence on any derivative added under the ω integral. Thus here the form of the expansion may affect the convergence with respect to both the partial waves and cutoff. The hope is that by direct application of equation (2.53) to the Green function expansion and careful manipulation of intermediate terms we will obtain a form of the density that will converge rapidly with cutoff.

2.3.2 Fermion Green function expansion

The method used here to derive the derivative expansion involves an explicit expansion of the fermion Green function in momentum space. This method was first introduced by Chan [27], who used it to calculate the expansion for the boson Green function up to terms with four derivatives. Since then many others have made use of this technique in different forms. Wasson [21], for instance, used this method to expand the energy trace of the fermion Green function in $1+1$ dimensions. Another benefit of this method is that the terms are represented in momentum space in a simple manner, which makes it easy to expanded in a partial wave sum in $3+1$ dimensions. This method is necessary not only to improve numerical convergence but also to allow extrapolation away from the DE result in cases where it does not rapidly converge. Here we make an explicit expansion of the fermion Green function in arbitrary dimension under the influence of a background scalar field. The necessary traces are evaluated at the end of the calculation, so that the expansion can be used to directly give either the energy or the density.

As only the diagonal spatial elements of the fermion Green Function are required, we can write

$$\begin{aligned}
S(x,x;i\omega) &= \langle x|S(i\omega)|x\rangle \\
&= -\langle x|\frac{1}{(-i\not{\partial}+\sigma(x))}|x\rangle \\
&= -\frac{1}{(2\pi)^{2d}}\int d^dp\ d^dp'\ \langle x|p\rangle\langle p|\frac{1}{-i\not{\partial}+\sigma(x)}|p'\rangle\langle p'|x\rangle \\
&= -\frac{1}{(2\pi)^{d}}\int d^dp\ e^{ipx}\ \frac{1}{-\not{p}+\sigma(i\frac{\partial}{\partial p})}\ e^{-ipx} \\
&= -\mathrm{Tr}_{\vec{p}}\ \ (e^{ipx}\ \frac{1}{-\not{p}+\sigma(i\frac{\partial}{\partial p})}\ e^{-ipx}). \qquad (2.54)
\end{aligned}$$

Here the d denotes the number of spatial dimensions, $d = D-1$, and the sign in the denominator is introduced for later convenience. To proceed we note that the

translation operator e^{-ipx} obeys the following relation:

$$f(i\frac{d}{dp})\ e^{-ipx} \ = \ e^{-ipx}\ f(x+i\frac{d}{dp}). \tag{2.55}$$

This can be easily proven by doing a Taylor series expansion of the function f. Therefore,

$$S(x,x;i\omega) \ = \ -\mathrm{Tr}_{\vec{p}}\ \frac{1}{-\not{p}+\sigma(x+i\frac{\partial}{\partial p})}\ . \tag{2.56}$$

Next the following two expansion equations are introduced:

$$\begin{aligned} f(x+i\frac{\partial}{\partial p}) \ &= \ \sum_{m=0}^{\infty}\frac{i^m}{m!}\left(\frac{\partial}{\partial x^{\mu_1}}\cdots\frac{\partial}{\partial x^{\mu_m}}f(x)\right)\frac{\partial^m}{\partial p_{\mu_1}\cdots\partial p_{\mu_m}} \\ &= \ f(x)+i(\partial_\mu f(x))\frac{\partial}{\partial p_\mu}-\frac{1}{2!}(\partial_\mu\partial_\nu f(x))\frac{\partial^2}{\partial p_\mu\partial p_\nu}+\ldots \end{aligned} \tag{2.57}$$

$$\begin{aligned} \frac{1}{X+Y} \ &= \ \sum_{m=0}^{\infty}\frac{1}{X}\left(-Y\frac{1}{X}\right)^m \\ &= \ \frac{1}{X}-\frac{1}{X}Y\frac{1}{X}+\frac{1}{X}Y\frac{1}{X}Y\frac{1}{X}+\ldots \end{aligned} \tag{2.58}$$

Equation (2.57) is the covariant Taylor series expansion for the function f about x, while equation (2.59) is an inverse operator series expansion where X and Y are operators. The choice of the separation of an operator into X and Y defines the nature of the expansion being made. With respect to (2.56), two useful choices are given below.

(i) For instance, to expand the interacting fermion Green function about the free field configuration, where $\sigma(x)=\sigma_0$ is simply the mass of the fermion, we let

$$\begin{aligned} X \ &= \ -\not{p}+\sigma_0, \\ Y \ &= \ \sigma(x+i\frac{\partial}{\partial p})-\sigma_0 \ \equiv \ \tilde{\sigma}(x+i\frac{\partial}{\partial p}). \end{aligned} \tag{2.59}$$

Then $-1/X=S_0(i\omega)$, the free fermion Green Function, and

$$\begin{aligned} S(x,x;i\omega) \ = \ \mathrm{Tr}_{\vec{p}}\Big(&S_0(i\omega)+S_0(i\omega)\ \tilde{\sigma}(x+i\frac{\partial}{\partial p})\ S_0(i\omega) \\ &+\ S_0(i\omega)\ \tilde{\sigma}(x+i\frac{\partial}{\partial p})\ S_0(i\omega)\ \tilde{\sigma}(x+i\frac{\partial}{\partial p})S_0(i\omega)\ +\ldots\Big). \end{aligned} \tag{2.60}$$

This form of the expansion will be useful for deriving the necessary counterterms in momentum space.

(ii) The derivative expansion is obtained by a slightly different choice of X and Y:

$$\begin{aligned} X &= -\not{p} + \sigma(x), \\ Y &= \sigma(x + i\frac{\partial}{\partial p}) - \sigma(x) \\ &= i(\partial_\mu \sigma(x))\frac{\partial}{\partial p_\mu} - \frac{1}{2!}(\partial_\mu \partial_\nu \sigma(x))\frac{\partial^2}{\partial p_\mu \partial p_\nu} + \ldots \end{aligned} \tag{2.61}$$

In fact both of the above expansions can be handled simultaneously. Before proceeding with the expansion we convert to a slightly different form of the Green function S. This is done to reduce the number of terms that must be kept in the inverse operator expansion (2.59), as well as to bring the spin structure to the numerator, which makes taking internal traces straightforward. We put

$$\begin{aligned} S(x,x;i\omega) &= -\langle x|\frac{1}{(-i\not{\partial} + \sigma(x))}|x\rangle \\ &= -\langle x|\frac{(i\not{\partial} + \sigma(x))}{(i\not{\partial} + \sigma(x))}\,\frac{1}{(-i\not{\partial} + \sigma(x))}|x\rangle \\ &= -\langle x|\frac{i\not{\partial} + \sigma(x)}{\partial^2 + \sigma^2(x) + i\,[\not{\partial}, \sigma(x)]}|x\rangle \;=\; \ldots \\ &= -\mathrm{Tr}_{\vec{p}}\left[\left(\not{p} + \sigma(x + i\frac{\partial}{\partial p})\right)\frac{1}{-p^2 + \sigma^2(x + i\frac{\partial}{\partial p}) + i\not{\partial}\sigma(x + i\frac{\partial}{\partial p})}\right], \end{aligned} \tag{2.62}$$

where $p^2 = p_0^2 - \vec{p}^{\,2} = -\omega^2 - \vec{p}^{\,2}$. Again we will make use of the expansion (2.59) for the inverse operator term. The two expansions (i) and (ii) can be obtained by setting:

	Counterterm Expn.	Derivative Expn.
$X:$	$-p^2 + \sigma_0^2$	$-p^2 + \sigma(x)^2$
$Y:$	$\sigma^2(x + i\frac{\partial}{\partial p}) - \sigma_0^2 + i\not{\partial}\sigma(x + i\frac{\partial}{\partial p})$	$\sigma^2(x + i\frac{\partial}{\partial p}) - \sigma(x)^2 + i\not{\partial}\sigma(x + i\frac{\partial}{\partial p})$

(2.63)

By using equation (2.57), the contributions in the Y term can be written as a series in momentum derivatives. To treat both cases in the table simultaneously, we work with the following notation:

$$\begin{aligned} X &\rightarrow \Delta^{-1} \\ Y &\rightarrow \left(A + B_\mu \frac{\partial}{\partial p_\mu} + C_{\mu\nu} \frac{\partial^2}{\partial p_\mu \partial p_\nu} + \mathcal{O}(\frac{d^3\sigma(x)}{dx^3}) + \ldots \right) \end{aligned} \tag{2.64}$$

where

$$\begin{aligned} \Delta &= \frac{1}{-p^2 + \sigma_0^2} \qquad \text{or} \qquad \Delta = \frac{1}{-p^2 + \sigma(x)^2} \\ A &= \sigma^2(x) - \sigma_0^2 + i\not{\partial}\sigma(x) \qquad \text{or} \qquad A = i\not{\partial}\sigma(x) \\ B_\mu &= 2i\sigma(x)\partial_\mu\sigma(x) - \gamma^\nu \partial_\nu \partial_\mu \sigma(x) \\ C_{\mu\nu} &= -\left(\partial_\mu\sigma(x)\right)\left(\partial_\nu\sigma(x)\right) - \sigma(x)\,\partial_\mu\partial_\nu\sigma(x) + \mathcal{O}(\frac{d^3\sigma(x)}{dx^3}) \end{aligned} \tag{2.65}$$

With this formulation only three terms in the inverse operator expansion must be retained to derive the counterterms and obtain the derivative expansion up to second order. To see this we can count powers of momentum and notice that the first convergent piece (under $\int d^4p$) has p^{-5} dependence. Terms beyond the third are of order p^{-6} or higher and are therefore not relevant to finding the counterterms. For the derivative expansion we see that each factor of Y contributes at least one derivative, so terms beyond the third (which has two Y's) are order (d^3/dx^3) and higher. In fact, due to the covariance of the expansion, only even numbers of derivatives appear, so that the next terms will be of order (d^4/dx^4).

Looking again at our definitions in (2.65) we see that Δ contains all of the p dependence. Spacetime derivatives of Δ can be taken easily, and to simplify our formula we will denote a p_μ derivative of Δ by Δ^μ. The coefficients $A, B_\mu, C_{\mu\nu}$ and the factor $\not{p} + \sigma(x + i\frac{\partial}{\partial p})$ contain the scalar field derivatives as well as the spinor matrix structure. Using equations (2.57), (2.59), and (2.64) in (2.62), we have

$$
\begin{aligned}
& S(x,x;i\omega) \\
&= -\mathrm{Tr}_{\vec{p}}\,\left(\not{p}+\sigma(x+i\frac{\partial}{\partial p})\right)\,\{\Delta-\Delta Y\Delta+\Delta Y\Delta Y\Delta+\ldots\} \\
&= -\mathrm{Tr}_{\vec{p}}\,\Big[\left(\not{p}+\sigma(x+i\frac{\partial}{\partial p})\right) \\
&\quad\times\Big\{\Delta-\ \Delta^2 A-\Delta\Delta^\mu B_\mu-\Delta\Delta^{\mu\nu}C_{\mu\nu}+\Delta^3A^2+\Delta^2\Delta^\mu AB_\mu \\
&\qquad +\Delta^2\Delta^{\mu\nu}AC_{\mu\nu}+\Delta(\Delta^2)^\mu B_\mu A+\Delta(\Delta^2)^{\mu\nu}C_{\mu\nu}A+\Delta(\Delta\Delta^\mu)^\nu B_\mu B_\nu\Big\} \\
&\quad +\mathcal{O}(\frac{d^3}{dx^3})\ \Big] \\
&= -\mathrm{Tr}_{\vec{p}}\Big[\\
&\quad(\not{p}+\sigma(x))\,\Big\{\Delta-\ \Delta^2 A-\Delta\Delta^\mu B_\mu-\Delta\Delta^{\mu\nu}C_{\mu\nu}+\Delta^3A^2+\Delta^2\Delta^\mu AB_\mu \\
&\qquad +\Delta^2\Delta^{\mu\nu}AC_{\mu\nu}+\Delta(\Delta^2)^\mu B_\mu A+\Delta(\Delta^2)^{\mu\nu}C_{\mu\nu}A+\Delta(\Delta\Delta^\mu)^\nu B_\mu B_\nu\Big\} \\
&\quad +(i\partial_\lambda\sigma(x))\,\Big\{\Delta^\lambda-(\Delta^2)^\lambda A-(\Delta\Delta^\mu)^\lambda B_\mu+(\Delta^3)^\lambda A^2 \\
&\qquad\qquad +(\Delta^2\Delta^\mu)^\lambda AB_\mu+(\Delta(\Delta^2)^\mu)^\lambda B_\mu A\Big\} \\
&\quad +(i\partial_\lambda\partial_\tau\sigma(x))\,\left\{\Delta^{\lambda\tau}-(\Delta^2)^{\lambda\tau}A+(\Delta^3)^{\lambda\tau}A^2\right\}\ +\ \mathcal{O}(\frac{d^3}{dx^3})\ \Big]\,. \qquad (2.66)
\end{aligned}
$$

Recall that the scalar field is time independent, so when the four-momenta that appear in the derivatives are contracted with the corresponding field derivatives they contribute only through the spacelike part. After simplifying the multiple p derivatives we can reduce the above equation by noting that under the momentum trace $\mathrm{Tr}_{\vec{p}}$ terms with odd powers of $\vec{p}$ vanish. Hence

$$
\begin{aligned}
& S(x,x;i\omega) \\
&= -\mathrm{Tr}_{\vec{p}}\Big[\\
&\quad \not{p}\,\Big\{\Delta-\ \Delta^2 A-\Delta\Delta^\mu B_\mu-\Delta\Delta^{\mu\nu}C_{\mu\nu}+\Delta^3A^2+3\Delta^2\Delta^\mu AB_\mu \\
&\qquad +3\Delta^2\Delta^{\mu\nu}AC_{\mu\nu}+2\Delta\Delta^\mu\Delta^\nu AC_{\mu\nu}+\Delta^2\Delta^{\mu\nu}B_\mu B_\nu+\Delta\Delta^\mu\Delta^\nu B_\mu B_\nu\Big\} \\
&\quad +\sigma(x)\,\Big\{\Delta-\ \Delta^2 A-\Delta\Delta^{\mu\nu}C_{\mu\nu}+\Delta^3A^2+\Delta^2\Delta^{\mu\nu}AC_{\mu\nu}+2\Delta^2\Delta^{\mu\nu}AC_{\mu\nu}
\end{aligned}
$$

$$
\begin{aligned}
&+2\Delta\Delta^{\mu}\Delta^{\nu}AC_{\mu\nu}+\Delta^{2}\Delta^{\mu\nu}B_{\mu}B_{\nu}+\Delta\Delta^{\mu}\Delta^{\nu}B_{\mu}B_{\nu}\Big\}\\
&+(i\partial_{\lambda}\sigma(x))\ \Big\{-\Delta^{\mu}\Delta^{\lambda}B_{\mu}-\Delta\Delta^{\mu\lambda}B_{\mu}+8\Delta\Delta^{\mu}\Delta^{\lambda}AB_{\mu}+3\Delta^{2}\Delta^{\mu\lambda}AB_{\mu}\Big\}\\
&+(i\partial_{\lambda}\partial_{\tau}\sigma(x))\ \Big\{\Delta^{\lambda\tau}-2\Delta^{\lambda}\Delta^{\tau}A-2\Delta\Delta^{\lambda\tau}A+6\Delta\Delta^{\lambda}\Delta^{\tau}A^{2}+3\Delta^{2}\Delta^{\lambda\tau}A^{2}\Big\}\\
&+\mathcal{O}(\frac{d^{3}}{dx^{3}})\ \Big]\ . \qquad (2.67)
\end{aligned}
$$

From this equation we can derive the general expansions for both the energy and the density using equations (2.50) and (2.53).

2.3.3 Energy and density expansions

For the energy (2.50), we see that by incorporating the ω integral into the trace we have an overall four-momentum trace of the form $\mathrm{Tr}_{p,x}\ (\omega\,\gamma_0 S(i\omega))$. Consider the reduction caused by the internal trace here. This can easily be done by recalling some well known trace theorems for the gamma matrices [7]:

$$
\begin{aligned}
\gamma_{\mu}\gamma_{\nu}+\gamma_{\nu}\gamma_{\mu} &= 2g_{\mu\nu}, && (2.68)\\
\mathrm{tr}(\gamma_{\mu 1}\cdots\gamma_{\mu n}) &= 0 \qquad (n \text{ odd}), && (2.69)\\
\mathrm{tr}(\gamma_{\mu}\gamma_{\nu}) &= Dg_{\mu\nu}. && (2.70)
\end{aligned}
$$

The γ matrices that appear in the coefficients $A, B_{\mu}, C_{\mu\nu}$ do not include γ_0 because this matrix appears multiplied by the vanishing time derivative of the scalar field. The trace of γ_0 times any number of γ_i $(i = 1, 2, 3)$ vanishes so these terms cannot contribute to the trace. The only remaining terms come from the $i\omega$ part of the $\not{p}$ terms. These are further reduced by the fact that some of the terms are now odd with respect to $\vec{p}$. The remaining contributions come from the following terms

$$
\begin{aligned}
E_{vac} &= -i\,\mathrm{Tr}^{int}_{p,x}\ \omega\,\gamma_0\,S(x,x;i\omega)\\
&= \mathrm{Tr}^{int}_{p,x}\ \omega^{2}\Big[\Delta-\ \Delta^{2}A'+\Delta^{3}(A^{2})'-\Delta\Delta^{\mu\nu}C'_{\mu\nu}+3\Delta^{2}\Delta^{\mu\nu}(AC_{\mu\nu})'\\
&\qquad +2\Delta\Delta^{\mu}\Delta^{\nu}(AC_{\mu\nu})'+\Delta^{2}\Delta^{\mu\nu}(B_{\mu}B_{\nu})'+\Delta\Delta^{\mu}\Delta^{\nu}(B_{\mu}B_{\nu})'\Big]. \qquad (2.71)
\end{aligned}
$$

The prime here denotes the parts of the coefficient(s) with an even number of gamma matrices.

Now consider the scalar density. Including the ω integral as part of the momentum trace we see from equation (2.53) that the density involves the factor $\mathrm{Tr}_p\ S(i\omega)$. The expression (2.67) can be reduced under this trace by vanishing internal traces as well as factors that are odd in $\vec{p}$. The remaining terms are

$$\begin{aligned}
\rho^s_{vac}(x) &= -\mathrm{Tr}^{int}_p\ S(x,x;i\omega) \\
&= -\mathrm{Tr}^{int}_p\Big[\\
&\quad \not{p}\left\{-\Delta\Delta^\mu B_\mu + 3\Delta^2\Delta^\mu A B_\mu + 3\Delta^2\Delta^{\mu\nu} A C_{\mu\nu} + 2\Delta\Delta^\mu\Delta^\nu A C_{\mu\nu}\right\} \\
&\quad +\sigma(x)\Big\{\Delta - \ \Delta^2 A' + \Delta^3 (A^2)' - \Delta\Delta^{\mu\nu} C_{\mu\nu}{}' + \Delta^2\Delta^{\mu\nu}(AC_{\mu\nu})' \\
&\qquad\qquad +2\Delta^2\Delta^{\mu\nu}(AC_{\mu\nu})' + 2\Delta\Delta^\mu\Delta^\nu(AC_{\mu\nu})' \\
&\qquad\qquad +\Delta^2\Delta^{\mu\nu}(B_\mu B_\nu)' + \Delta\Delta^\mu\Delta^\nu(B_\mu B_\nu)'\Big\} \\
&\quad +(i\partial_\lambda\sigma(x))\Big\{-\Delta^\mu\Delta^\lambda B_\mu{}' - \Delta\Delta^{\mu\lambda} B_\mu{}' + 8\Delta\Delta^\lambda\Delta^\mu(AB_\mu)' \\
&\qquad\qquad +3\Delta^2\Delta^{\mu\lambda}(AB_\mu)'\Big\} \\
&\quad +(i\partial_\lambda\partial_\tau\sigma(x))\Big\{\Delta^{\lambda\tau} - 2\Delta^\lambda\Delta^\tau A' - 2\Delta\Delta^{\lambda\tau} A' \\
&\qquad\qquad +6\Delta\Delta^\lambda\Delta^\tau(A^2)' + 3\Delta^2\Delta^{\lambda\tau}(A^2)'\Big\} \\
&\quad +\mathcal{O}(\frac{d^3}{dx^3})\Big]\ .
\end{aligned} \tag{2.72}$$

The prime again denotes the part of the coefficient that has an even number of gamma matrices.

To go further we must insert a form for the coefficients. We choose to insert the counterterm form of the coefficients, as it will be a simple exercise to obtain the derivative expansion form from the resulting equations, so that we then have both expansions. We note that since

$$\Delta = \Delta_0 = \frac{1}{(-p^2 + \sigma_0^2)}\ , \tag{2.73}$$

we have

$$\Delta^\mu = 2p^\mu \Delta^2. \tag{2.74}$$

Using this expression to evaluate derivatives, and taking all internal traces, we find the following form upon grouping like terms:

$$\begin{aligned}
E_{vac} \;=\; & \mathrm{Tr}_{p,x}\; D\; \omega^2 \Big[\\
& \Big\{ \Delta_0 - (\sigma^2(x) - \sigma_0^2)\; \Delta_0^2 + (\sigma^2(x) - \sigma_0^2)^2\; \Delta_0^3 + \ldots \Big\} \\
& \\
& + \sigma(x)(\partial_\mu \partial_\nu \sigma(x)) \Big\{ \Big(\; 8p^\mu p^\nu\; \Delta_0^4 + 2g^{\mu\nu}\; \Delta_0^3 \;\Big) \\
& \qquad + (\sigma^2(x) - \sigma_0^2) \Big(\; 32p^\mu p^\nu\; \Delta_0^5 + 6g^{\mu\nu}\; \Delta_0^4 \Big) + \ldots \Big\} \\
& \\
& + (\partial_\mu \sigma(x))(\partial_\nu \sigma(x)) \Big\{ \Big(8p^\mu p^\nu \Delta_0^4 + g^{\mu\nu} \Delta_0^3 \Big) \\
& \qquad - 4\sigma^2(x) \Big(12 p^\mu p^\nu \Delta_0^5 + 2 g^{\mu\nu} \Delta_0^4 \Big) \\
& \qquad - (\sigma^2(x) - \sigma_0^2) \Big(32 p^\mu p^\nu \Delta_0^5 + 6 g^{\mu\nu} \Delta_0^4 \Big) \Big\} \Big] \,,
\end{aligned} \tag{2.75}$$

$$\begin{aligned}
\rho^s_{vac}(x) = -\mathrm{Tr}_p\; D \Big[\\
\Big\{ \sigma(x)\; \Delta_0 - \sigma(x)(\sigma^2(x) - \sigma_0^2)\; \Delta_0^2 + \sigma(x)(\sigma^2(x) - \sigma_0^2)^2\; \Delta_0^3 + \ldots \Big\} \\
& \\
+ (\partial_\mu \partial_\nu \sigma(x)) \Big\{ - \Big(2p^\mu p^\nu\; \Delta_0^3 + g^{\mu\nu}\; \Delta_0^2 \Big) + \sigma^2(x) \Big(8p^\mu p^\nu\; \Delta_0^4 + 2g^{\mu\nu}\; \Delta_0^3 \Big) \\
\qquad + (\sigma^2(x) - \sigma_0^2) \Big(6p^\mu p^\nu\; \Delta_0^4 + 2g^{\mu\nu}\; \Delta_0^3 \Big) + \ldots \Big\} \\
& \\
+ (\partial_\mu \sigma(x))(\partial_\nu \sigma(x)) \Big\{ \sigma(x) \Big(20 p^\mu p^\nu\; \Delta_0^4 + 5 g^{\mu\nu}\; \Delta_0^3 \Big) \\
\qquad - \sigma^3(x) \Big(48 p^\mu p^\nu\; \Delta_0^5 + 8 g^{\mu\nu}\; \Delta_0^4 \Big) \\
\qquad - \sigma(x)(\sigma^2(x) - \sigma_0^2) \Big(128 p^\mu p^\nu\; \Delta_0^5 + 17 g^{\mu\nu}\; \Delta_0^4 \Big) \Big\} \Big] \,.
\end{aligned} \tag{2.76}$$

The form of these equations can now be simplified using various transformations that are valid under the momentum space trace. We must proceed with caution,

however, as making use of a transformation under the ω part of this trace will affect the convergence when a finite cutoff is placed on this integral. Any transformation that vanishes under the $\vec{p}$ trace will affect the termwise form of any partial wave expansion. This dependence will in fact allow us to consider which form converges the most rapidly. For purpose of illustration we consider the density. The first thing to note is that none of the terms p^μ will have an energy part contributing because the time derivative of the scalar field $\partial_0 \sigma(x)$ vanishes. This allows us to reduce the dependence $p^\mu p^\nu$ as follows:

$$\begin{aligned} \mathrm{Tr}_p(p^\mu p^\nu \ \Delta^n) &= g^{\mu i} \ g^{\nu j} \ \mathrm{Tr}^p(p_i \ p_j \ \Delta^n) \\ &= g^{\mu i} g^{\nu j} \ \frac{\delta_{ij}}{D-1} \mathrm{Tr}_p(\vec{p}^{\,2} \Delta^n) \\ &= -\frac{g^{\mu\nu}}{D-1} \ \mathrm{Tr}_p(\vec{p}^{\,2} \Delta^n). \end{aligned} \tag{2.77}$$

To make the partial wave expansion, we will find that it is useful to remove the $\vec{p}^{\,2}$ dependence from the numerator. This may be done by noting that

$$\vec{p}^{\,2} = (\Delta)^{-1} - \omega^2 - \sigma^2. \tag{2.78}$$

The equation for the density is then

$$\begin{aligned} \rho^s_{vac}(x) = -\mathrm{Tr}_p \ D \Big[& \\ & \Big\{ \sigma(x) \ \Delta - \sigma(x)(\sigma^2(x) - \sigma_0^2) \ \Delta^2 + \sigma(x)(\sigma^2(x) - \sigma_0^2)^2 \ \Delta^3 + \ldots \Big\} \\ & \\ & + (\partial^2 \sigma(x)) \Big\{ - \Big(\frac{1}{3}\Delta^3 + \frac{2}{3}(\omega^2 + \sigma^2(x))\Delta^3 \Big) - \frac{2}{3}\sigma^2(x) \Big(\Delta^3 - 4(\omega^2 + \sigma^2(x))\Delta \Big) \\ & \qquad + 2(\sigma^2(x) - \sigma_0^2) \Big((\omega^2 + \sigma^2(x))\Delta^4 \Big) + \ldots \Big\} \\ & \\ & + (\partial_\mu \sigma(x))^2 \Big\{ -\frac{5}{3}\sigma(x) \Big(\Delta^3 - 4(\omega^2 + \sigma^2(x))\Delta^4 \Big) \\ & \qquad + 8\sigma^3(x) \Big(\Delta^4 - 2(\omega^2 + \sigma^2(x))\Delta^5 \Big) \\ & \qquad + \frac{1}{3}\sigma(x)(\sigma^2(x) - \sigma_0^2) \Big(77\Delta^4 - 128(\omega^2 + \sigma^2(x))\Delta^5 \Big) \Big\} \Big] \ . \end{aligned} \tag{2.79}$$

So far we have done nothing to affect the convergence with cutoff or partial wave. We now consider a reduction that affects the partial waves but not the cutoff. Effectively what we do is to add the total divergence of a function under the $\vec{p}$ integral where the function is such that it vanishes at infinity. Although this term makes no net contribution, it's individual partial wave contributions may be nonzero. This mechanism may be implemented by letting

$$(\omega^2 + \sigma^2)\Delta^n = \Delta^{n-1} - \vec{p}^{\,2}\Delta^n, \tag{2.80}$$

and then taking

$$\int d^n p \frac{(\vec{p}^{\,2})^\beta}{(\vec{p}^{\,2} + M^2)^\alpha} = \frac{(n + 2\beta - 2)}{2(\alpha - 1)} \int d^n p \frac{1}{(\vec{p}^{\,2} + M^2)^{\alpha-1}} \ , \tag{2.81}$$

where the integral is over the n dimensional Euclidean $\vec{p}^{\,2}$. This gives us

$$\begin{aligned}
\rho^s_{vac}(x) = -\mathrm{Tr}_p \ D\Big[& \\
& \Big\{\sigma(x)\ \Delta_0 \ - \ \sigma(x)(\sigma^2(x) - \sigma_0^2)\ \Delta_0^2 \ + \ \sigma(x)(\sigma^2(x) - \sigma_0^2)^2\ \Delta_0^3 \ + \ldots\Big\} \\
& + (\partial^2\sigma(x)) \left\{-\frac{1}{2}\Delta_0^2 + \frac{2}{3}\sigma^2(x)\Delta_0^3 \ + \ (\sigma^2(x) - \sigma_0^2)\ \Delta_0^3 \ + \ldots\right\} \\
& + (\partial_\mu\sigma(x))^2 \left\{\frac{5}{3}\ \sigma(x)\Delta_0^3 - 2\sigma^3(x)\ \Delta_0^4 - \sigma(x)(\sigma^2(x) - \sigma_0^2)\Delta_0^4\right\} \Big] \ .
\end{aligned} \tag{2.82}$$

The purpose of the manipulations between (2.79) and (2.82) should be, however, to maximize the convergence of the partial wave series. It will be seen in the next section that in fact the expression (2.82) is the most useful. The purpose of these manipulations has been simply to allow us to consider other forms. In particular, once this choice has been established we see that expression (2.82) could have been obtained in a much simpler manner by simply using the following formula

$$\int d^d k \ \frac{k^i k^j}{(\omega^2 + k^2 + M^2)^\alpha} = \frac{\delta^{\,ij}}{2(\alpha - 1)} \int d^d k \ \frac{1}{(\omega^2 + k^2 + M^2)^{\alpha-1}}. \tag{2.83}$$

to reduce the form of the spatial part of the p integrals in (2.76).

It is important to note that we are not making use of the ω part of the p integration, so this reduction again affects only the partial waves. Also, as the energy contractions

vanish, formula (2.83) can be implemented by letting

$$\frac{p^\mu p^\nu}{(-p^2+M^2)^\alpha} \to -\frac{g^{\mu\nu}}{2(\alpha-1)}\ \frac{1}{(-p^2+M^2)^{\alpha-1}}. \tag{2.84}$$

Applying this shortcut to the energy expression (2.75) gives

$$\begin{aligned} E_{vac} &= \mathrm{Tr}_{p,x}\ D\ \omega^2\Big[\\ &\quad \Big\{\Delta_0 - (\sigma^2(x)-\sigma_0^2)\Delta_0^2 + (\sigma^2(x)-\sigma_0^2)^2\ \Delta_0^3 + \ldots\Big\} \\ &\quad +\sigma(x)(\partial^2\sigma(x))\left\{\frac{2}{3}\Delta_0^3 + 2(\sigma^2(x)-\sigma_0^2)\ \Delta_0^4 + \ldots\right\} \\ &\quad +(\partial_\mu\sigma(x))^2\Big\{-\frac{1}{3}\Delta_0^3 - 2\sigma^2(x)\Delta_0^4 - 2(\sigma^2(x)-\sigma_0^2)\Delta_0^4\Big\}\ \Big]\ . \end{aligned} \tag{2.85}$$

2.3.4 Counterterms

To see which of the terms in the expressions (2.82) and (2.85) are divergent, we can count powers of p and consider whether the integral over all p space will converge in the dimension we are considering. Alternatively we can make use of the following formulas (see [3] for method of derivation):

$$\frac{1}{(2\pi)^D}\int d^Dp \frac{\omega^2}{(-p^2+M^2)^\alpha} = \frac{-i(-1)^\alpha\pi^{-D/2}}{2M^{2\alpha-D-2}}\ \frac{\Gamma(\alpha-1-D/2)}{\Gamma(\alpha)}\ , \tag{2.86}$$

$$\frac{1}{(2\pi)^D}\int d^Dp \frac{1}{(-p^2+M^2)^\alpha} = \frac{i(-1)^\alpha\pi^{-D/2}}{M^{2\alpha-D}}\ \frac{\Gamma(\alpha-D/2)}{\Gamma(\alpha)} \tag{2.87}$$

Terms that may diverge in 4 or fewer dimensions are

$$\begin{aligned} E_{vac} &= -\frac{i}{2}\ D\ \pi^{-D/2}\ M^{D+2}\ \mathrm{Tr}_x\Big[\\ &\quad \left\{\frac{-\Gamma(-D/2)}{M^2} - (\sigma^2(x)-\sigma_0^2)\frac{\Gamma(1-D/2)}{M^4} - (\sigma^2(x)-\sigma_0^2)^2\frac{\Gamma(2-D/2)}{2M^6}\right\} \\ &\quad +\sigma(x)(\partial^2\sigma(x))\left\{-\frac{\Gamma(2-D/2)}{3M^6}\right\} + (\partial_\mu\sigma(x))^2\left\{\frac{\Gamma(2-D/2)}{6M^6}\right\}\ \Big]\ , \end{aligned} \tag{2.88}$$

$$\begin{aligned} \rho^s_{vac}(x) &= -i\ D\ \pi^{-D/2}\ M^D\Big[\\ &\quad \left\{-\sigma(x)\frac{\Gamma(1-D/2)}{M^2} - \sigma(x)(\sigma^2(x)-\sigma_0^2)\frac{\Gamma(2-D/2)}{M^4}\right\} \\ &\quad +(\partial^2\sigma(x))\left\{-\frac{\Gamma(2-D/2)}{2M^4}\right\}\ \Big]\ . \end{aligned} \tag{2.89}$$

Divergent terms are then the terms where a Γ function will be evaluated at a pole. If we regularize our expressions under the p integral, the terms that must be included in the counter term expression are the terms in (2.85) and (2.82) that correspond to the divergent terms in (2.88) and (2.89). Depending on the renormalization scheme, other finite terms may also be included in the subtraction. The mechanism for determining a scheme is simply to make our expressions reduce to those which satisfy the appropriate relations placed upon the coefficients in equation (2.3). This reduction is accomplished by evaluating the renormalized momentum integral.

2.3.5 Derivative expansion expressions

Looking back at (2.64) we see that expressions for the derivative expansion can easily be determined from the above counterterm equations by simply replacing $(-p^2+\sigma_0^2)$ with $(-p^2+\sigma^2(x))$ and removing all factors containing $(\sigma^2(x)-\sigma_0^2)$. From (2.85) and (2.82) we have

$$\begin{aligned} E_{vac} &= \mathrm{Tr}_{p,x}\ D\ \omega^2\ \Big[\frac{1}{(-p^2+\sigma^2(x))}+\frac{2}{3}\frac{\sigma(x)\partial^2\sigma(x)}{(-p^2+\sigma^2(x))^3} \\ &\qquad -\frac{1}{3}\frac{(\partial_\mu\sigma(x))^2}{(-p^2+\sigma^2(x))^3}-2\frac{\sigma^2(x)(\partial_\mu\sigma(x))^2}{(-p^2+\sigma^2(x))^4}\Big], \qquad (2.90) \\ \rho^s_{vac}(x) &= -\mathrm{Tr}_p\ D\ \Big[\frac{\sigma(x)}{(-p^2+\sigma(x)^2)}-\frac{1}{2}\frac{\partial^2\sigma(x)}{(-p^2+\sigma(x)^2)^2}+\frac{2}{3}\frac{\sigma^2(x)\partial^2\sigma(x)}{(-p^2+\sigma(x)^2)^3} \\ &\qquad +\frac{5}{3}\frac{\sigma(x)(\partial_\mu\sigma(x))^2}{(-p^2+\sigma(x)^2)^3}-2\frac{\sigma^3(x)(\partial_\mu\sigma(x))^2}{(-p^2+\sigma(x)^2)^4}\Big\}\ \Big]\ . \qquad (2.91) \end{aligned}$$

These expressions agree with [19, 21] in $1+1$ dimensions, and in $3+1$ dimensions the energy agrees with the results of [23, 24]. The new expression here is that for the $3+1$ dimension density in momentum space.

2.4 Termwise convergence

In this section we evaluate the momentum integrals obtained above. When this is done, we regain the original expressions which we quoted in section 2.1. The results

obtained will agree with any other method that may have been used to derive the DE energy and density. Our purpose here is to consider the termwise convergence of our derivative expansion expressions for the energy and the density in $3+1$ dimensions. The direct derivative expansion for the energy can be evaluated by choosing the counterterms that correspond to the $3+1$ dimensional divergences in (2.88) and subtracting them from (2.90). We obtain a result for which the p trace can be evaluated and which agrees with the value given in section (2.1) with the choice:

$$f_0 = 0, \quad f_1 = 2, \quad f_2 = -7, \quad f_3 = 6, \quad f_4 = -\frac{3}{2}. \tag{2.92}$$

Including the fourth order derivative terms from section (2.1), and writing the energy grouped in orders of the derivatives, we have

$$\begin{aligned}
E_{vac}(\sigma) &= E_0(\sigma) + E_2(\sigma) + E_4(\sigma), && (2.93)\\
E_0 &= \mathrm{Tr}_{\vec{x}}\ \frac{-1}{16\pi^2}\left(\sigma^4\ \ln(\frac{\sigma^2}{\sigma_0^2}) - \frac{1}{2}(3\sigma^2 - \sigma_0^2)(\sigma^2 - \sigma_0^2)\right), && (2.94)\\
E_2 &= \mathrm{Tr}_{\vec{x}}\ \frac{-1}{16\pi^2}\ \ln(\frac{\sigma^2}{\sigma_0^2})(\nabla\sigma)^2, && (2.95)\\
E_4 &= \mathrm{Tr}_{\vec{x}}\ \frac{-1}{160\pi^2}\left(\frac{(\nabla^2\sigma)^2}{\sigma^2} - \frac{11(\nabla\sigma)^2(\nabla^2\sigma)}{9\sigma^3} + \frac{11(\nabla\sigma)^4}{18\sigma^4}\right), && (2.96)
\end{aligned}$$

where $\sigma = \sigma(x)$. Note that the method of renormalization is such that

$$E_0(\sigma_0) = 0, \qquad \frac{dE_0(\sigma_0)}{d\sigma} = 0, \qquad \frac{d^2E_0(\sigma_0)}{d^2\sigma} = 0, \qquad E_2(\sigma_0) = 0. \tag{2.97}$$

The derivative expansion for the density can be evaluated by subtracting the counterterms corresponding to those in (2.89) from (2.91). A finite term given by the term in (2.82) with $\sigma^2(x)\partial^2\sigma(x)$ dependence is also subtracted. By doing this we will see that our expressions agree up to second order with the ones found by applying equation (2.25) or (2.51) to the energy. As the fourth order derivative term is not subject to renormalization and all traces have been performed, we can obtain the fourth order density term from the energy by using equation (2.25) or (2.51):

$$\rho^s_{vac}(r) = \rho_0(r) + \rho_2(r) + \rho_4(r), \tag{2.98}$$

$$\rho_0(r) = -\frac{1}{4\pi^2}\left(\sigma^3\,\ln(\frac{\sigma^2}{\sigma_0^2}) - \sigma^3 + \sigma\sigma_0^2\right), \tag{2.99}$$

$$\rho_2(r) = \frac{1}{8\pi^2}\left(\frac{(\nabla\sigma)^2}{\sigma} + \nabla^2\sigma\,\ln(\frac{\sigma^2}{\sigma_0^2})\right), \tag{2.100}$$

$$\begin{aligned}\rho_4(r) = -\frac{1}{80\pi^2\sigma^2}\Big(&\nabla^4\sigma - \frac{4\nabla\sigma\cdot\nabla(\nabla^2\sigma)}{\sigma} - \frac{16(\nabla^2\sigma)^2}{9\sigma} \\ &-\frac{11(\partial^2\sigma/\partial^2 r)^2}{9\sigma} + \frac{43(\nabla\sigma)^2(\nabla^2\sigma)}{9\sigma^2} \\ &+\frac{44(\nabla\sigma)^2(\partial^2\sigma/\partial^2 r)}{9\sigma^2} - \frac{11(\nabla\sigma)^4}{3\sigma^3}\Big).\end{aligned} \tag{2.101}$$

Note that the terms in $\rho_4(r)$ with second derivatives of r appear from covariant expressions like $(\partial_\mu\partial_\nu\sigma)^2$ etc. All operators ∇ are derivatives with respect to r, and all operators ∇^2 indicate the radial part of the Laplacian.

We could now put the coupling explicitly back into these expressions for the energy and density. However, we find it more useful to simply rescale these equations in terms of the free field mass, $M = g\,\sigma_0$, so that all quantities are dimensionless and explicitly coupling free:

$$\sigma(x)' = \frac{\sigma(x)}{\sigma_0}, \qquad\qquad x' = x\sigma_0. \tag{2.102}$$

With this choice our energy is expressed in units of M^4 and density in units of M^3. Also, the explicit dependence on the coupling has been folded into the x' variable and will thus only appear in the rescaled field as $\sigma'(x) \to \sigma'(x')$. (The rescaling in (2.102) may be implemented by simply setting $g\sigma_0 = 1$.) To test the convergence of these derivative expansions we pick a representative analytic form for the field. We choose a spherically symmetric field potential, $\sigma'(r)$, which has a form similar to that of a shifted hyperbolic secant:

$$\sigma(r) = \sigma_0 - \frac{a(1+f)}{e^{b\,r^n} + f e^{-b\,r^n}} \quad \to \quad \sigma'(r') = 1 - \frac{a'(1+f)}{e^{b'\,r'^n} + f e^{-b'\,r'^n}}\ , \tag{2.103}$$

where $a' = a$ and $b' = b/(g\sigma_0)^n$ are positive numbers, and n is an integer greater than 0. Note that $\sigma'(0) = 0$ in all cases ($n \geq 1$) and that $\sigma'(r \to \infty) = 1$. This choice of

boundary conditions ensures that our field σ remains smooth at $r = 0$, and decays to a constant value at infinity (the fermion mass). The effect of the parameters in (2.103) are that

- a' controls the depth of the potential at the origin,
- b' affects the width and maximum slope of the potential,
- n controls how long the potential remains flat near the origin,
- f affects the "slope" of this flat piece near the origin.

From the definition of b' we see an implicit dependence on the coupling g. For a fixed background field, increasing g effectively decreases b' and therefore gives a potential with larger radius of effect. As g is a coupling this behavior is as expected. The parameter f is included to make the Laplacian of the potential nonzero at $r' = 0$. The interesting case is where $n = 2$, as

$$\nabla^2 \sigma'(r' = 0) = \frac{12ab(1-f)}{(1+f)}. \tag{2.104}$$

For the purposes of the figures in this section, g was fixed at a value of 25. As mentioned, a different value of g amounts to a redefinition of the given b's.

We begin by examining how the terms in the energy contribute as compared to those in the density. For this purpose we look at the value of the density at the origin $r = 0$. In figure 2.3 we see that for the energy the expansion appears to be convergent for all a whereas for the density it definitely is not. Notice that the expansion is increasingly divergent as we increase the depth of the potential.

This behavior of the energy versus the density is of fundamental importance to remember when solving the Euler-Lagrange equations. In this case it is the density which is the quantity of interest. Even though we are minimizing the energy functional

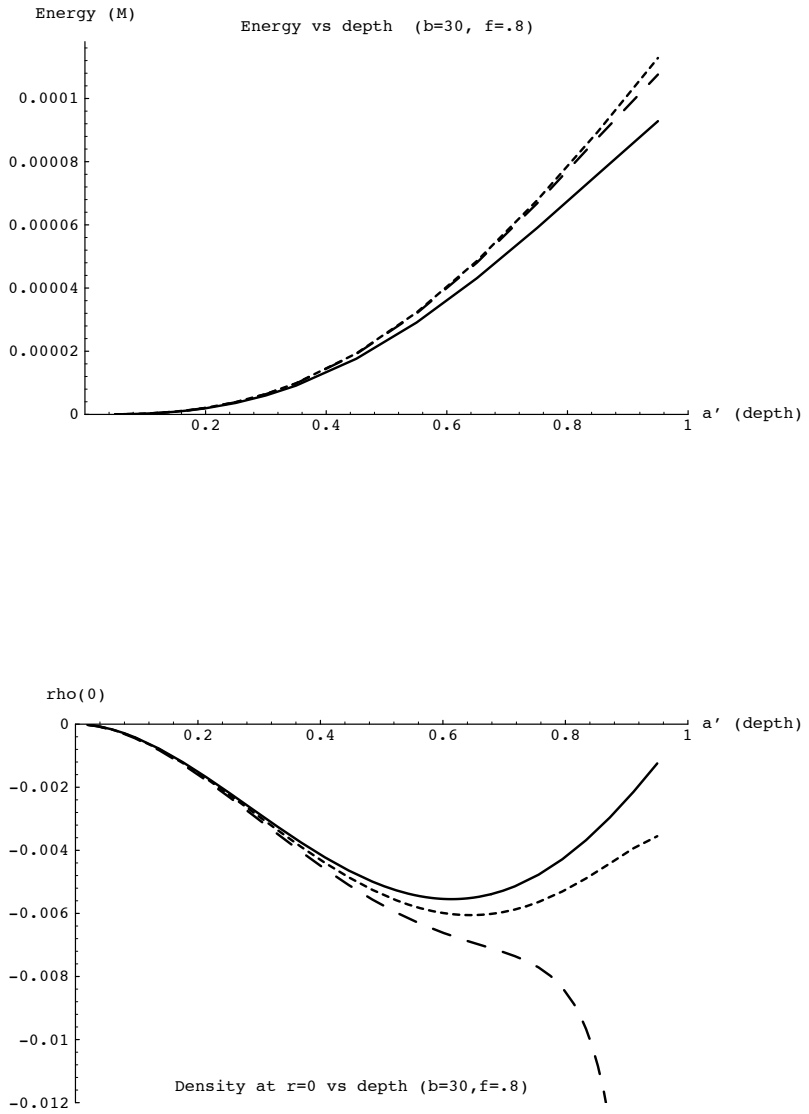

Figure 2.3: Comparison of the energy and density DE versus depth of the scalar background potential. The solid line is LDA, small dashes are DE to 2nd order and large dashes include the DE 4th order term.

by our choice of scalar field, to do so in an exact manner we must solve the equations of motion which involve the density. We now confine our interest to the density terms.

In figure 2.4 we consider the termwise behavior for potentials of different width and fixed $a = .5$. Small values of b give convergent behavior in a similar manner to what was found for small values of a. In the figure the plots shown are concentrated in the region of small widths (large b). At the origin the behavior is predictable, with steeper potentials having larger and larger contributions from the higher derivatives. At a nonzero value of r, increasing b is effectively pushing this point from a location on the flat part of the potential near the origin, up the steep boundary and then into the asymptotic region. Here this has been done for the point $r = .1$, which is fairly close to the origin. Notice that for smaller b the DE shows oscillatory convergence, but that this behavior disappears as our point moves out. In the asymptotic region the dominant contribution is that of the fourth order derivative terms.

To complete the analysis of our potential parameters we give plots of the density at a fixed spatial point versus n and f, figure 2.5. The depth and width are fixed at the reasonable values $a = .5$ and $b = 30$. In the first plot we see a similar effect for n as was seen for parameter b at $r = .1$. The points with $n \geq 2$ are on the flat part at the bottom of the potential, while smaller n start up the slope. Looking at the f plot, we see the value of f can completely control how different terms in the DE contribute to $\rho^s_{vac}(r = 0)$. A value $f = 1$ makes derivatives of second and higher order zero at the origin, so that the 4th and higher DE terms can not contribute. Smaller values of f make the flat piece of the potential at the origin slightly convex, while larger values of f make it concave. We will favor a value of $f = .8$ for our fixed backgrounds as giving representative behavior while not suppressing the effects of higher derivatives.

Finally, consider the shape of the entire vacuum density $\rho^s_{vac}(r)$. An interesting question is what effect the width of our potential has on the termwise convergence at various points. In figures 2.6 and 2.7 we see three plots of $\rho^s_{vac}(r)$ versus r. As

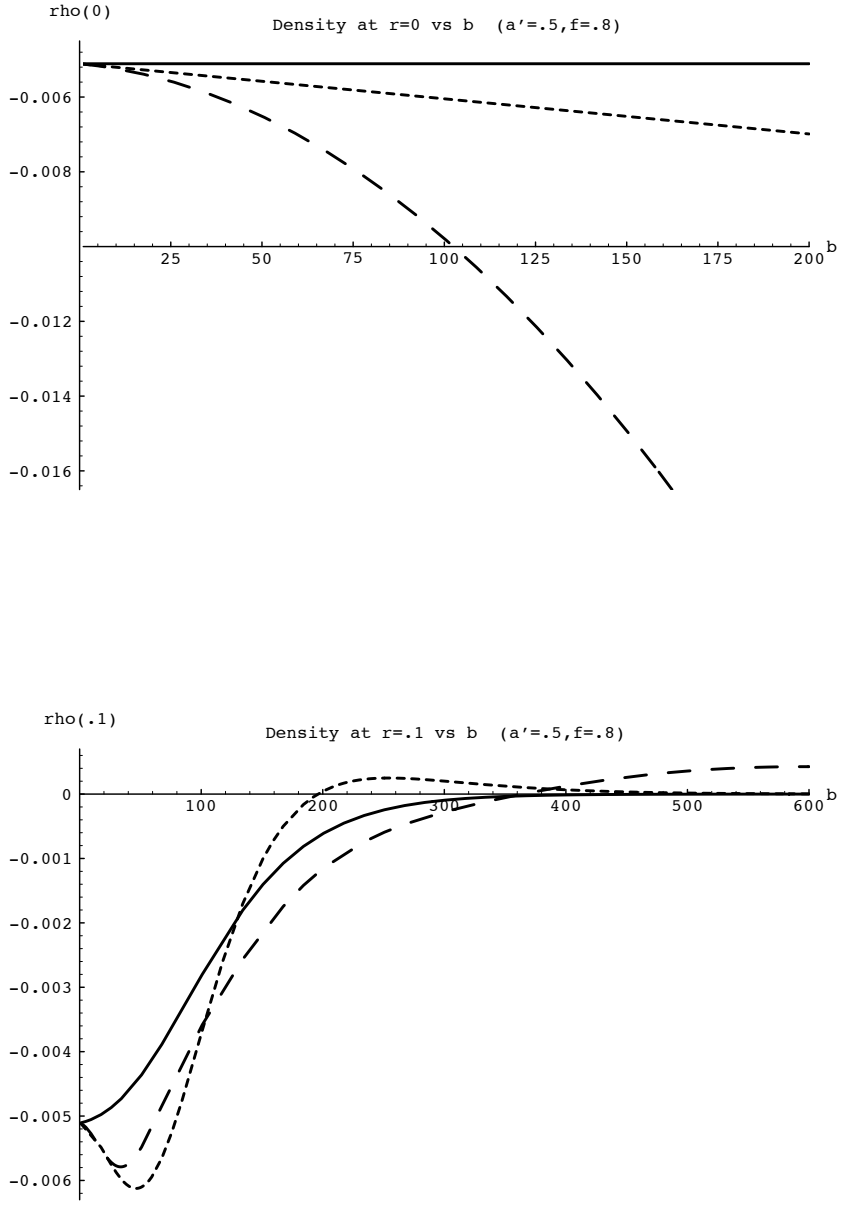

Figure 2.4: Density at the fixed values $r = 0, 0.1$ versus width parameter b.

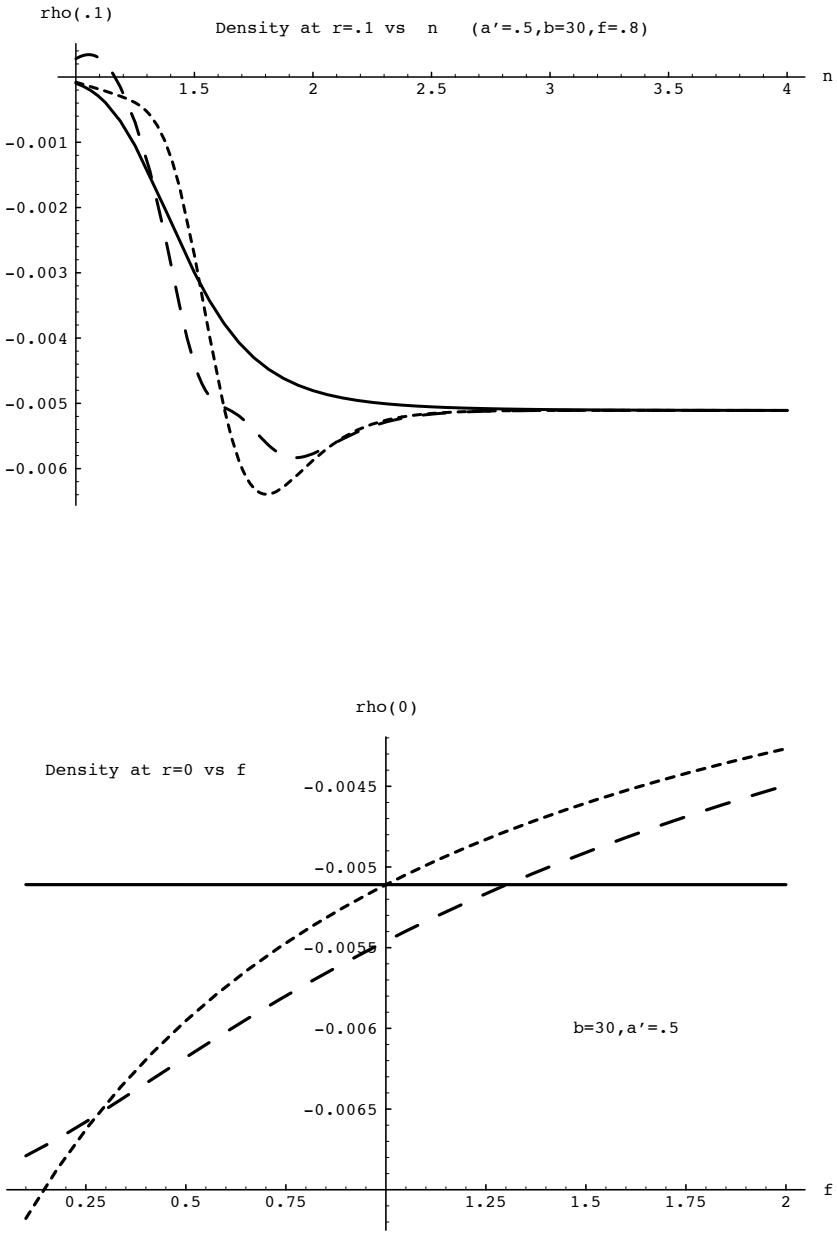

Figure 2.5: The density at the origin for the parameters n and f in our background potential.

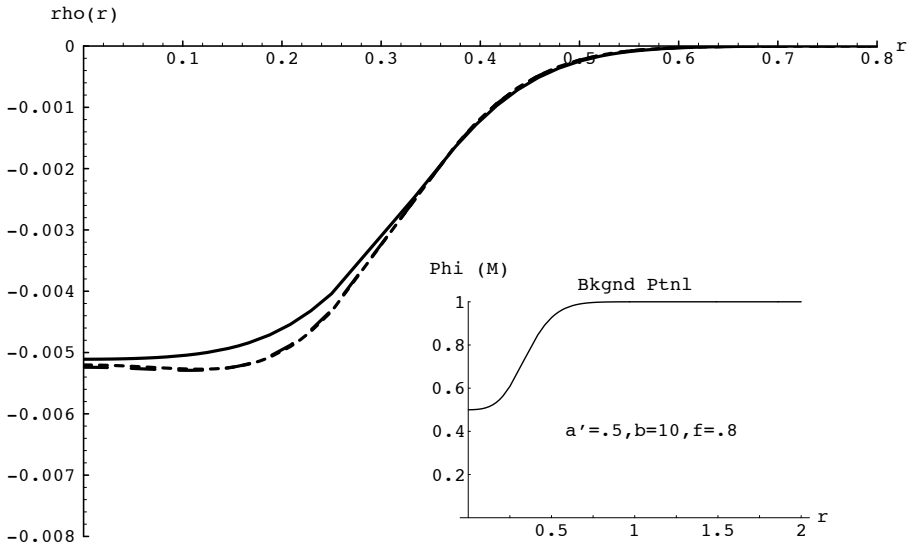

Figure 2.6: DE density terms for a background where the DE converges at all points.

the width is decreased higher derivative terms contribute substantially to the vacuum density at the origin. In the $b = 30$ plot of figure 2.7 the 2nd order expansion is still qualitatively correct. For higher b we definitely need more terms.

We may also ask what effect the potential depth has on the pointwise convergence. Starting with the parameters of figure 2.6 and increasing a we see in figure 2.8 that again the higher order terms contribute near the origin. Notice that keeping only the 2nd order terms gives an anomalous parabolic form which is removed at 4th order. In this case we are on the borderline of being able to see what the vacuum density looks like using only the derivative expansion.

Finally, in figure 2.9 the potential is taken to be a very deep well. Note the interesting appearance of a local maximum and two minima in the density structure

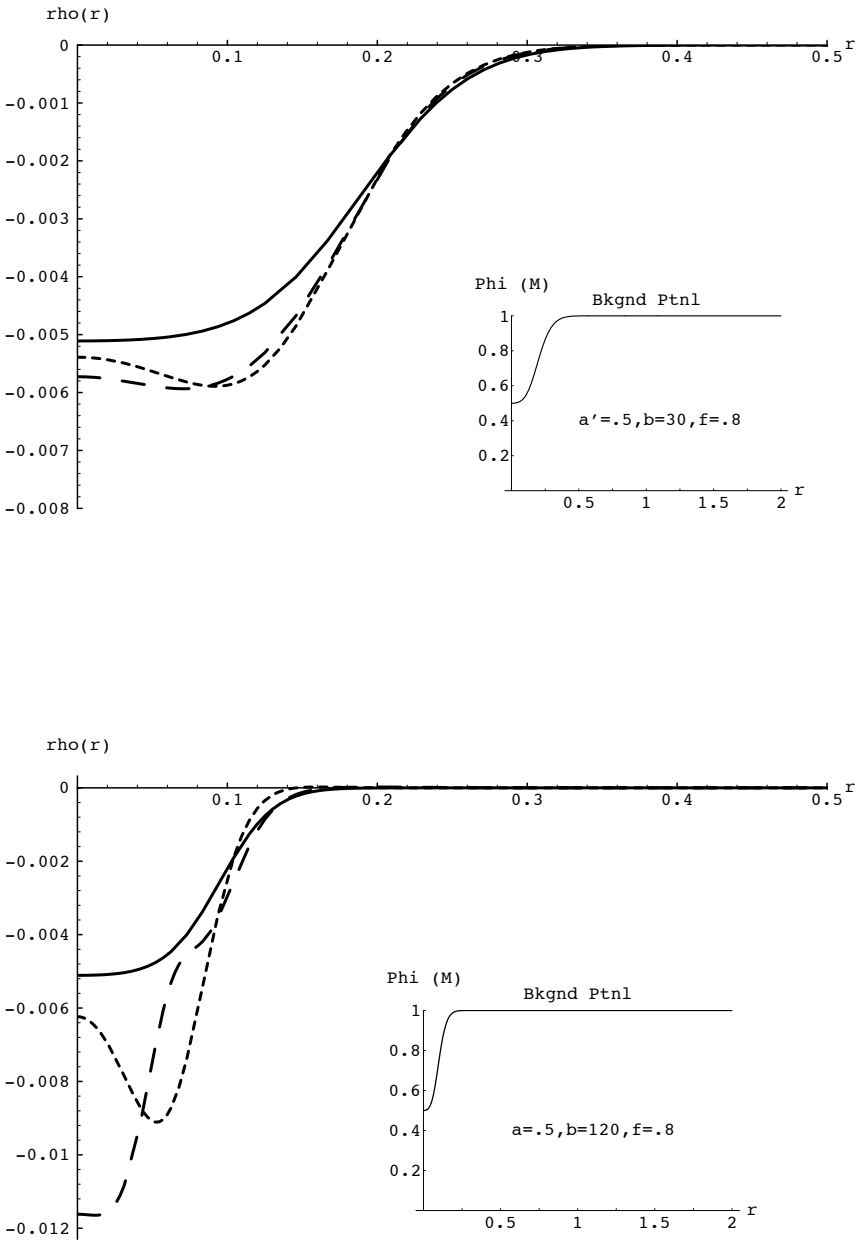

Figure 2.7: DE density terms for fixed potentials of smaller width.

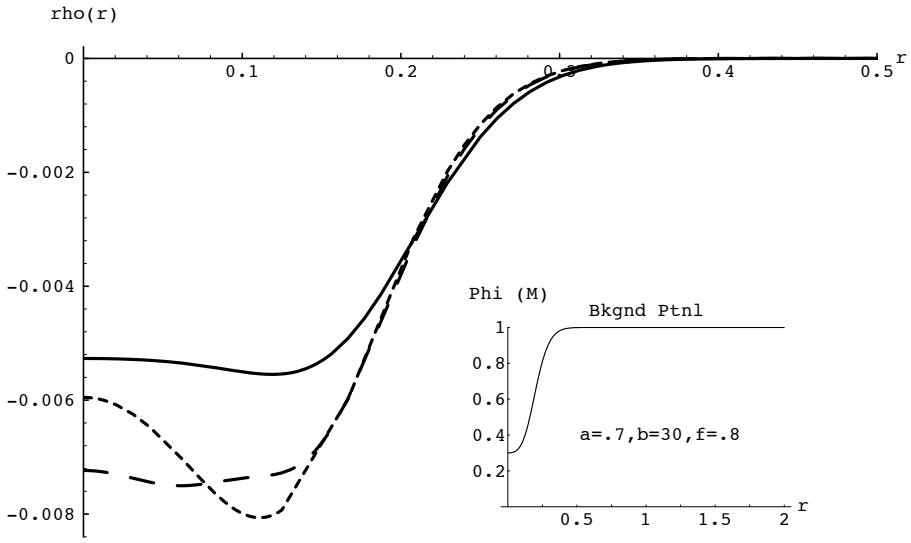

Figure 2.8: DE density terms for a fixed potential of larger depth.

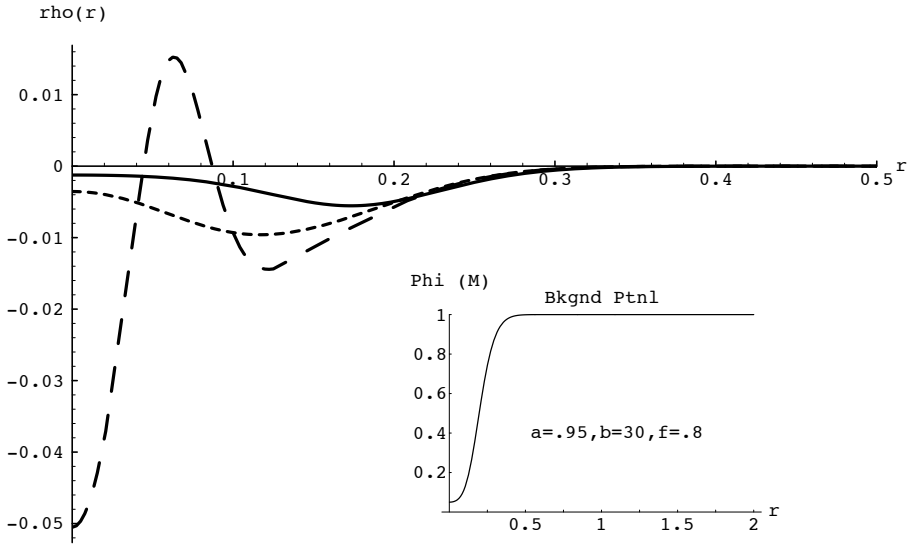

Figure 2.9: DE density terms for a very deep potential.

when the 4th order terms are included. However, at this point it is entirely unclear that we can interpret the form of the vacuum density using just terms from the DE.

It is interesting to note that the 2nd order DE seems to do qualitatively quite well at approximating the vacuum scalar density. We can see the essential shape of the vacuum density for potentials of depth of up to $a = 0.8$.

Chapter 3

EXACT CALCULATIONS AND DERIVATIVE EXPANSION IMPROVED CONVERGENCE

3.1 Exact fermion vacuum scalar density in $1+1$ *dimensions*

As the next step in our formalism, we consider testing and improving the derivative expansion series with exact calculations. In this section we restrict ourselves to the 1+1 dimensional case. The usefulness of the 1+1 dimensional DE has been considered previously by several authors [18, 19, 20, 21]. Our purpose here will be to illustrate an important idea about the numerical convergence of calculations with a finite cutoff. This is done by making use of the framework given by Wasson [21], where calculation of the $1+1$ dimensional scalar fermion density is discussed. To evaluate the one-loop vacuum contributions exactly we must solve for the full interacting fermion Green function. Thus we must solve the equation

$$(i\gamma^0\omega + i\gamma^1\partial_x - g\sigma(x))S(x,x';i\omega) = \delta(x-x'), \tag{3.1}$$

where $g\sigma(x) = M - g_s\phi(x)$ is the background scalar field contribution, and $\gamma^0 = \sigma_y$ and $\gamma^1 = i\sigma_z$ following the notation in [21]. The Wick-rotated Green function in momentum space may then be written,

$$S(i\omega) = \frac{1}{i\gamma^0\omega + i\gamma^1\partial_x - g\ \sigma(x)}\ . \tag{3.2}$$

The propagator $S(x,x')$ can be written in terms of the homogeneous solutions of this equation [19] by the Wichmann-Kroll method [36]. (This is often referred to as the Green function method.) This will allows us to solve for the trace in equation

(2.53) for each value of ω. Then, by subtracting the appropriate counterterms and integrating over all ω, obtain a solution for $\rho^s(x)$.

To consider the convergence of this exact method Wasson [21] works with a fixed classical kink soliton background given by

$$\sigma(x) = \tanh(x/\sqrt{2}). \tag{3.3}$$

As $\sigma(\infty) = 1$, the fermion has a bare mass g. Thus the convergence of the DE at large distances depends on the size of $1/g$. Also, this field has a zero at $x = 0$, so the derivative expansion is divergent at this point. Therefore, we subtract the appropriate counterterms and calculate the vacuum density exactly up to a cutoff Λ in the ω integral. Wasson's expression for this contribution in our notation is

$$\begin{aligned} \rho^{s,E}_{vac}(\Lambda, x) &= -\frac{1}{2\pi}\int_{-\Lambda}^{\Lambda} d\omega \left(\operatorname{tr} S(i\omega) - g\sigma(x)\frac{\omega^2}{(\omega^2 + (g\sigma_0)^2)^{3/2}} \right) \\ &\quad -\frac{1}{2\pi}\,\Lambda \operatorname{tr}\left[S(i\Lambda) + S(-i\Lambda)\right]. \end{aligned} \tag{3.4}$$

The renormalization terms are displayed explicitly here. The superscript E denotes that this is the exact result, up to the cutoff Λ.

The tail of the integral was then calculated using the derivative expansion, which will not diverge over this interval because the integrand is bounded away from zero. Wasson derives his derivative expansion density by first calculating the energy DE expression and then taking its variation, $\delta E/\delta\phi$ (see equations (2.25) and 2.51)). As this is a one dimensional calculation, the ω integral can be evaluated exactly. This gives an analytic form with respect to cutoff for the tail of the density under the derivative expansion approximation. However, because we are dealing with a cutoff parameter, the way in which the derivative expansion is derived may effect its convergence — the differences being total derivatives under the integrand. This density can also be calculated using the Green function expansion, equation (2.91), in $1+1$ dimensions. Including the same counterterm as in (3.4) above, this latter

method gives

$$\rho_{vac}^{s,DE}(x) = -\frac{1}{2\pi}\int d\omega\Big(\frac{g\sigma(x)}{(\omega^2+(g\sigma(x)^2))^{1/2}}+\frac{1}{4}\frac{g\,\omega^2\partial^2\sigma(x)}{(\omega^2+g^2\sigma^2(x))^{5/2}} -\frac{5}{8}\frac{g^3\omega^2\sigma(x)(\partial_\mu\sigma(x))^2}{(\omega^2+g^2\sigma^2(x))^{7/2}}\Big). \tag{3.5}$$

Evaluating this expression over the tails $(-\infty,-\Lambda)$ and (Λ,∞), and adding in the exact contribution (3.4) for the interval $(-\Lambda,\Lambda)$, we have the derivative expansion improved result

$$\rho_{vac}^{s,E+DE}(\Lambda,x) = \rho^{s,E}(\Lambda,x)+\frac{1}{\pi}\Bigg[g\sigma(x)\,\ln\left(\frac{\Lambda+\sqrt{\Lambda^2+g^2\sigma^2(x)}}{\Lambda+\sqrt{\Lambda^2+g^2\sigma_0^2}}\right) -\frac{\partial^2\sigma(x)}{12g\sigma^2(x)}\left(1-\frac{\Lambda^3}{(\Lambda^2+g^2\sigma^2(x))^{3/2}}\right) +\frac{(\partial_\mu\sigma(x))^2}{g^2\sigma^3(x)}\left(1-\frac{\Lambda^3(2\Lambda^2+5g^2\sigma^2(x))}{2(\Lambda^2+\sigma^2(x))^{5/2}}\right)\Bigg]. \tag{3.6}$$

This expression can be regarded as an interpolation scheme between the full DE result, corresponding to $\Lambda = 0$, and the exact Green function result, corresponding to $\Lambda \to \infty$. When (3.6) is used rather than equation (3.15) of Wasson's paper [21], the convergence with cutoff Λ is improved[1]. This can be seen in table 3.1. The first two columns of this table reproduce the results found in table 1 of reference [21]. The last column shows the results using (3.6). Notice that at a cutoff of $\Lambda/G = 0.5$, the variational method gets only 27% of the way to the exact result, whereas the direct Green function method gets 80% of the way there. The direct Green function method becomes asymptotic at a lower value of Λ. We anticipate that this result will be even more important in $3+1$ dimensions, as higher partial waves converge at a higher cutoff. In light of this result, we will use the direct expression (2.53) in $3+1$ dimensions rather than taking the functional derivative of an energy expression.

---

[1] A special thanks to Peter Blunden for writing the numerical code for this calculation in one dimension.

Table 3.1: Convergence of various methods for calculating the fermion scalar density of the kink soliton. Shown is density at $x = 0.5$ with coupling $G = g/\sqrt{2} = 2$.

Λ/G	$\rho^s(x = 0.5)$		
	$\rho^{s,E}$	$\rho^{s,E+DE}$ $(\delta E/\delta\phi)$	$\rho^{s,E+DE}$ $(\mathrm{tr}\, S)$
0.0	0.0000	0.0713	0.0713
0.5	-0.0069	0.0344	-0.0357
1.0	-0.0249	-0.0495	-0.0589
2.0	-0.0463	-0.0606	-0.0612
5.0	-0.0584	-0.0613	-0.0613
10.0	-0.0606	-0.0613	-0.0613
20.0	-0.0611	-0.0613	-0.0613

We can see the importance of using the DE density term to evaluate the high energy tails by comparing figures 3.1 and 3.2. The former shows the convergence with cutoff when just the exact calculation is performed. The latter includes equation (3.6) to evaluate the tail and obtains much more rapid convergence. Also shown are the LDA and 2nd order DE approximation. It is clear that neither can adequately describe the density for this kink soliton. In fact, we see explicitly that the DE blows up at the origin as mentioned previously.

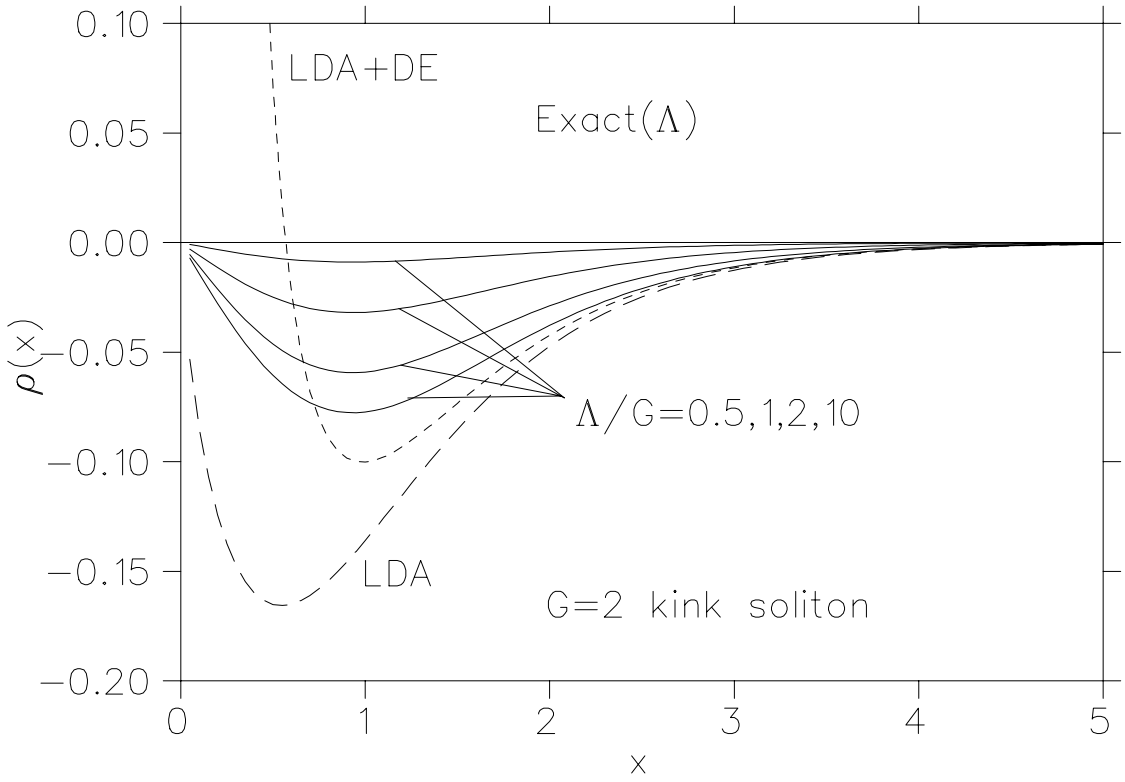

Figure 3.1: Convergence of the exact density expression (3.4) with cutoff for the kink soliton. ($G = g/\sqrt{2}$)

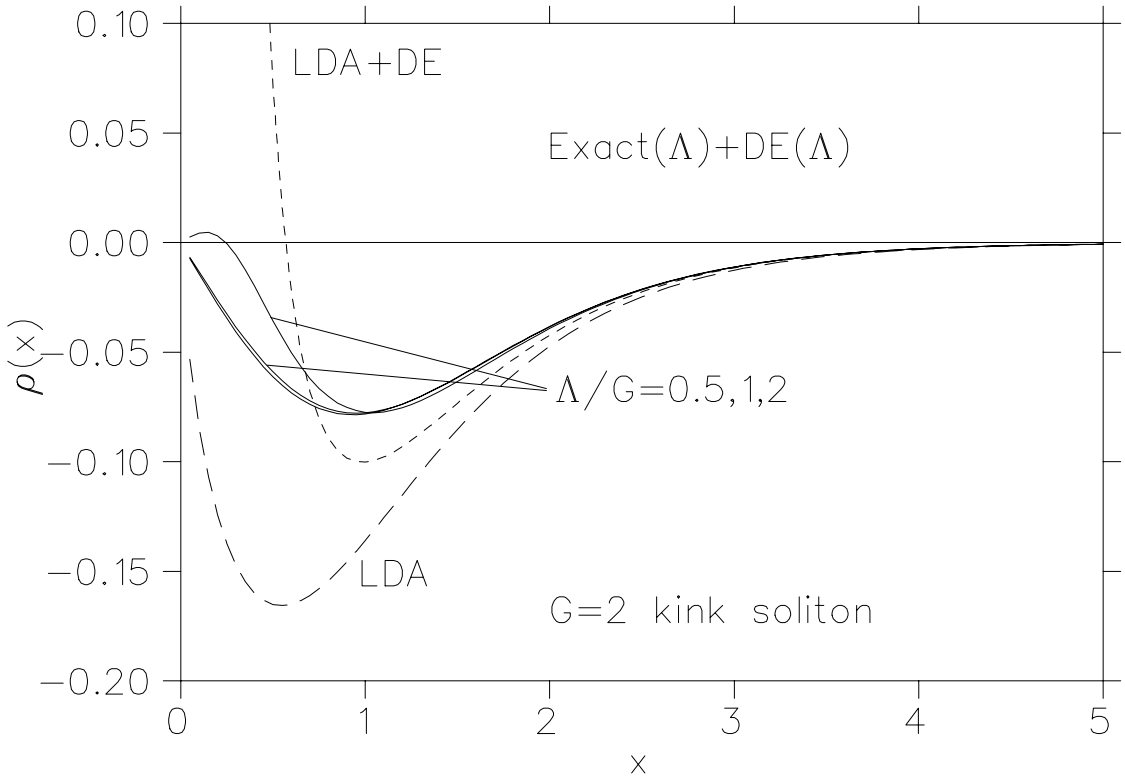

Figure 3.2: Convergence of the DE improved density expression (3.6) with cutoff for the kink soliton. ($G = g/\sqrt{2}$)

3.2 Convergence in $3+1$ dimensions

3.2.1 Exact calculation by partial waves

In $3+1$ dimensions we may attempt to carry out a procedure analogous to that of the last section for calculating the exact one-loop density. The solution, however, is now complicated by the presence of angular momentum states. Here we must solve

$$(i\gamma_0\omega + i\vec{\gamma}\cdot\nabla - g\sigma(x)\ )\ S(\vec{x}\,,\vec{x}\,';i\omega) = \delta^{(3)}(\vec{x}\,-\vec{x}\,'). \tag{3.7}$$

For a spherically symmetric scalar potential $\sigma = \sigma(r)$, equation (3.7) can only be solved exactly for each partial wave. The full Green function is then expressed as a sum of the contribution from each partial wave. This exact solution in partial waves was previously considered by Li, Perry, and Wilets in their examination of the effective energy [18, 24]. Here it is the density that we are interested in, so we review the method of partial wave expansion in this context. To expand equation (3.7) in partial waves, we use

$$S(\vec{x}\,,\vec{x}\,';i\omega) = \frac{1}{rr'}\sum_{\kappa,m} S_\kappa(r,r';i\omega)\otimes\mathcal{Y}_{\kappa m}\mathcal{Y}^\dagger_{\kappa m}, \tag{3.8}$$

$$\delta^{(3)}(\vec{x}\,-\vec{x}\,') = \frac{1}{rr'}\delta(r-r')\sum_{\kappa m}\mathcal{Y}_{\kappa m}\mathcal{Y}^\dagger_{\kappa m}. \tag{3.9}$$

With the conventions of reference [3], we have

$$(\vec{\sigma}\cdot\vec{\nabla}\,)\left(\frac{G(r)}{r}\mathcal{Y}_{\kappa m}\right) = -\frac{1}{r}\left(\frac{d}{dr}+\frac{\kappa}{r}\right)G(r)\mathcal{Y}_{-\kappa m}. \tag{3.10}$$

The upper components of the 4×4 matrix $S_\kappa(r,r';i\omega)$ couple to $\mathcal{Y}_{\kappa m}$, while the lower components couple with $\mathcal{Y}_{-\kappa m}$. The result is the following equation for the radial Green function:

$$\begin{pmatrix} i\omega - g\sigma & -\dfrac{d}{dr}+\dfrac{\kappa}{r} \\ -\dfrac{d}{dr}-\dfrac{\kappa}{r} & -i\omega - g\sigma \end{pmatrix} S_\kappa(r,r';i\omega) = \delta(r-r'). \tag{3.11}$$

The Wichmann and Kroll reduction of equation (3.11) can be written

$$S_{-\kappa}(r,r';i\omega) = \frac{-\gamma_0\left(U_\kappa(r)V_\kappa^\top(r')\theta(r'-r) + V_\kappa(r)U_\kappa^\top(r')\theta(r-r')\right)}{\mathcal{W}_\kappa(\omega)}, \tag{3.12}$$

where $\mathcal{W}_\kappa(\omega)$ is the r independent Wronskian

$$\mathcal{W}_\kappa(\omega) = U_\kappa^2(r)V_\kappa^1(r) - U_\kappa^1(r)V_\kappa^2(r), \tag{3.13}$$

(1 and 2 representing the upper and lower components respectively). The homogeneous solutions satisfied by U_κ and V_κ are:

$$\begin{pmatrix} -i\omega + g\sigma & -\dfrac{d}{dr} - \dfrac{\kappa}{r} \\ \dfrac{d}{dr} - \dfrac{\kappa}{r} & -i\omega - g\sigma \end{pmatrix} (U_\kappa \text{ or } V_\kappa) = 0. \tag{3.14}$$

The boundary conditions are fixed by the conditions on the scalar field

$$\begin{aligned} &\text{(i)} \quad \text{outward solution } U_\kappa: \quad \left.\frac{d\sigma(r)}{dr}\right|_{r=0} = 0, \\ &\text{(ii)} \quad \text{inward solution } V_\kappa: \quad \sigma(r\to\infty) = \sigma_0. \end{aligned} \tag{3.15}$$

To smooth the singular nature of the homogeneous solutions we follow the method given in [2], and scale the solutions componentwise by dividing out the known free solutions:

$$\begin{pmatrix} U_\kappa^1 \\ U_\kappa^2 \end{pmatrix} = \begin{pmatrix} U_{\kappa 0}^1 \tilde{U}_\kappa^1 \\ U_{\kappa 0}^2 \tilde{U}_\kappa^2 \end{pmatrix}, \qquad \begin{pmatrix} V_\kappa^1 \\ V_\kappa^2 \end{pmatrix} = \begin{pmatrix} V_{\kappa 0}^1 \tilde{V}_\kappa^1 \\ V_{\kappa 0}^2 \tilde{V}_\kappa^2 \end{pmatrix}, \tag{3.16}$$

where

$$U_{\kappa 0} = \begin{pmatrix} r i_{\kappa-1}(z_{0\omega} r) \\ \dfrac{r z_{0\omega} i_\kappa(z_{0\omega} r)}{g\sigma_0 + i\omega} \end{pmatrix}, \qquad V_{\kappa 0} = \begin{pmatrix} r k_{\kappa-1}(z_{0\omega} r) \\ \dfrac{-r z_{0\omega} k_\kappa(z_{0\omega} r)}{g\sigma_0 + i\omega} \end{pmatrix}. \tag{3.17}$$

Here $z_{0\omega} = \sqrt{g^2\sigma_0^2 + \omega^2}$, and i_κ, k_κ are modified spherical Bessel functions of order κ. This scaling is an important step for the density calculation, as it turns out that

the solution must be extremely accurate near the origin ($r = 0$). This is a result of the fact that the Green function solution and r-dependent counterterms blow up as $r \to 0$. For the scaled solutions, the new equations we must solve are

$$\begin{pmatrix} (g\sigma(r) - i\omega)\ \mathcal{F}(r,\omega) & -\dfrac{d}{dr} - (g\sigma_0 - i\omega)\ \mathcal{F}(r,\omega) \\ \dfrac{d}{dr} + \dfrac{(g\sigma_0 + i\omega)}{\mathcal{F}(r,\omega)} & -\dfrac{(g\sigma(r) + i\omega)}{\mathcal{F}(r,\omega)} \end{pmatrix} \left(\tilde{U}_\kappa \text{ or } \tilde{V}_\kappa\right) = 0, \tag{3.18}$$

where

$$\mathcal{F}(r,\omega) \;=\; \begin{cases} \dfrac{(g\sigma_0 + i\omega)}{z_{0\omega}}\ \dfrac{i_{\kappa-1}(z_{0\omega}r)}{i_\kappa(z_{0\omega}r)} & \text{outward,} \\ -\dfrac{(g\sigma_0 + i\omega)}{z_{0\omega}}\ \dfrac{k_{\kappa-1}(z_{0\omega}r)}{k_\kappa(z_{0\omega}r)} & \text{inward.} \end{cases} \tag{3.19}$$

The boundary conditions for this new differential equation can be derived from the boundary conditions on the scalar field (3.15). For the outward solution we solve the equations near the origin by making Taylor series expansions of the r-dependent terms. This is necessary as the function $\mathcal{F}(r)$ is singular at the origin. With

$$\begin{aligned} U^1_\kappa(r \to 0) &= a_0 + a_1 r + a_2 r^2 + a_3 r^3 + a_4 r^4 + \ldots \\ U^2_\kappa(r \to 0) &= b_0 + b_1 r + b_2 r^2 + b_3 r^3 + b_4 r^4 + \ldots \\ \sigma(r \to 0) \pm i\omega &= s_0^\pm + s_1 r + s_2 r^2 + s_3 r^3 + s_4 r^4 + \ldots \end{aligned} \tag{3.20}$$

we find

$$\begin{aligned} a_0 &= 1, \qquad a_1 = 0, \qquad a_2 = \frac{(s_0^+ s_0^- - z_{0\omega}^2)}{2(2\kappa+1)}, \\ a_3 &= \frac{(b_1 s_0^+ + b_0 s_1) z_{0\omega}^2}{3(2\kappa+1)(\phi_0 + i\omega)}, \\ a_4 &= \frac{z_{0\omega}^2 \left(\dfrac{(b_1 s_1 + b_0 s_2 + b_2 s_0^+)}{(\phi_0 + i\omega)} - a_2 \right)}{4(2\kappa+1)} + \frac{z_{0\omega}^4 \left(1 + \dfrac{b_0 s_0^+}{(\phi_0 + i\omega)} \right)}{4(2\kappa+1)^2(2\kappa+3)}, \end{aligned} \tag{3.21}$$

and

$$
\begin{aligned}
b_0 &= \frac{s_0^-(g\phi_0+i\omega)}{z_{0\omega}^2}, \qquad b_1=\frac{(2\kappa+1)(g\phi_0+i\omega)s_1}{(2\kappa+2)z_{0\omega}^2},\\
b_2 &= \frac{(2\kappa+1)(g\phi_0+i\omega)(a_2s_0^-+s_2)}{(2\kappa+3)z_{0\omega}^2},\\
b_3 &= \frac{(s_1(\phi_0+i\omega)-b_1z_{0\omega}^2)}{(2\kappa+3)(2\kappa+4)}+\frac{(2\kappa+1)(\phi_0+i\omega)}{(2\kappa+4)z_{0\omega}^2}(s_3+a_3s_0^++a_2s_1),\\
b_4 &= \frac{((\phi_0+i\omega)(s_2+a_2s_0^-)-b_2C_\omega^2)}{(2\kappa+3)(2\kappa+5)}.\\
&\qquad +\frac{(2\kappa+1)(\phi_0+i\omega)}{(2\kappa+5)C_\omega^2}(s_4+s_3a_2+s_1a_3+s_0^-a_4). \qquad (3.22)
\end{aligned}
$$

The boundary condition (i) corresponds to setting $s_1=0$ in these equations. This extends the results in [2], which gives a_0 and b_0. The large number of terms will enable us to find the components of the Green function with great precision near the origin. Also, it is possible to test the sensitivity to the boundary condition near the origin by including a certain number of these terms. The reason for which such accuracy is necessary is because when we solve for the Green function components by making a Taylor series expansion near the origin, it is found that the leading order terms to the density under the ω integral are

$$
\frac{1}{3\pi}\,\frac{\sigma(r)}{r}\;+\;\left(\frac{\Re(\mathcal{W}^{-1})\;c_1}{z_{0\omega}}-\sigma(r)\;z_{0\omega}\right)+\mathcal{O}(r), \qquad (3.23)
$$

where $\Re$ is the real part. Here c_1 and $\mathcal{W}$ are unknown quantities (the former is the upper component of V_κ at the origin). By making similar expansions of the DE and counter term densities we find that an identical $1/r$ piece appears. Therefore the true information for the density at the origin comes from the next term in (3.23), and depends on the numerically determined c_1, and $\mathcal{W}$. This requires a numerical evaluation of the Green function that is valid to 12 digits, and therefore a very accurate boundary condition near $r=0$.

We solve the equations for $r\to\infty$ by similarly making an expansion in $1/r$ of the the r-dependent terms

$$
V_\kappa^1(r\to\infty) \;=\; a_0+a_1/r+\ldots
$$

$$\begin{aligned} V_\kappa^2(r\to\infty) &= b_0 + b_1/r + \ldots \\ \sigma(r\to\infty) \pm i\omega &= c_0^\pm + c_1/r + \ldots \end{aligned} \tag{3.24}$$

and find

$$a_0 = 1, \qquad b_0 = 1, \tag{3.25}$$

to be sufficient if these conditions are applied at fairly large r. This specifies the boundary conditions for the incoming solution.

To define the partial wave contribution to the density, we combine (2.53) and (3.8) to find

$$\rho_{vac}^{s,E}(r) = -\frac{1}{2\pi}\int_{-\infty}^{\infty} d\omega \sum_{\kappa=-\infty}^{\infty} \frac{2|\kappa|}{4\pi r^2}\,\mathrm{tr}\, S_\kappa(r,r;i\omega). \tag{3.26}$$

Here the angular integral and sum over magnetic substates m have been collapsed to give the factor $2|\kappa|/4\pi r^2$. We proceed by noting that

$$\begin{aligned} S_\kappa(r,r';-i\omega) &= \sigma_1\; S_{-\kappa}(r,r';i\omega)\;\sigma_1, && (3.27)\\ \mathrm{tr}\, S_\kappa(r,r';-i\omega) &= \mathrm{tr}\, S_{-\kappa}(r,r';i\omega), && (3.28)\\ \mathrm{tr}\,(S_\kappa(r,r';i\omega) + S_{-\kappa}(r,r';i\omega)) &= 2\Re\,\mathrm{tr}\, S_\kappa(r,r';i\omega). && (3.29) \end{aligned}$$

The first equation here can easily be seen from (3.11) by multiplying by σ_1 on the left and right, and by introducing a σ_1^2 term between the operator matrix and the Green function. The second then follows immediately, while the third can be seen by taking the complex conjugate of (3.11). With this reduction, we can express the result for the exact density as

$$\begin{aligned} \rho_{vac}^{s,E}(r) &= \sum_{\kappa=1}^{\infty} \kappa\rho_\kappa^E(r), && (3.30)\\ \rho_\kappa^E(r) &= -\frac{1}{2\pi}\;4\int_{-\infty}^{\infty} d\omega\;\frac{1}{4\pi r^2}\;\Re\,\mathrm{tr}\, S_\kappa(r,r;i\omega). && (3.31) \end{aligned}$$

3.2.2 Partial wave DE expansion

Next we turn to the evaluating the derivative expansion as given by equation (2.91). In $3+1$ dimensions

$$\rho_{vac}^{s,DE}(x) = -\mathrm{Tr}_p\ 4\ \Big[\frac{\sigma(x)}{(-p^2+\sigma(x)^2)} + \frac{1}{2}\frac{\nabla^2\sigma(x)}{(-p^2+\sigma(x)^2)^2} - \frac{2}{3}\frac{\sigma^2(x)\nabla^2\sigma(x)}{(-p^2+\sigma(x)^2)^3} - \frac{5}{3}\frac{\sigma(x)(\nabla\sigma(x))^2}{(-p^2+\sigma(x)^2)^3} + 2\frac{\sigma^3(x)(\nabla\sigma(x))^2}{(-p^2+\sigma(x)^2)^4}\ \Big]\ . \tag{3.32}$$

As the exact density in $3+1$ dimensions could only be calculated in a partial wave sum we must also decompose the derivative expansion in order to test its validity. This can be done for a radially dependent potential $\sigma(r)$ which is assumed in our form of the RHA. To decompose our expression (3.32) for the density we again follow the method used by Li, Perry and Wilets [2, 23]. The utility of their method can be summed up in the following manner. For a constant scalar field $\sigma = \sigma_0$ the second order form of the radial Dirac equation is diagonal, and the partial wave solutions are known. Therefore the form of the radial Green function can be written explicitly. The Green function can also be expressed as a spectral sum [37]

$$S(x,x';p_0) = \sum_\alpha \frac{\psi_\alpha(x)\bar{\psi}_\alpha(x')}{p_0-\epsilon_\alpha}, \tag{3.33}$$

from which we derive the expression for higher powers of the Green function

$$S^n(x,x';p_0) = \sum_\alpha \frac{\psi_\alpha(x)\bar{\psi}_\alpha(x')}{(p_0-\epsilon_\alpha)^n} = \frac{(-1)^{n-1}}{(n-1)!}\ \frac{d^{(n-1)}}{dp_0^{(n-1)}}\ S(x,x';p_0). \tag{3.34}$$

An equation for the momentum space factors can then be written using the following procedure [23]. First we take the trace of expression (3.34) for S^n in momentum space and then make use of equation (3.8) to expand this in partial waves. This implements the same partial wave expansion that we did for the exact Green function. We then use equation (3.12) evaluated for the free particle solutions (3.17), whereupon taking the trace we obtain the sum $\Delta^n_{\kappa-1} + \Delta^n_\kappa$ given in equation (3.37) below. We then have

$$\int d^3p \frac{1}{(w^2+\vec{p}^2+\sigma^2)^n} = (-1)^n \sum_{\kappa=1}^{\infty} \kappa \Upsilon_\kappa^n, \tag{3.35}$$

$$\Upsilon_\kappa^n = \frac{1}{4\pi r^2}(\Delta_{\kappa-1}^n + \Delta_\kappa^n), \tag{3.36}$$

$$\Delta_\kappa^n = -\frac{1}{(n-1)!}\left(\frac{1}{2z_\omega}\frac{d}{dz_\omega}\right)^{n-1} z_\omega r^2 i_\kappa(z_\omega r) k_\kappa(z_\omega r), \tag{3.37}$$

where $z_\omega = (\omega^2+\sigma^2)^{1/2}$, and i_κ, k_κ are the modified spherical Bessel functions of order κ. The free particle Wronskian is

$$\mathcal{W}(\omega) = \frac{z_{0\omega}}{g\sigma_0 + i\omega}. \tag{3.38}$$

Note that when σ is radially dependent we still require only the value of the density at a fixed radial point, say r', specified on the LHS of equation (3.37). Therefore any potential that agrees with $\sigma(r)$ at point r' will give the same result. In particular, we can make the simplest choice of a constant potential $\sigma = \sigma(r')$. Actually we are just restating the fact that the derivative expansion is local. Therefore (3.36) can be used without regard to the radial dependence of σ. The derivative expansion density is therefore

$$\rho_{vac}^{s,DE}(r) = \sum_{\kappa=1}^{\infty} \kappa\, \rho_\kappa^{DE}(r), \tag{3.39}$$

$$\rho_\kappa^{DE}(r) = -\frac{1}{2\pi} 4 \int d\omega \left(-\sigma(r)\Upsilon_\kappa^1 + \frac{1}{2}\nabla^2\sigma(r)\Upsilon_\kappa^2 + \frac{2}{3}\sigma(r)^2\nabla^2\sigma(r)\Upsilon_\kappa^3 + \frac{5}{3}\sigma(r)(\sigma'(r))^2\Upsilon_\kappa^3 + 2\sigma^3(r)(\sigma'(r))^2\Upsilon_\kappa^4 \right), \tag{3.40}$$

where z_ω is now dependent on both ω and r. This differs from the $1+1$ dimensional case in that here we cannot easily evaluate the ω integral over a particular range of ω. This is a result of the more complex form of the integrand as products of modified spherical Bessel functions, along with derivatives of such products. Numerical evaluation, however, is possible.

The same partial wave expansion as was done for the DE can be made for the counterterm expansion in an identical manner. We take the terms in (2.82) that

correspond to the divergent terms from (2.89) in $3+1$ dimensions. This gives the following counter term expression which must be subtracted from the DE and Exact expressions (3.40), (3.31) to give a finite result.

$$\begin{aligned}
\delta\rho^{s}_{vac}(r) &= \sum_{\kappa=1}^{\infty} \kappa\, \delta\rho_{\kappa}(r), \\
\delta\rho_{\kappa}(r) &= -\frac{1}{2\pi} 4 \int d\omega \left(-\sigma(r)\Upsilon^{1}_{0\kappa} - (\sigma(r)^2 - \sigma_0^2)\ \Upsilon^{2}_{0\kappa} \right. \\
&\qquad \left. + \frac{1}{2}\nabla^{\,2}\sigma(r)\Upsilon^{2}_{0\kappa} - \frac{2}{3}\sigma_0^2\Upsilon^{3}_{0\kappa} \right), \qquad (3.41)
\end{aligned}$$

where $\Upsilon_{0\kappa}$ is the Υ in (3.37) with $z_{0\omega} = (\omega^2 + \sigma_0^2)^{1/2}$ for z_{ω}.

3.2.3 Interpolation scheme and the numerical procedure

Now that equations for both the exact and derivative expansion densities have been derived, we are interested in the numerical convergence of our expressions. The aim in this subsection is to observe how the finite quantity

$$\tilde{\rho}^{s,E}_{vac}(r) = \rho^{s,E}_{vac}(r) - \delta\rho^{s}_{vac}(r), \qquad (3.42)$$

can be determined with the least amount of numerical effort. The way in which the actual shape of the background potential affects the convergence and size of the correction will be discussed in the next subsection. The quantity $\tilde{\rho}^{s,E}_{vac}(r)$ can be written as follows:

$$\begin{aligned}
\tilde{\rho}^{s,E}_{vac}(r) &= \sum_{\kappa=1}^{\infty} \left(\rho^{E}_{\kappa}(r) - \delta\rho_{\kappa}(r) \right) \qquad (3.43) \\
&= \tilde{\rho}^{s,DE}_{vac}(r) + \sum_{\kappa=1}^{\infty} \left(\rho^{E}_{\kappa}(r) - \rho^{DE}_{\kappa}(r) \right), \qquad (3.44)
\end{aligned}$$

where the tilde indicates a renormalized expression. Note that in the latter of the two expressions the difference between the exact and derivative expansion partial wave densities gives a result that is independent of renormalization. The renormalization is entirely taken care of in the DE term $\tilde{\rho}^{s,DE}_{vac}(r)$. Writing $\Delta\rho_{\kappa} = \rho^{E}_{\kappa} - \rho^{DE}_{\kappa}$, and

inserting a finite cutoff on the ω integral, we have that

$$\begin{aligned}\Delta\rho_\kappa(\Lambda,r) &= -\frac{1}{2\pi^2}\int_{-\Lambda}^{\Lambda} d\omega\Big(\frac{1}{r^2}\Re\,\mathrm{tr}\,S_\kappa(r,r';i\omega)+\sigma(r)\Upsilon_\kappa^1-\frac{1}{2}\nabla^{\,2}\sigma(r)\Upsilon_\kappa^2 \\ &\quad -\frac{2}{3}\sigma(r)^2\nabla^{\,2}\sigma(r)\Upsilon_\kappa^3-\frac{5}{3}\sigma(r)(\sigma'(r))^2\Upsilon_\kappa^3-2\sigma^3(r)(\sigma'(r))^2\Upsilon_\kappa^4\Big). \quad (3.45)\end{aligned}$$

All quantities here are even with respect to ω, so

$$\begin{aligned}\Delta\rho_\kappa(\Lambda,r) &= -\frac{1}{\pi^2}\int_{0}^{\Lambda} d\omega\Big(\frac{1}{r^2}\Re\,\mathrm{tr}\,S_\kappa(r,r';i\omega)+\sigma(r)\Upsilon_\kappa^1-\frac{1}{2}\sigma''(r)\Upsilon_\kappa^2 \\ &\quad -\frac{2}{3}\sigma(r)^2\sigma''(r)\Upsilon_\kappa^3-\frac{5}{3}\sigma(r)(\sigma'(r))^2\Upsilon_\kappa^3-2\sigma^3(r)(\sigma'(r))^2\Upsilon_\kappa^4\Big). \quad (3.46)\end{aligned}$$

The exact one-loop density is then

$$\tilde{\rho}_{vac}^{s,E}(r) \;=\; \tilde{\rho}_{vac}^{s,DE}(r) \;+\; \sum_{\kappa=1}^{\infty}\lim_{\Lambda\to\infty}\Delta\rho_\kappa(\Lambda,r). \quad (3.47)$$

The renormalization for the exact density is accounted for in the expression for the DE, and the partial wave sum acts as a correction. Since the former is analytically known (c.f. section 2.1) the problem is simply to calculate the latter.

The form of our numerical calculation of (3.46) is as follows. For a fixed κ we evaluate the ω integral numerically. For *each* value of ω we must solve a set of complex coupled first order equations (the Wick rotated radial Dirac equation in the presence of a scalar source). This calculation is performed twice, once going in from the boundary condition at ∞ and once out from the condition at the origin. We must also calculate both the modified spherical Bessel functions and their derivatives because these appear as coefficients in the differential equations as well as explicitly in the integrand through the factors Υ_κ^n. Note that for each value ω the integrand is determined by this procedure for all r. Finally, we calculate the ω integral out from the origin to a value of the cutoff where convergence has occurred for all r. This entire process may then be repeated for the next value of κ.

Because of the large degree of cancelation between terms in (3.46) our calculations must be very accurate. In particular the differential equations are solved with 12

significant figures, and all the modified spherical Bessel functions are also calculated to greater than 12 digits accuracy. This has been found to give sufficient accuracy, after various manipulations, to determine the integrand over a wide range of r and ω. The required programs were written using double numerical precision in Fortran. The code is essentially an adaptation of standard routines from [38]. The ω integration is performed through a Romberg integration over a particular interval in ω, refining the value by the n^{th} stage of the extended trapezoidal rule, and then extrapolating to zero step size using Neville's algorithm. This process is repeated over another such interval until the contributions are shown to be asymptotic. (An estimate may then be made for the remainder by fitting a second order polynomial in $1/\omega^2$ if this is desired.) The Bessel functions are calculated using the standard iterative procedures, where special attention is paid to the required accuracy. In particular, large and small values of the argument are found by using the appropriate series expansions. Derivatives are also found using iteration, and when this proves unreliable, by expansion. Finally, the differential equations are solved using an adaptive stepsize 5th order Runge Kutta routine [38]. Modifications are made to incorporate a minimum r mesh on which the Green function must be found. In particular, the entire routine will run on any predetermined minimum mesh in r. All of these routines are combined into a correction subroutine which, given a background scalar potential, derives a corrected vacuum density. This makes the routine portable enough for inclusion in a self-consistent calculation (which is done in chapter 5).

One method by which we can test our numerical code is to recall that our partial wave method is based on that of [2]. Therefore, with our code, it is a simple matter to evaluate the expressions that these authors give for the energy of the DE and exact calculation in each partial wave. Doing this, we obtain the numbers in table 3.2, which at most disagree by 1 or 2 in the last digit of the numbers quoted in reference [2].

Table 3.2: Partial wave energies for the soliton potential of reference [2]. (Consistency check)

κ	DE Energy	Exact Energy
1	0.2240459×10^{0}	0.221799×10^{0}
2	0.1496159×10^{0}	0.148745×10^{0}
3	0.1027586×10^{0}	0.102322×10^{0}
4	0.7202294×10^{-1}	0.717738×10^{-1}
5	0.5136474×10^{-1}	0.512104×10^{-1}
6	0.3721826×10^{-1}	0.371170×10^{-1}
7	0.2737292×10^{-1}	0.273035×10^{-1}
8	0.2041825×10^{-1}	0.203691×10^{-1}
9	0.1543499×10^{-1}	0.154003×10^{-1}
10	0.1181852×10^{-1}	0.117921×10^{-1}
11	0.9158048×10^{-2}	0.913817×10^{-2}
12	0.7177235×10^{-2}	0.716210×10^{-2}

3.2.4 Examining the convergence

The overall goal for testing the convergence of the correction is to see how many partial waves and what value of the cutoff Λ are sufficient to correct $\rho_{vac}^{s,DE}$ to give the exact result within a required accuracy. Consider the convergence with cutoff Λ. In figure 3.3, the benefit of using the expression (3.44) with $\Delta\rho_\kappa(r)$ rather than calculating the full exact $\tilde{\rho}_\kappa$ in (3.43) can be seen. The derivative expansion corrected series is seen to converge to an asymptotic form faster with respect to the cutoff. This behavior is also seen in the second and higher partial waves.

The finite cutoff in equation (3.47) can alternatively be viewed as a parameter that

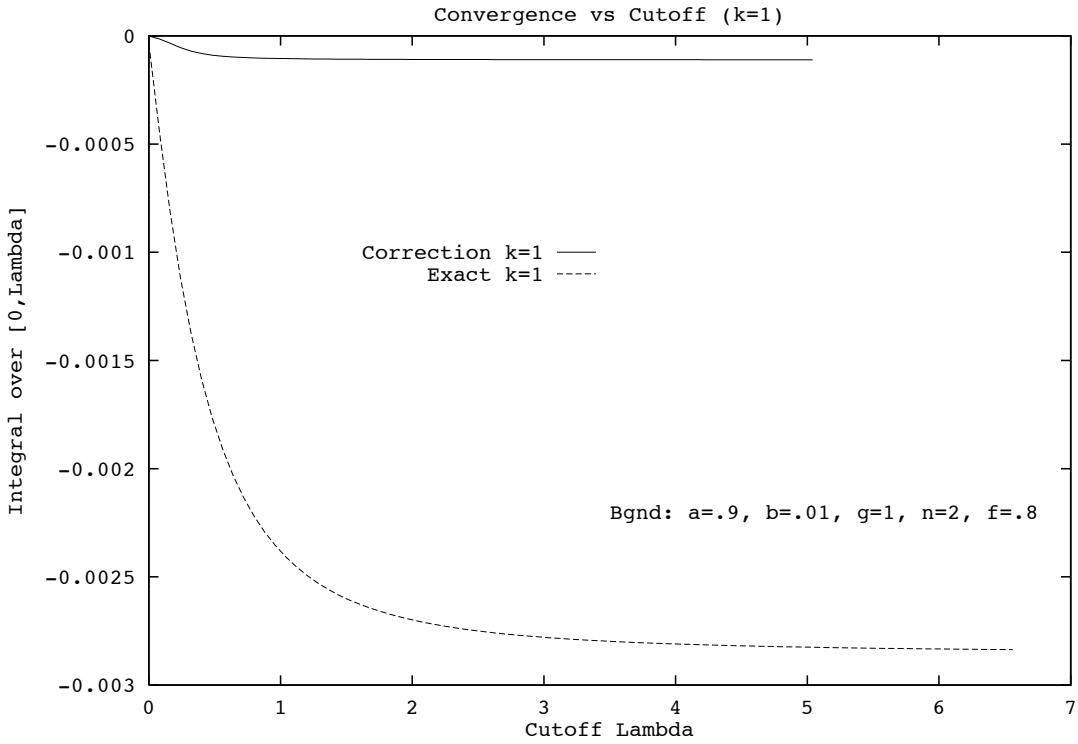

Figure 3.3: Comparison of the convergence with cutoff between the exact and DE improved correction calculations. The integrand is given for $r = 0.01$ and $\kappa = 1$.

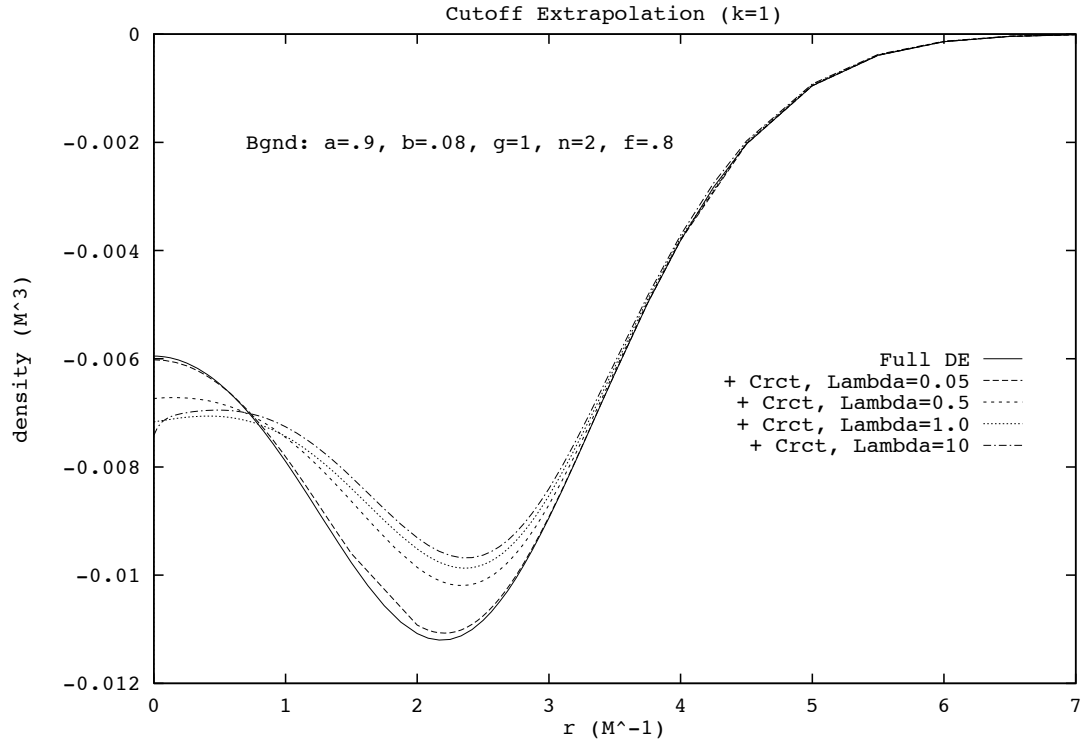

Figure 3.4: Implementation of the cutoff extrapolation scheme for $\kappa = 1$. The curves shown extrapolate between the DE and the exact result.

makes a continuous smooth extrapolation from the DE result at $\Lambda = 0$ to the exact result as $\Lambda \to \infty$. In $1 + 1$ dimensions this was the view exploited by Wasson [21], as explained in section 3.1 . In $3 + 1$ for a given partial wave this provides a smooth extrapolation for including the exact correction for that partial wave. In figure 3.4, plotting the density for various values of cutoff Λ, we can see how the density function converges at different values of r. This figure shows the extrapolation mechanism for $\kappa = 1$. Note that the largest cutoff curve plotted is a factor of ten bigger than the preceding curve. This interpolation mechanism turns out to be an important tool when self-consistent solutions are attempted (see chapter 5).

The final issue of convergence is that of the partial wave series. In particular, it

was noted that the form of the derivative expansion was at one point manipulated in a way that affected the termwise definition of partial wave contributions (although not the entire sum). We can make use of this manipulation by considering three different forms of the partial wave derivative expansion and examining the partial wave convergence of these. Two of these forms were derived above, one being (3.40) (form 1), and the second being the analogous partial wave decomposition of (2.79) (form 5). The third is a partial wave decomposition that was made of a form obtained by Blunden [26] (form 4) by expanding the first order form (2.56). The equations for these three forms are given here for reference:

Form 1:

$$\begin{aligned}\rho_\kappa^{DE}(r) &= -\frac{1}{2\pi}\,4\int d\omega\Big(-\sigma\Upsilon_\kappa^1+\nabla^2\sigma\left\{\frac{1}{2}\Upsilon_\kappa^2+\frac{2}{3}\sigma^2\Upsilon_\kappa^3\right\}\\ &\qquad +(\sigma')^2\left\{\frac{5}{3}\sigma\Upsilon_\kappa^3+2\sigma^3(r)\Upsilon_\kappa^4\right\}\Big),\end{aligned}\tag{3.48}$$

Form 4:

$$\begin{aligned}\rho_\kappa^{DE}(r) &= -\frac{1}{2\pi}\,4\int d\omega\Big(-\sigma\Upsilon_\kappa^1+\nabla^2\sigma\Big\{\frac{5}{24}\Upsilon_\kappa^2-(\frac{2}{3}\omega^2+\sigma^2)\Upsilon_\kappa^3+(\omega^4-\sigma^4)\Upsilon_\kappa^4\Big\}\\ &\quad+\ (\sigma')^2\Big\{-\frac{25}{48}\sigma\Upsilon_\kappa^3-\frac{1}{4}(17\omega^2+5\sigma^2)\sigma\Upsilon_\kappa^4-\sigma(5\omega^4+2\sigma^2\omega^2-3\omega^4)\Upsilon_\kappa^5\Big\}\Big),\end{aligned}\tag{3.49}$$

Form 5:

$$\begin{aligned}\rho_\kappa^{DE}(r) &= -\frac{1}{2\pi}\,4\int d\omega\Big(-\sigma\Upsilon_\kappa^1+\nabla^2\sigma\Big\{\frac{1}{3}\Upsilon_\kappa^2-\frac{2}{3}(\omega^2+2\sigma^2)\Upsilon_\kappa^3-\frac{8}{3}(\omega^2+\sigma^2)\sigma^2\Upsilon_\kappa^4\Big\}\\ &\quad-\ (\sigma')^2\Big\{\frac{5}{3}\sigma\Upsilon_\kappa^3+\frac{4}{3}(5\omega^2+11\sigma^2)\sigma\Upsilon_\kappa^4+16\sigma^3(\omega^2+\sigma^2)\Upsilon_\kappa^5\Big\}\Big).\end{aligned}\tag{3.50}$$

Using these expressions we may now form the corresponding density correction to (3.46). In figures 3.5 to 3.10 the partial wave terms from these forms are shown for two different background potentials. The DE is only mildly divergent for the $a = .5$ case and is quite divergent for $a = .8$ case. It appears that forms 4 and 5 may converge faster with partial wave than the reduced form 1 does. However, form 1 has the advantage of being the simplest form and also does not contain any Υ_κ^5 term. Due to this numerical advantage, form 1 will be used exclusively here. Form 1 gives

one less derivative of the modified spherical Bessel functions that we must calculate to 12 significant digits. Another feature to notice is that the solutions pictured in figures 3.8 to 3.10 have at most one zero crossing unlike the situation in figure 2.9 with the fourth order derivatives.

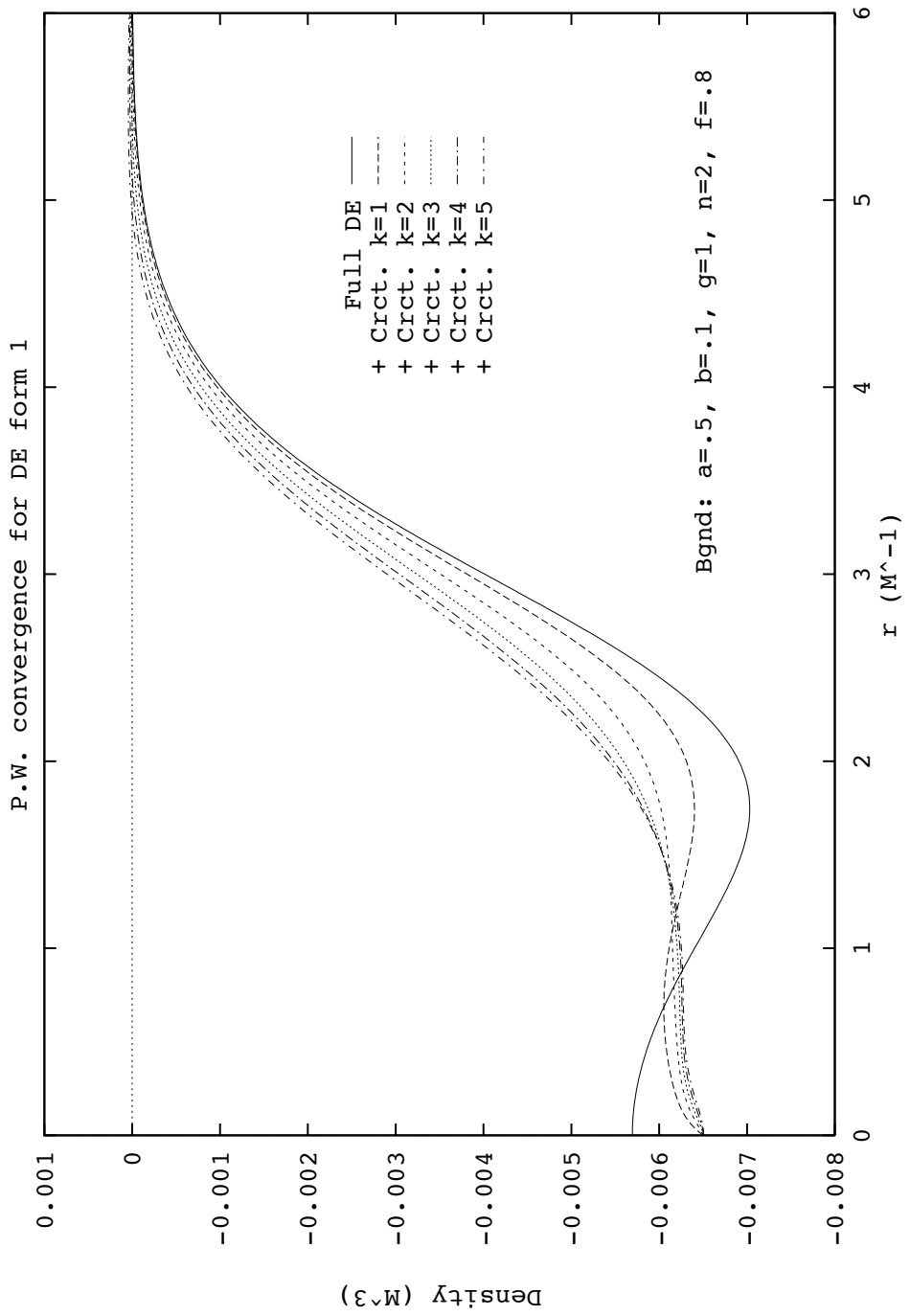

Figure 3.5: Convergence with partial wave for Form 1 of the correction functional in a sizeable background.

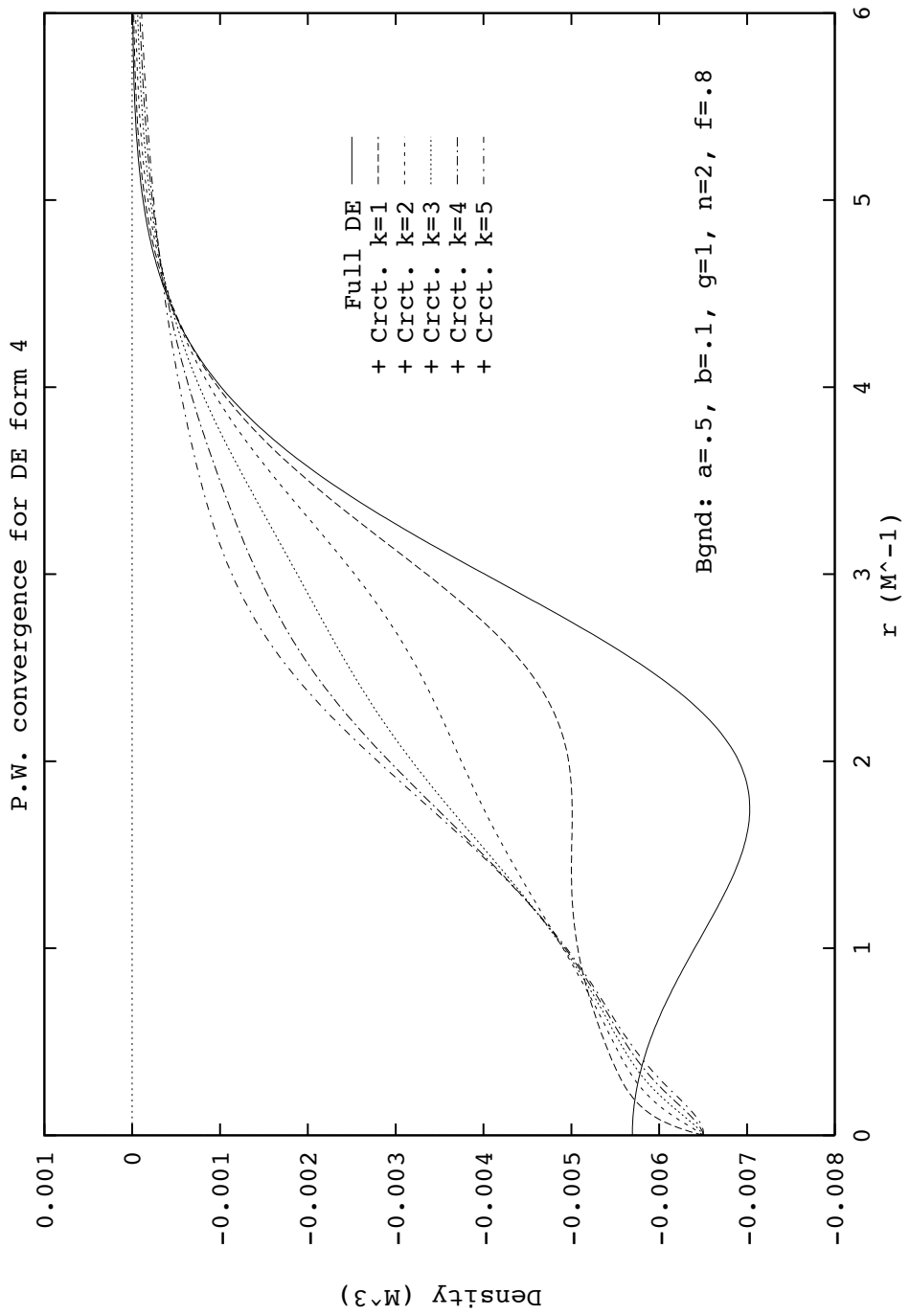

Figure 3.6: Convergence with partial wave for Form 4 of the correction functional in a sizeable background.

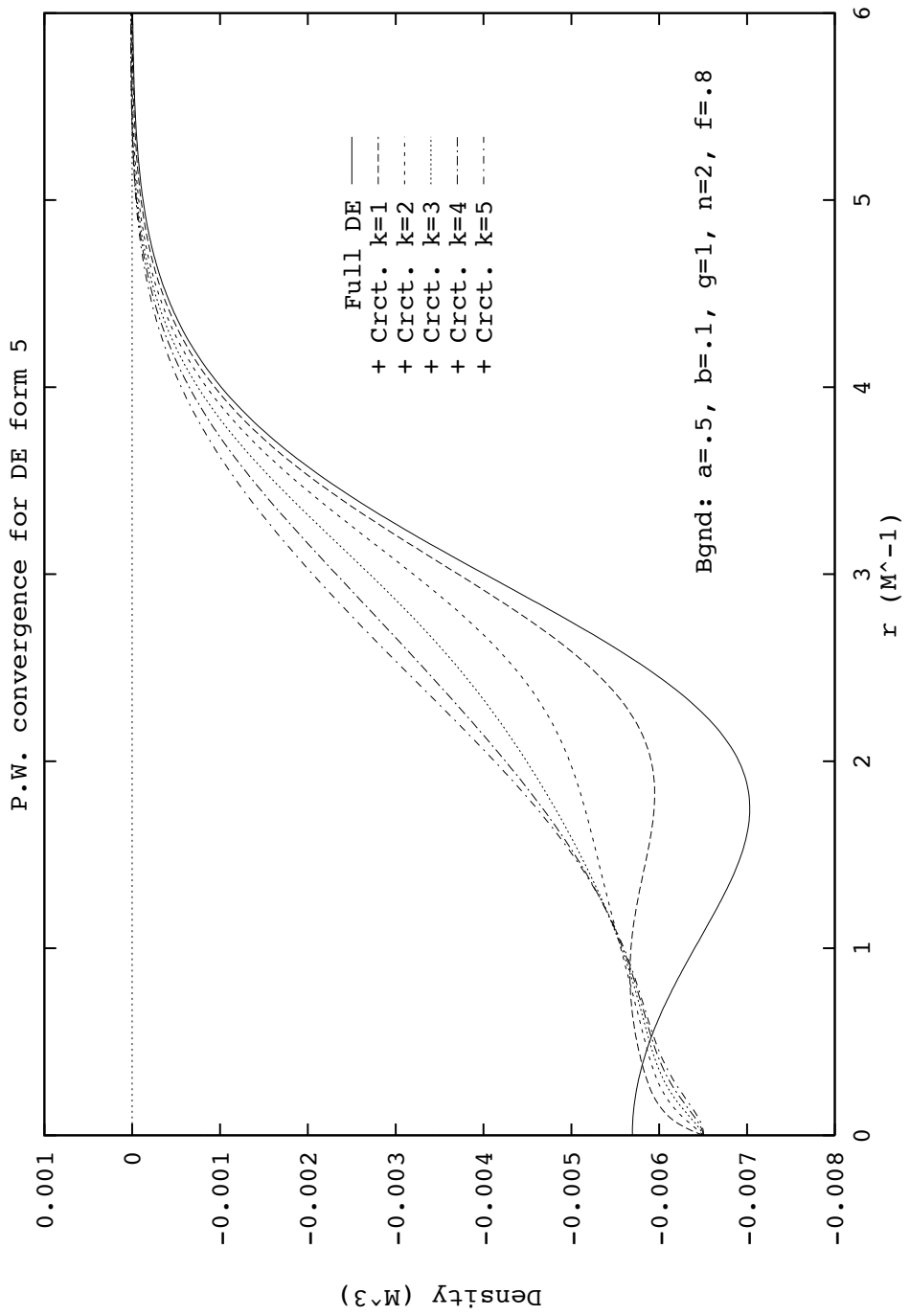

Figure 3.7: Convergence with partial wave for Form 5 of the correction functional in a sizeable background.

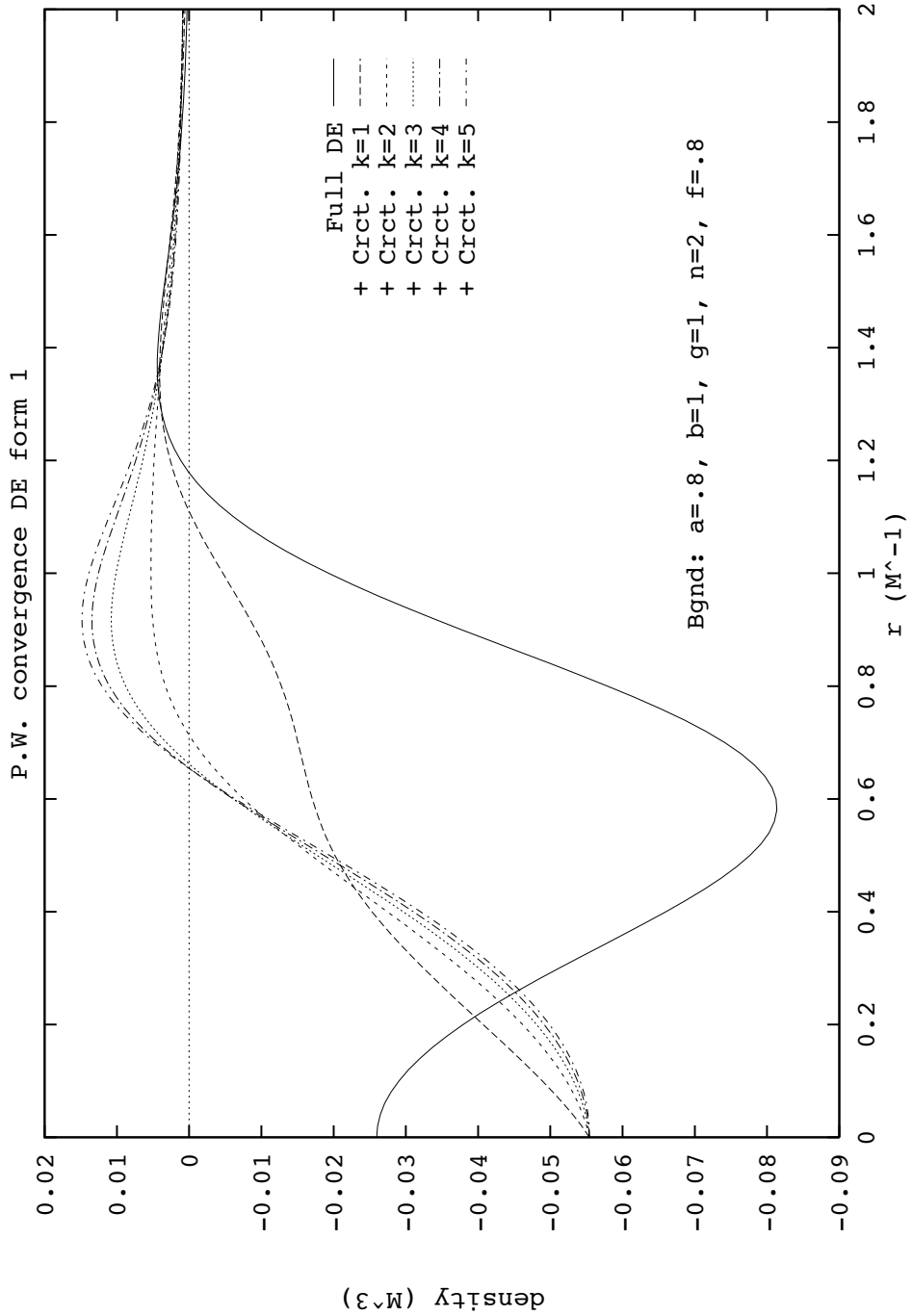

Figure 3.8: Convergence with partial wave for Form 1 of the correction functional in a deep narrow background.

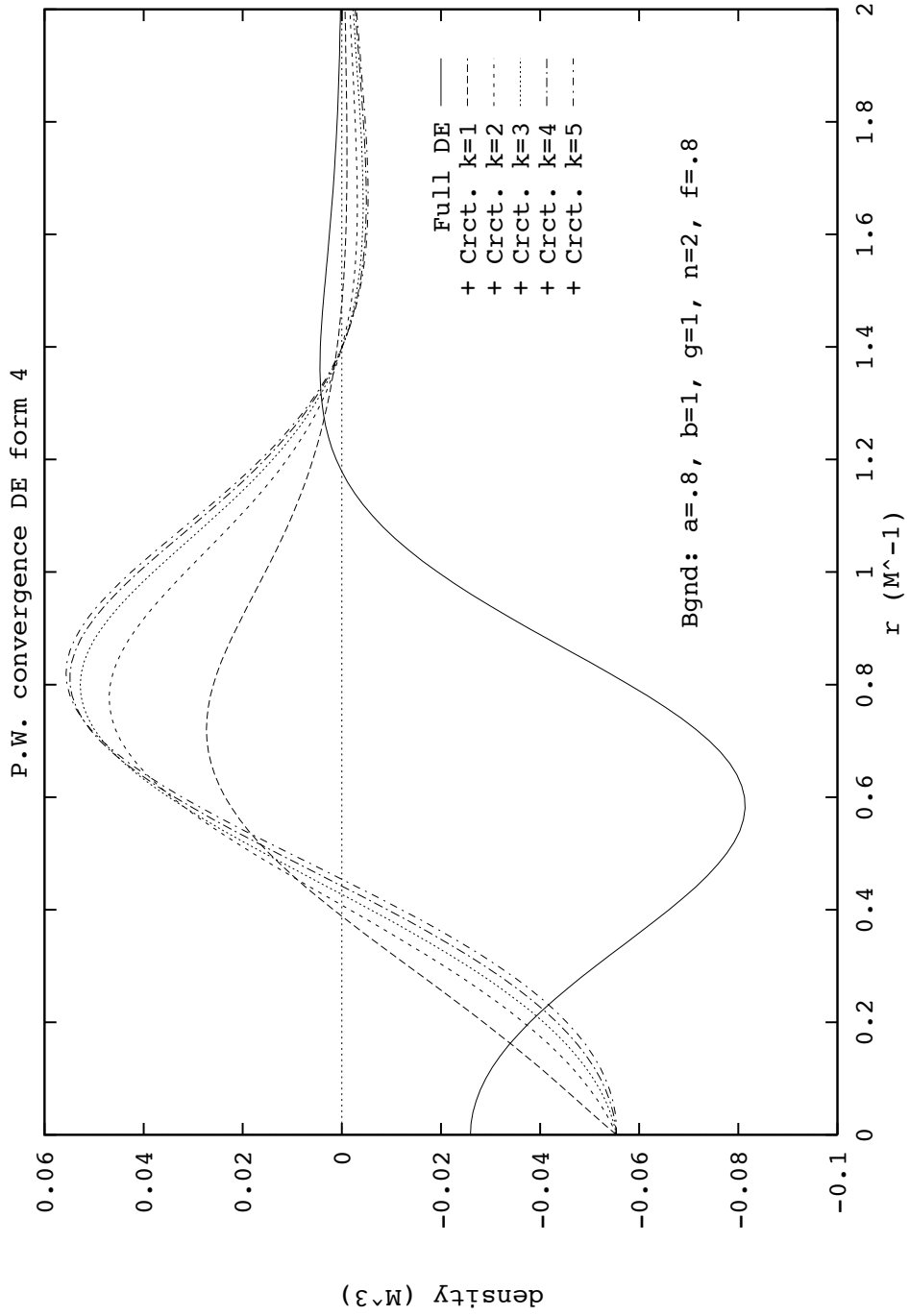

Figure 3.9: Convergence with partial wave for Form 4 of the correction functional in a deep narrow background.

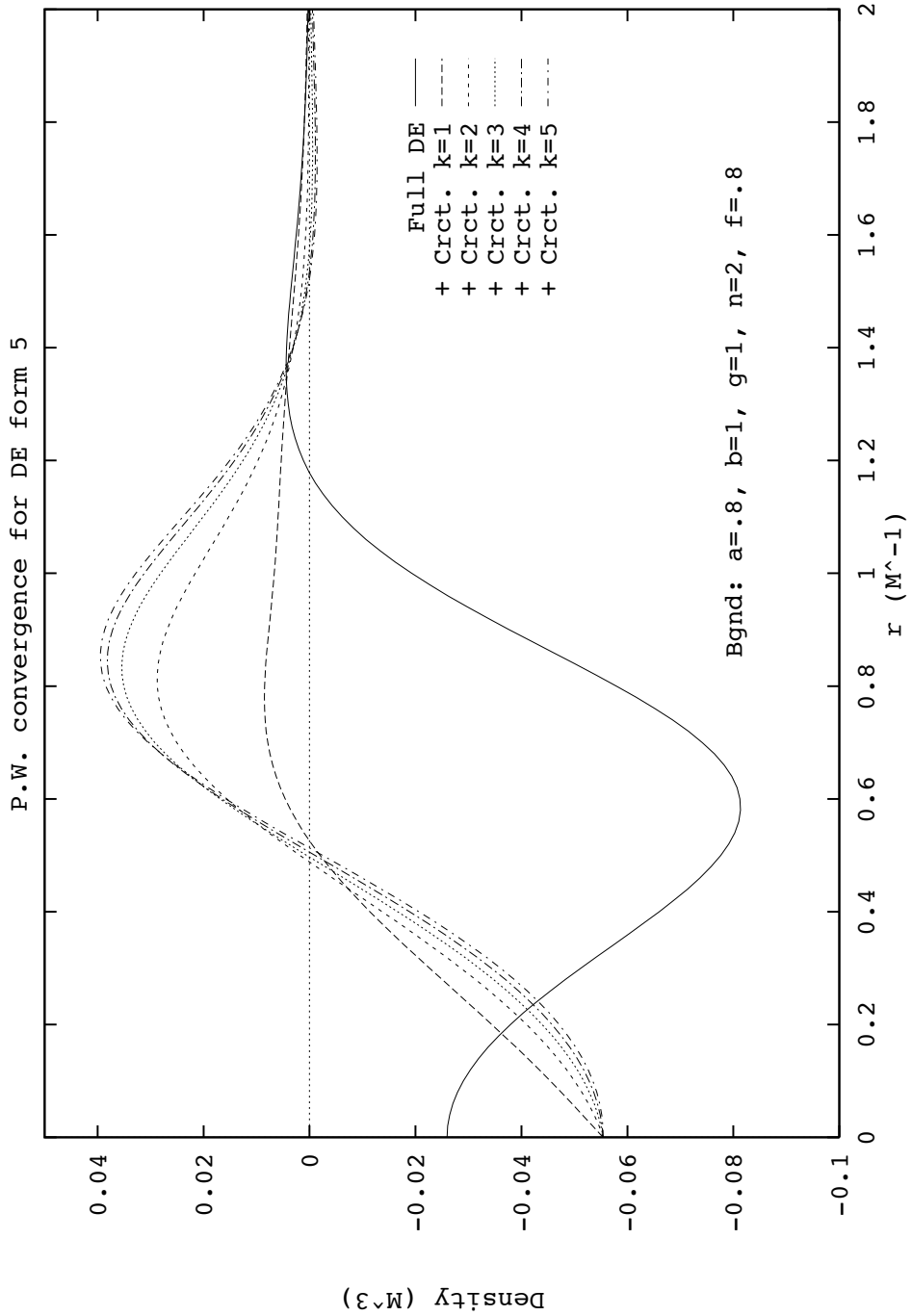

Figure 3.10: Convergence with partial wave for Form 5 of the correction functional in a deep narrow background.

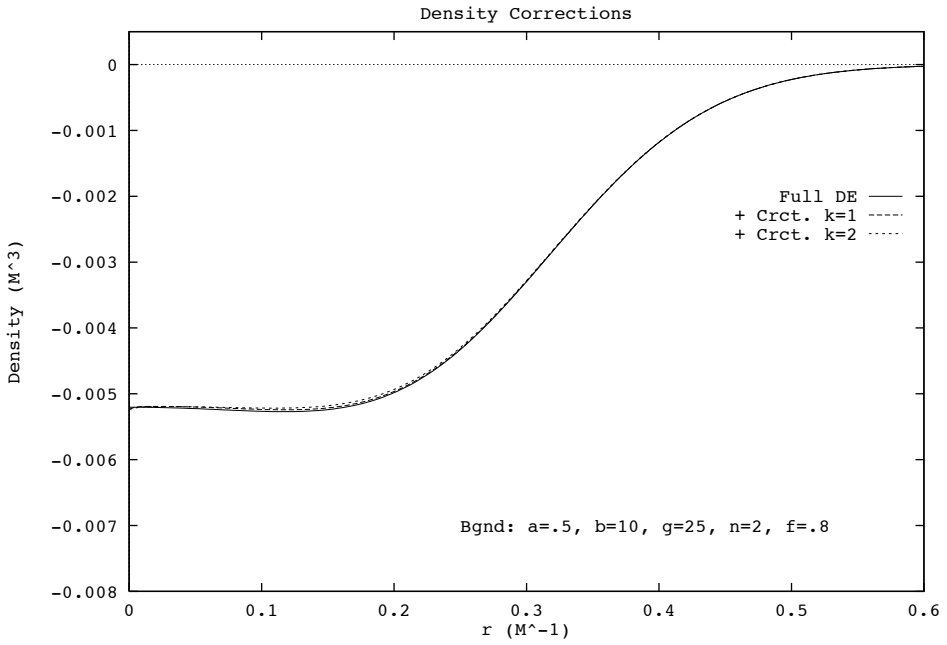

Figure 3.11: Vanishing correction when the DE is convergent. The partial wave corrections are shown to be consistent, with essentially zero correction for a case where we expect the 2nd order DE to be convergent

3.2.5 Size of the correction for different background fields

Here we consider how varying the shape of the background field affects the size of the correction. The graphic approach here is analogous to the approach taken in section 2.4. In particular, we will be able to pinpoint the region where the derivative expansion is convergent by second order. The shape of the potential is varied by changing the parameters (a and b) while ($g = 25$, $n = 2$, $f = .8$) are fixed. For consistency we first consider the case analogous to figure 2.6, where we expect that the DE will have converged for all r by second order. In figure 3.11 we see the result of correcting the 2nd order DE (in the manner of equation (3.47)) with two partial wave terms is essentially no change.

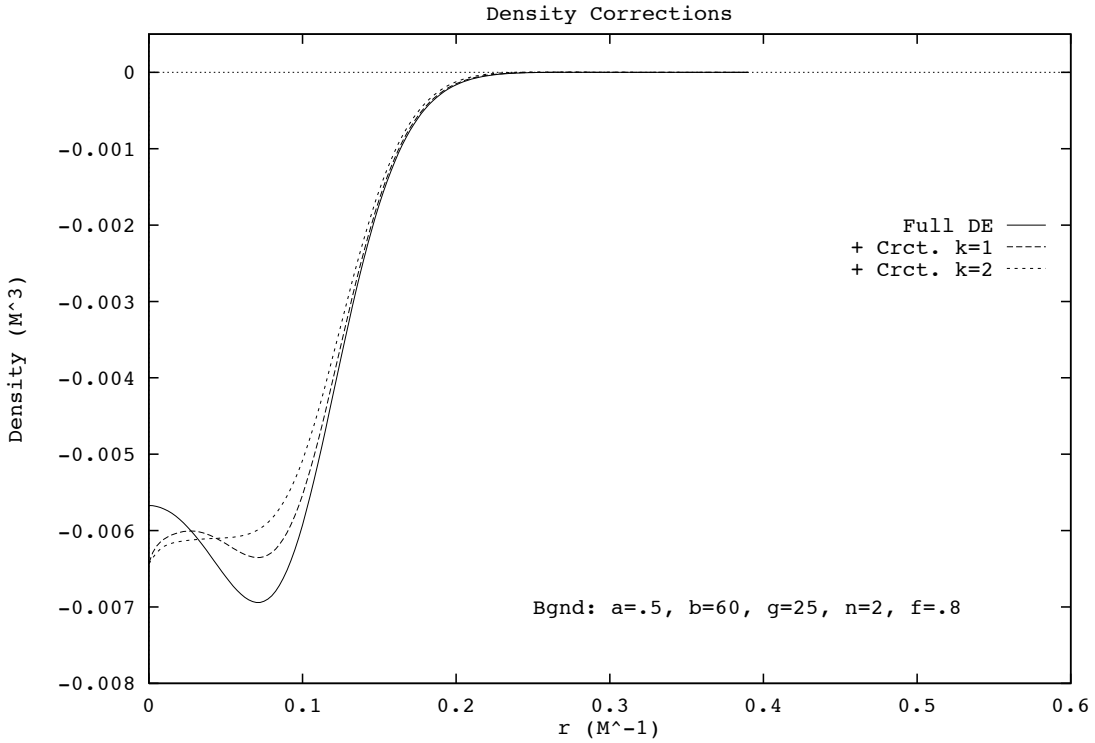

Figure 3.12: Partial wave corrections for a narrow potential.

Now consider changing the width of the potential for a fixed depth of $a = .5$. As we decrease the width, figure 3.12, the DE begins to break down near the origin and a nonzero correction appears. In figure 3.13 we squeeze the potential even more and see that the correction is needed even further out from $r = 0$. The densities here have at most one internal zero.

Finally consider what happens when we increase the depth. The sequence of plots in figures 3.14 and 3.15 have a fixed $b = 30$ and various a. Notice that for many potentials we require more partial wave contributions than the two shown to obtain the exact result. However, we do obtain the *exact* result at $r = 0$ as only $\Delta\rho_1$ is nonzero there.

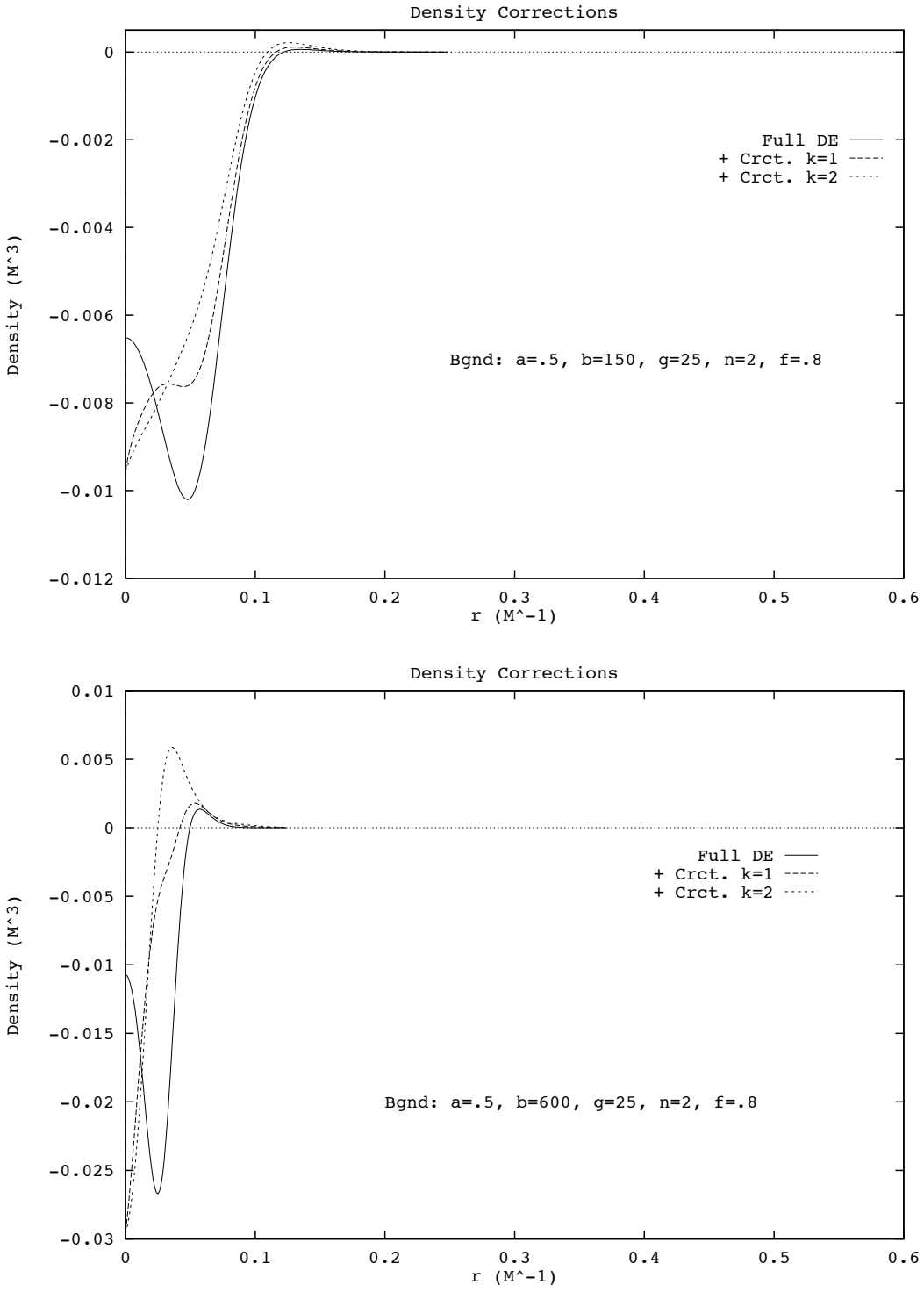

Figure 3.13: Partial wave corrections for very narrow potentials.

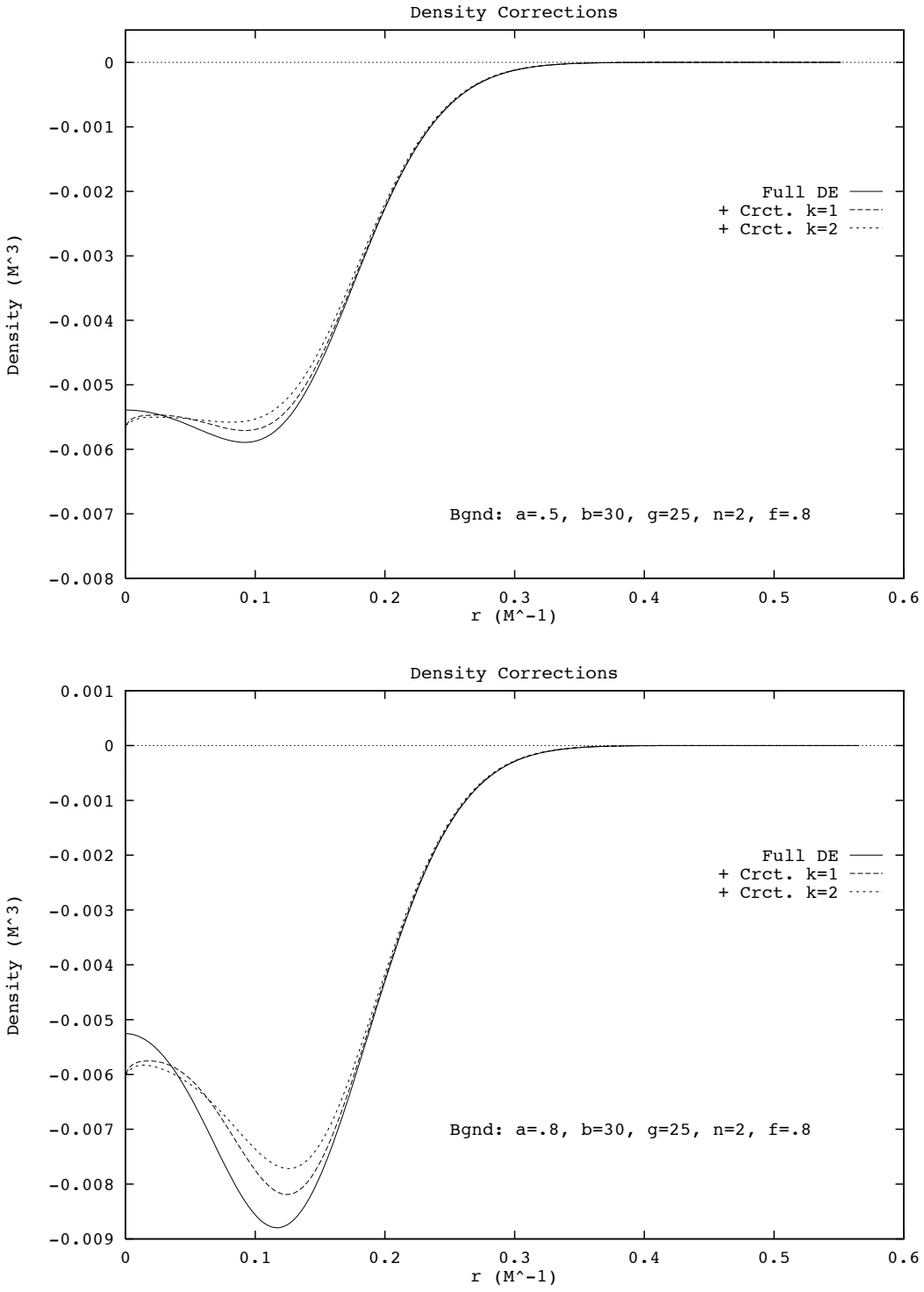

Figure 3.14: Partial wave contributions for deep potentials.

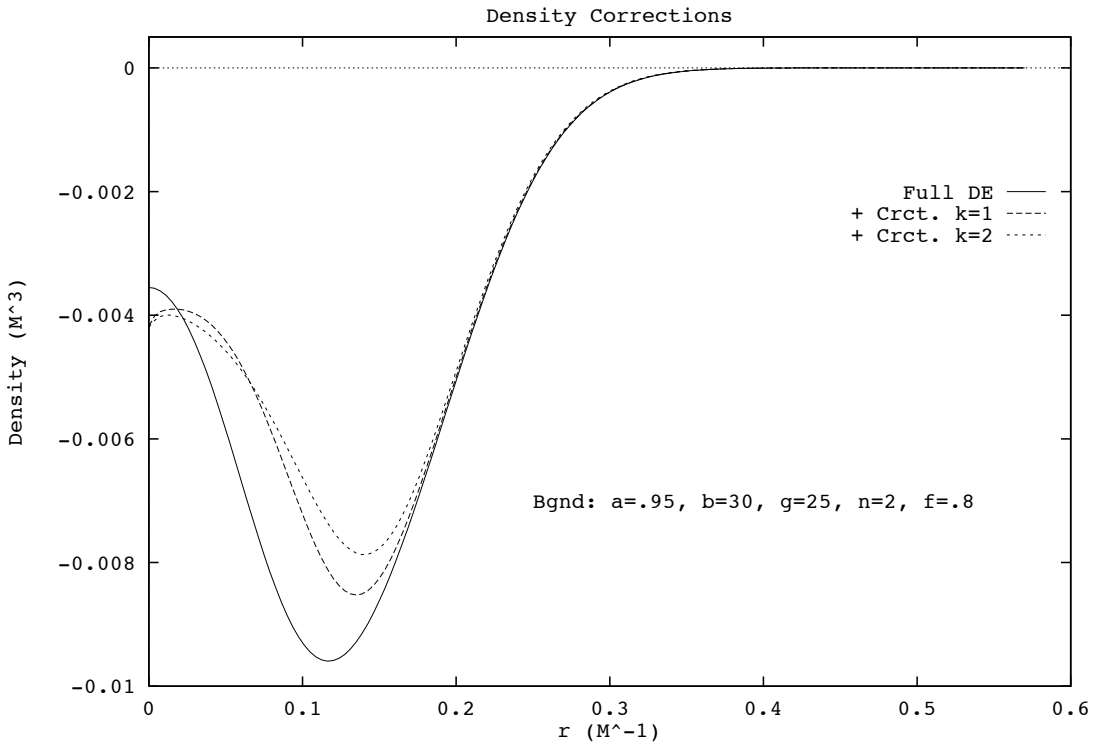

Figure 3.15: Partial wave corrections for a very deep potential.

Chapter 4

QHD SELF-CONSISTENT CALCULATION

Here we consider the effect of including the one-loop vacuum effects via the DE in the context of a relativistic bound state calculation. In this chapter we consider a case where the DE expansion is convergent when terms up to second order in the derivatives are included. This enables us to investigate the vacuum effects in a non-trivial model, while dealing directly with the coupled nonlinear dynamical equations. We consider a renormalizable relativistic meson exchange theory with interacting fermions (nucleons ψ), scalar bosons (sigma ϕ), and vector bosons (omega V_0, rho b_0, and photon A_0) referred to as QHDII [3]. The size of DE effects for finite nuclei was first considered by Perry [17] for the fixed background field obtained from a LDA self-consistent solution (often referred to as the relativistic Hartree approximation, RHA). Self consistent solutions including the derivative terms have been performed by Wasson [39]. Though unpublished, it is known that these effects were also considered by Fox[1]. The aim of using this model to describe finite nuclei here will be to generalize the results of references [39] and [40]. These previous results are extended by including the nonlinear scalar interaction terms along with their associated derivative expansion, and the use of a more general renormalization method. We also take the photon as coupling to the charge of the protons in nuclei (as opposed to the method of [39]). It is important to keep in mind the aim of observing the effect of the vacuum terms in a self-consistent calculation. We will reduce the number of free parameters in the finite nuclei model by requiring the energy per nucleon to saturate

[1] W. R. Fox, Ph.D. thesis, referred to by [15].

at a specified Fermi level in nuclear matter.

Current phenomenological models of finite nuclei and nuclear matter often take more complicated forms than this older prototype model. For example, more recent relativistic models of finite nuclei often include the pion and other mesons, and possibly the effects of chiral symmetry [41, 42]. Note that even though the pion is the lightest meson, no pions are included here. This is acceptable because the neutral scalar and vector mesons are the most important for modeling bulk properties [15]. For models of infinite nuclear matter, higher orders in the loop expansion have been considered [43]. Also, the possibility of forming neutral or charged kaon condensates is of theoretical interest [44]. It is in the interest of illustrating the one-loop effects that we choose not to overcomplicate the model described below.

4.1 QHD model

A model of finite nuclei is desired that can reproduce the shell structure of bound valence nucleons. Essentially we will extend the model used by Fox [40] by including the derivative terms in the vacuum densities derived from both fermionic and bosonic loops. Also, in the manner of Rudaz et. al. [45], we will vary the choice of our three and four body renormalization point for the fermion loops. The Lagrangian density for finite nuclei is [3]

$$\begin{aligned}\mathcal{L}_{QHDII} &= \bar{\psi}[i\partial\!\!\!/ - g_v\gamma_0 V_0 - g_\rho\tau_3\gamma_0 b_0 - e\tfrac{1}{2}(1+\tau_3)\gamma_0 A_0 - (M - g_s\phi)]\psi \\ &\quad + \left((\tfrac{1}{2}\partial_\mu\phi)^2 - U(\phi)\right) - \tfrac{1}{2}\left((\partial_\mu V_0)^2 - m_v^2 V_0^2\right) - \tfrac{1}{2}(\partial_\mu A_0)^2 \\ &\quad - \tfrac{1}{2}\left((\partial_\mu b_0)^2 - m_\rho^2 b_0^2\right). \end{aligned} \tag{4.1}$$

Here the scalar field interaction is written

$$U(\phi) = \frac{m_s^2}{2}\phi^2 + \frac{\kappa}{3!}\phi^3 + \frac{\lambda}{4!}\phi^4. \tag{4.2}$$

An extension is made here of the field equations given in [3] by including vacuum density terms, as well as the general scalar interactions via $U(\phi)$:

$$\begin{aligned}
\nabla^2\phi - U'(\phi) &= -g_s(\rho^s_{val} + \rho^s_{vac} + \rho^{nl}_{vac}) && (4.3)\\
\nabla^2 V_0 - m_v^2 V_0 &= -g_v(\rho^v_{val} + \rho^v_{vac}) && (4.4)\\
\nabla^2 b_0 - m_\rho^2 b_0 &= -g_\rho(\rho^b_{val}) && (4.5)\\
\nabla^2 A_0 &= -e(\rho^\gamma_{val}) && (4.6)\\
\mathcal{M}_r \begin{pmatrix} G_\kappa(r) \\ F_\kappa(r) \end{pmatrix} &= 0 \qquad \text{with} \quad \int_0^\infty dr \left(|G_\kappa|^2 + |F_\kappa|^2\right) = 1. && (4.7)
\end{aligned}$$

Here $\mathcal{M}_r$ is the 2×2 operator which implements the radial Dirac equation,

$$\mathcal{M}_r = \mathbf{1}\frac{d}{dr} + \sigma_{\mathbf{3}}\frac{\kappa}{r} - i\sigma_{\mathbf{2}}(E - g_v V_0 - t_a g_\rho b_o - (t_a + \tfrac{1}{2})eA_0) - \sigma_{\mathbf{1}}(M - g_s\phi). \quad (4.8)$$

The valence fermion density contributions are

$$\begin{aligned}
\rho^s_{val} &= \sum_a \left(\frac{2j_a+1}{4\pi r^2}\right)\left[|G_\kappa|^2 - |F_\kappa|^2\right] && (4.9)\\
\rho^v_{val} &= \sum_a \left(\frac{2j_a+1}{4\pi r^2}\right)\left[|G_\kappa|^2 + |F_\kappa|^2\right] && (4.10)\\
\rho^b_{val} &= \sum_a \left(\frac{2j_a+1}{4\pi r^2}\right)\left[|G_\kappa|^2 + |F_\kappa|^2\right](-1)^{t_a - 1/2} && (4.11)\\
\rho^\gamma_{val} &= \sum_a \left(\frac{2j_a+1}{4\pi r^2}\right)\left[|G_\kappa|^2 + |F_\kappa|^2\right](t_a + \tfrac{1}{2}). && (4.12)
\end{aligned}$$

The filled shells are characterized by the quantum numbers $a = (n, \kappa, t)$ and $j = |\kappa| - \frac{1}{2}$. The isospin parameter $t_a = \pm\frac{1}{2}$ differentiates between the proton and neutron states.

Note in (4.6) that only the scalar sigma meson and the vector omega meson have terms representing vacuum contributions. The sigma meson equation is the only one whose vacuum contribution will contribute at the LDA level. The others don't contribute as a consequence of isovector and electromagnetic current conservation and the conservation of baryon number. For the derivative expansion there will

be contributions to all of the boson equations, however only the sigma and omega contributions will be significant [15].

It is sufficient to evaluate the vacuum density contributions using the DE to second order. The validity of this statement can easily be seen from the characteristic size of the scalar field. It turns out that the size of this field can be modeled by the parameters from section 2.4 as (a=.3, b=.005, f=.7, n=2, g=1). Thus, the depth is approximately one-third the mass of a nucleon and the width corresponds to about 3 fm, or 0.6 M^{-1}. In figures 2.6 and 3.11 we saw that even for a deeper narrower potential no corrections beyond the 2nd order DE are necessary.

The choice of renormalization here is as follows. For the self interactions of the scalar sigma field, we renormalize in such a way so that the first nonzero contributions occur beyond the four body term,

$$\frac{d^n U_B(\phi_0)}{d\phi^n} = 0, \qquad n = 0, 1, \ldots, 4. \tag{4.13}$$

The parameters in (2.13) are therefore [15]

$$\begin{aligned} W(x) &= m_s^2 + \kappa\phi + \frac{\lambda}{2}\phi^2, \\ W_0 &= m_s^2, \\ f_b(\phi) &= -\frac{1}{3}\left(\frac{\kappa\phi}{m_s^2}\right)^2\left(\frac{\kappa\phi}{m_s^2} + \frac{3\lambda\phi^2}{2m_s^2}\right) + \frac{1}{12}\left(\frac{\kappa\phi}{m_s^2}\right)^4. \end{aligned} \tag{4.14}$$

Thus the couplings κ and λ will not be shifted by the self interacting scalar vacuum. For the fermionic contribution we renormalize following [45]:

$$\begin{aligned} \frac{d^n U_s(\phi_0)}{d\phi^n} &= 0 \quad (n = 0, 1, 2), \qquad \frac{d^3 U_s(\mu)}{d\phi^3} = 0, \\ \frac{d^4 U_s(\mu)}{d\phi^4} &= 0, \qquad\qquad Z_{1s}(\sigma = \sigma_0) = 0. \end{aligned} \tag{4.15}$$

This fixes the parameters in (2.6) as

$$\begin{aligned} f_0 = \ln(\mu/\sigma_0), \qquad f_1 &= 1 - 4\ln(\mu/\sigma_0), \qquad f_2 = -\frac{7}{2} + 6\ln(\mu/\sigma_0), \\ f_3 = \frac{25}{3} - 4\frac{\mu}{\sigma_0}, \qquad f_4 &= -\frac{25}{12}, \qquad\qquad z_{1s} = 0. \end{aligned} \tag{4.16}$$

Here and in the following we will make use of the notation

$$\sigma(x) = M - g_s\phi(x), \quad \text{and} \quad \sigma_0 = M, \tag{4.17}$$

to simplify and connect the form of the equations to our previous results. The utility of the renormalization (4.16) is essentially to allow three and four body effective vacuum forces to contribute along with the nuclear matter mean field many body terms. Note that we have reduced the generality of the model by allowing contributions here from only fermionic and not bosonic loops. The parameter μ is now not independent of κ and λ, but really gives a one-loop renormalization of their values. With these specifications the vacuum densities to 2nd order in the DE are

$$\begin{aligned}\rho^s_{vac}(r) &= -\frac{1}{4\pi^2}\Big(\sigma^3(4\ \ln(\frac{\sigma}{\mu})+1) - f_1M^3 - 2f_2M^2g_s\phi \\ &\qquad -3f_3M(g_s\phi)^2 - 4f_4(g_s\phi)^3\Big) \\ &\quad -\frac{1}{4\pi^2}\left(2\ln(\frac{\sigma}{M})g_s^2\phi''(r) - \frac{1}{\sigma}((g_s\phi'(r))^2 + \frac{2}{3}(g_vV_0'(r))^2)\right), \end{aligned} \tag{4.18}$$

$$\rho^v_{vac}(r) = -\frac{1}{3\pi^2}\left(\ln(\frac{\sigma}{M})g_vV_0''(r) - \frac{1}{\sigma}g_vg_sV_0'(r)\phi'(r)\right), \tag{4.19}$$

$$\begin{aligned}\rho^{nl}_{vac}(r) = -\frac{m_s^4}{64\pi^2g_s}\Big\{2\left(\frac{\kappa+\lambda\phi}{m_s^2}\right)\left[\left(\frac{1+\kappa\phi+\frac{1}{2}\lambda\phi^2}{m_s^2}\right)\ln\left(\frac{1+\kappa\phi+\frac{1}{2}\lambda\phi^2}{m_s^2}\right)\right] \\ -\left(\frac{\kappa\phi+\frac{1}{2}\lambda\phi^2}{m_s^2}\right) - \left(\frac{\kappa\phi}{m_s^2}\right)\left(\kappa\phi+\tfrac{1}{2}\lambda\phi^2\right) + \frac{1}{3}\left(\frac{\kappa}{m_s^2}\right)^4\phi^3\Big\} \\ - \frac{1}{48\pi^2g_s}\frac{(\kappa+\lambda\phi)}{(m_s^2+\kappa\phi+\frac{1}{2}\lambda\phi^2)}\left(-\frac{(2\lambda m_s^2-\kappa^2)(\phi'(r))^2}{(m_s^2+\kappa\phi+\frac{1}{2}\lambda\phi^2)} - 2(\kappa+\lambda\phi)\phi''(r)\right). \end{aligned} \tag{4.20}$$

Now that all quantities have been specified, we can proceed with the solution of the equations of this section. The method employed is that of relatively straight forward iteration. The radial Dirac equation is solved using 4th order Runge-Kutta techniques to shoot to a matching point. Continuity at this point enables us to obtain a new estimate for the appropriate eigenvalue. The Poisson-like equations are solved using finite difference methods, while iteratively including nonlinear terms. Some

degree of technique is required to keep the routine stable, but as a whole the method is very successful.

4.2 Fitting the parameters

Having completed the specification of our model we now consider the requirements that are imposed on the parameters ($M, m_s, m_v, m_\rho, g_s, g_v, g_\rho, e, \kappa$, and λ). Of these, the following masses are fixed at their experimental values:

$$M = 939 \text{ MeV}, \quad m_v = 783 \text{ MeV}, \quad m_\rho = 770 \text{ MeV}, \tag{4.21}$$

with the exception that we use the true nucleon masses for the proton and neutron (M_p=938.28 MeV, M_n=939.57 MeV) when solving the radial Dirac equation. Two couplings are also fixed:

$$\alpha = \frac{e^2}{4\pi} = \frac{1}{137.035}, \qquad \text{and} \qquad g_\rho = 4.038. \tag{4.22}$$

The first is the accepted value (at our energy scale) for the electromagnetic coupling, while the latter is the value fit from requiring a symmetry energy of 35 MeV for the Mean Field Model of nuclear matter [15, 40]. As these previous models have found very little sensitivity to the parameter g_ρ, we simplify our description by fixing it at this value, even though, for complete generality g_ρ should be fit self-consistently with the other parameters that are determined in nuclear matter.

In nuclear matter for a given m_s we fit the couplings g_s and g_v by requiring a binding energy per nucleon of -15.75 MeV at $k_F = 1.30$ fm^{-1}. To model infinite nuclear matter (an equal infinite number of neutrons and protons) several simplifications can be made to the model of finite nuclei described in the last section. We may neglect electromagnetic effects and, as mentioned above, also the rho meson. The remaining scalar and vector mesons fields are then fixed at constant values by the translational symmetry of the infinite medium. The field equations fix the vector meson field in terms of the baryon number density. The nucleon equation has the standard form of

a plane wave solution with shifted mass and energy, as noted previously (section 1.4). The only equation that remains to be solved is the specification of the scalar field. The scalar field will depend on the nucleon field solution, which also has nontrivial scalar field dependence. Therefore, there remains a single transcendental equation to solve for ϕ which minimizes the effective energy. Note that the LDA vacuum densities contribute to this equation, but the higher order DE terms do not. The equation may be written [15]

$$\begin{aligned}\sigma &= M - \frac{g_s^2}{m_s^2 2\pi^2}\left(\sigma^3\ln(\sigma) + k_F\sigma(k_F^2+\sigma^2)^{\frac{1}{2}} - \sigma^3\ln(k_F+(k_F^2+\sigma^2))^{\frac{1}{2}}\right) \\ &\quad -\frac{g_s^2}{m_s^2}\left(\rho_s^{vac}+\rho_{nl}^{vac}\right) \qquad \text{with no derivative terms} \\ &\quad +\frac{g_s^s}{m_s^2}\left(\frac{\kappa\phi^2}{2g_s^3}+\frac{\lambda\phi^3}{6g_s^4}\right). \end{aligned} \tag{4.23}$$

Finally, we fix one parameter in finite nuclei, the scalar mass m_s. The parameter m_s is set to a value that gives the correct charge radius for ^{40}Ca. When the nonlinear couplings κ and λ are nonzero, the nuclear matter calculation will depend explicitly on the value of m_s, and we must iterate the two calculations to reach final values. This is not a problem when the nonlinear terms are left out. In this case the coupling g_s will scale with m_s in the same manner throughout the nuclear matter equations, so that the value of m_s may then be independently determined in the finite nucleus calculation.

The remaining unspecified parameters in this model are the many body couplings (κ, λ, μ), which as we mentioned above, can be regrouped into renormalized couplings at the one-loop level

$$\kappa' = \kappa + \frac{6g_s^3}{\pi^2 M}\left(1 - \frac{\mu}{M} + \ln(\frac{\mu}{M})\right), \tag{4.24}$$

$$\lambda' = \lambda - \frac{6g_s^3}{\pi^2}\ln(\frac{\mu}{M}). \tag{4.25}$$

Usually in a renormalization procedure, we have a physical idea or quantity which we use to fix the *meaning* of the parameters in our model. (For example, we renormalize

so that a mass m is the physically observable mass, which from unitarity must be taken as the pole in the exact propagator [12].) However, here we have not made such a choice to define the physical meaning of the parameters κ and λ. Instead they are treated as an additional manner in which we can adjust the model. If a physical specification had been made, then the original coupling parameters of the theory may be modified at one-loop, giving us new couplings κ' and λ' which satisfy this specification. The value of the parameter μ would then telling us how the original couplings were modified to maintain our specification.

Equations (4.24) and (4.25) allows us the freedom of removing the μ dependence in the fermion renormalization by including it explicitly in the new parameters κ' and λ'. Instead we choose to use the equations as given previously, and simply note that this functional inter-dependence exists.

4.3 Nuclear matter

The quality of different models (κ, λ, μ) can be assessed by looking at experimentally determined quantities. A representative range of models is given in table 4.1.

The first four models do not include nonlinear scalar terms, and simply consider the effect of μ. The fifth model is the MFA, and is the only model which does not include any vacuum terms. Models six through eight have nonlinear self-coupling terms and both fermionic and bosonic one-loop contributions. Two of the parameter sets here (6,7) were chosen to correspond to the most promising nonlinear models considered in [40]. The last model, number 9, has nontrivial μ ($\mu/M = 1.2$), as well as nonlinear terms (nonzero κ and λ). All of the values in table 4.1 are a result of the fit to nuclear matter and finite nuclei using a value of $r_{rms}^{ch} = 3.483 \pm 0.001$ fm for the root mean square charge radius of ^{40}Ca.

In nuclear matter we have extracted the compressibility K, and skewness S/K

Table 4.1: Parameters from the self-consistent solution of the QHD model of nuclear matter and finite nuclei with derivative corrections.

Model No.	μ/M	κ/M	λ	K	S/K	σ/M	m_s	g_s	g_v
1	0.738277	0	0	149.4	3.881	0.738277	579	10.6250	9.9482
2	0.8	0	0	386.5	11.669	0.6567	790	15.4476	11.7172
3 (RHA)	1.0	0	0	452.5	5.933	0.7306	534	8.5840	10.1281
4	1.2	0	0	280.0	4.033	0.8111	423	6.2436	8.0181
5 (MFT)	1.0	0	0	546.8	9.938	0.5406	515.5	10.3835	13.8055
6	1.0	+5.3248	100	313.8	4.801	0.7826	560	8.6330	8.8253
7	1.0	−1.0650	10	492.5	5.999	0.7217	547	8.8147	10.3339
8	1.0	10.7029	400	397.3	4.241	0.8103	672	9.8886	8.0435
9	1.2	3.1949	100	237.6	3.416	0.8391	440	6.3285	7.1335

[45]

$$K = k_F^2 \frac{d^2}{dk_F^2}(E/A), \qquad S = k_F^3 \frac{d^3}{dk_F^3}(E/A), \tag{4.26}$$

as well as the effective mass ratio σ/M. We may then determine for which models they approach the experimentally favored ranges [15]

$$200 \text{ MeV} < K < 350 \text{ MeV}, \qquad 0.58 < \frac{\sigma}{M} < 0.65, \tag{4.27}$$

and where S/K fits breathing mode data [45]. Rudaz et. al. [45] have noted that for $\kappa = 0$, $\lambda = 0$ the effect of varying the parameter μ is to prescribe a semicircle in the K, S/K plane. The results for the models we are considering are summarized in figure 4.1. From this figure we see that models 4, 6, and 9 are favorable. However, when we examine the effective mass ratio σ/M in table 4.1, we see that these three models all fall outside the desired range. The models which have a more acceptable effective mass (2 and 5) do not satisfy both of the restrictions on K and S/K. This is known to be a generic feature of this type of finite nuclei model [15, 40].

As a result of the nuclear matter fit we would choose to favor models (2, 4, 6, and 9). Note that the limits from K and S/K make both the MFA and RHA unfavorable. The conclusion of [45] was to favor a value of $\mu = 1.2$, as not only does this value agree with the experimental limits, but also gives the most stable minimum for the effective scalar field potential. There is yet another aspect of this stability, which appears when we consider the effect of nonzero κ and λ. Changing these parameters has the effect of shrinking and shifting the μ semicircle, however the points corresponding to μ around 1.2 remain highly stationary. This can be seen in figure 4.2. This fact gives us an extra amount of freedom in the evaluation of this model for finite nuclei. With a value of $\mu = 1.2$ we can essentially adjust κ and λ for the finite nuclei without having much effect on K and S/K in nuclear matter. As a result of this, model 9 has been introduced. Since we are not that interested in finding a rigorous fit to the nuclei here, the nonlinear couplings of 9 were simply chosen.

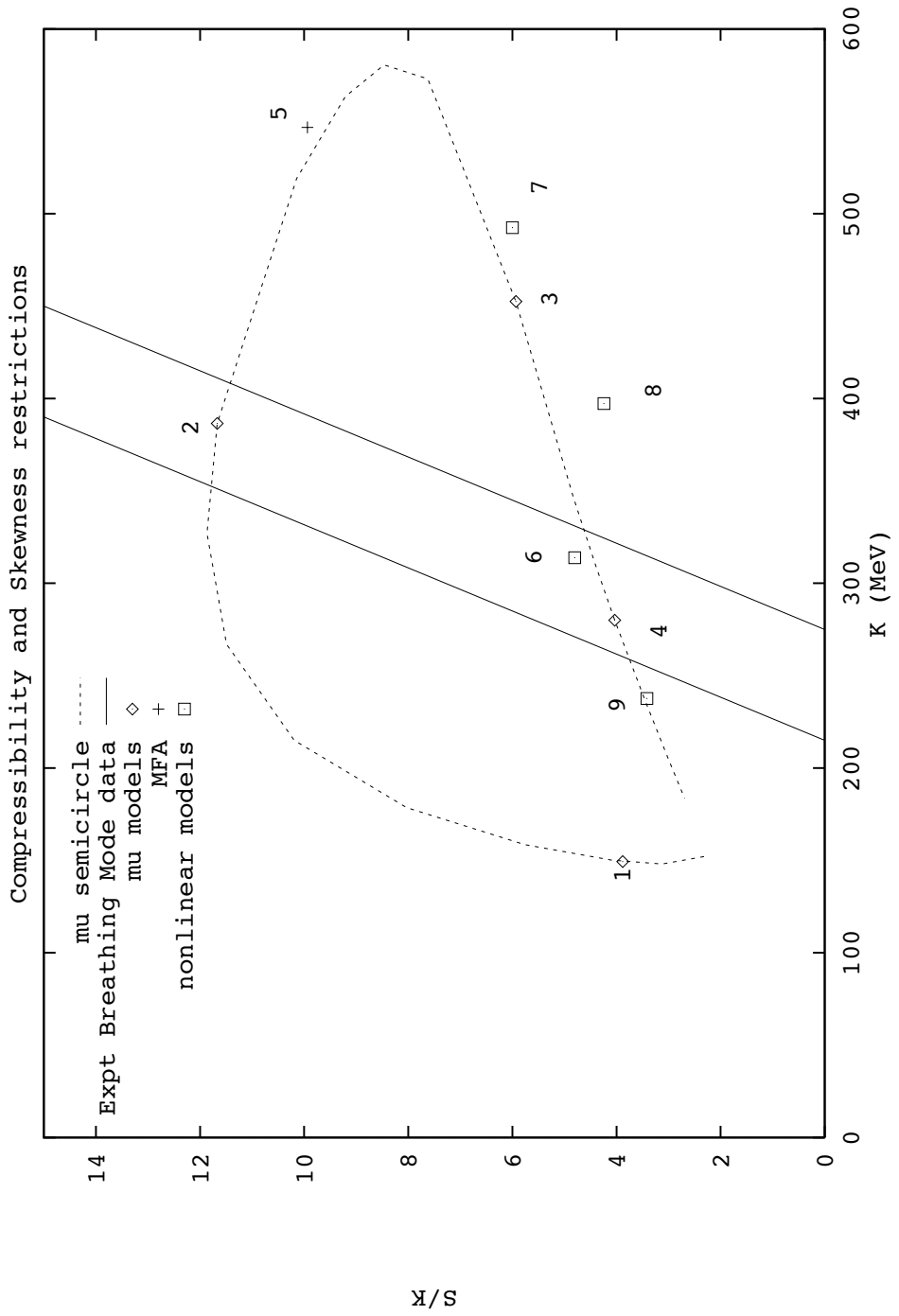

Figure 4.1: Nuclear matter models in K, S/K parameter space with experimental limits. The semicircle is inscribed by different values of the parameter μ.

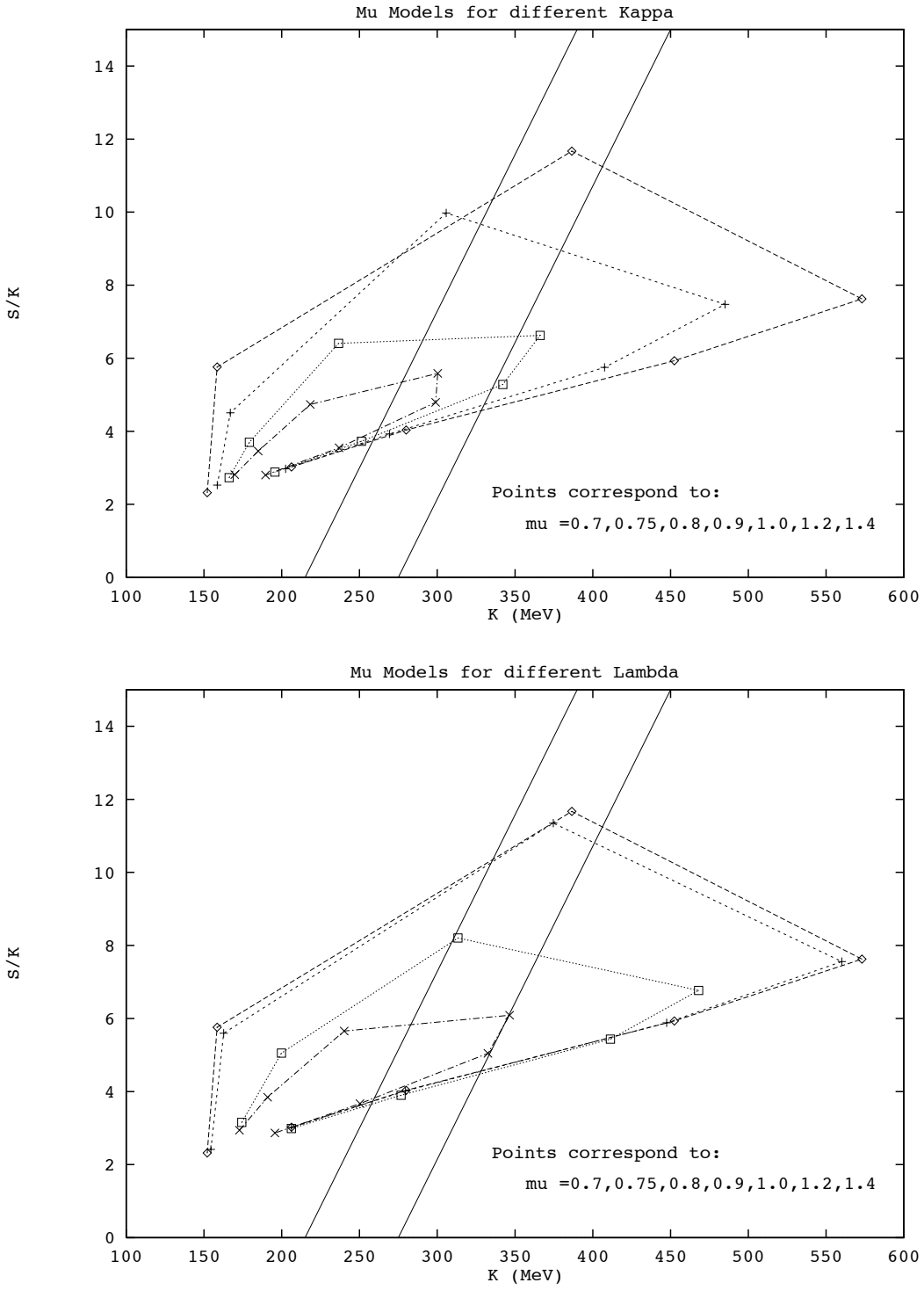

Figure 4.2: Effect of varying κ and λ on the μ curve in K, S/K parameter space.

4.4 Finite nuclei with derivative corrections

Consider the effect that the second order DE terms have in fitting the charge radius of ^{40}Ca. In figure 4.3 and table 4.2 we see the magnitude of the DE effects.

A generic feature of the solution for all models is that the DE terms smooth out the form of the bosonic fields. This can be seen in the first plot of figure 4.3, which shows the scalar field of model 3 and the change in this model when the DE terms are dropped with the parameters left fixed. The second plot of this figure shows the separate contributions to the fermion scalar vacuum density at the point of self-consistent solution. The results are for model 7. One place where the effect of the DE terms can be physically seen is in the single particle nucleon energies in table 4.2. The energy results here are in qualitative agreement with what was found previously for model 3 [39]. We see in our table, that the DE terms have caused the nucleons to become more bound for models 6 and 4. Note that we have refit the models at the LDA level. The DE is observed to have only a small effect on the results in this table. This also shows up in the charge density distribution; for model 3 the DE effect was considered by Wasson, and was also found to be small [39].

The reason for this behavior is that the fields must rearrange themselves to satisfy a new parameter fit in the LDA. In particular, the couplings and scalar mass had to be changed as follows:

	LDA	DE
Model 6	$g_s = 4.4555$	$g_s = 8.6330$
	$g_v = 5.9842$	$g_v = 8.8253$
	$m_s = 310.$	$m_s = 560.$
Model 4	$g_s = 5.7565$	$g_s = 6.2436$
	$m_s = 390.$	$m_s = 423.$

We see that the internal setup of a model is changed to a great extent by the DE, but that the physical predictions are comparable in the end.

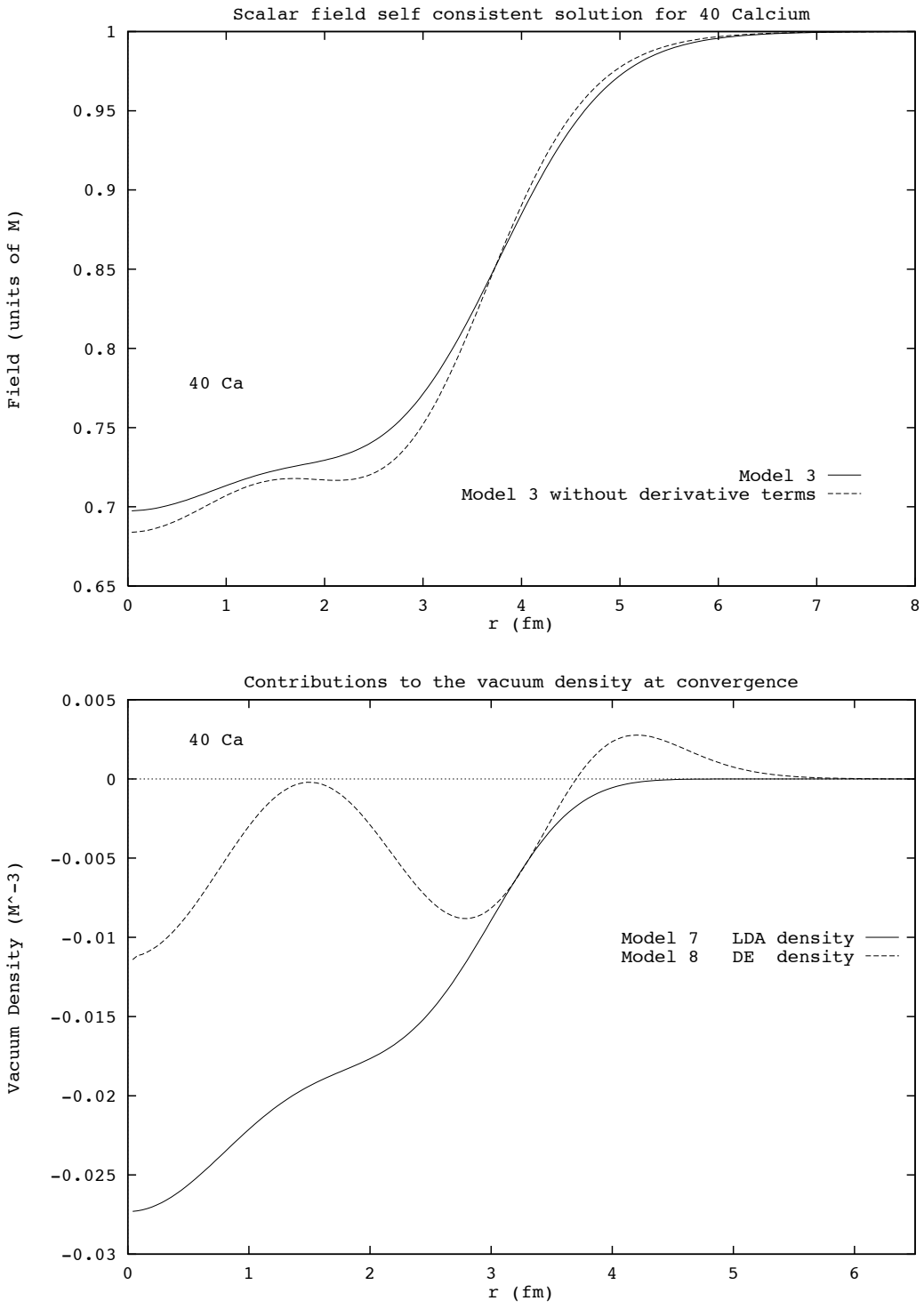

Figure 4.3: Effects of derivative terms on the self-consistent solution.

Table 4.2: Effect of the DE on the single particle nucleon self-consistent energies (in MeV) for models 6 and 4.

Particles	Level	Model 6		Model 4	
		LDA	DE (2nd order)	LDA	DE (2nd order)
protons:	$1s_{\frac{1}{2}}$	−33.3355	−35.1092	−34.2227	−34.3206
	$1p_{\frac{3}{2}}$	−22.7095	−23.8810	−23.1299	−23.3027
	$1p_{\frac{1}{2}}$	−22.0688	−22.5072	−21.9989	−22.1817
	$1d_{\frac{5}{2}}$	−11.2440	−11.7730	−11.2361	−11.4091
	$1s_{\frac{1}{2}}$	−8.5722	−7.7375	−7.8065	−7.8260
	$1d_{\frac{3}{2}}$	−10.1577	−9.4602	−9.3347	−9.5188
neutrons:	$1s_{\frac{1}{2}}$	−41.3730	−43.2126	−42.2908	−42.4019
	$1p_{\frac{3}{2}}$	−30.4489	−31.6770	−30.8943	−31.0806
	$1p_{\frac{1}{2}}$	−29.8193	−30.3201	−29.7779	−29.9744
	$1d_{\frac{5}{2}}$	−18.6638	−19.2512	−18.6774	−18.8686
	$1s_{\frac{1}{2}}$	−15.9263	−15.1593	−15.1722	−15.2224
	$1d_{\frac{3}{2}}$	−17.5819	−16.9375	−16.7739	−16.9785

To examine the usefulness of models we consider a standard complement of even-even nuclei: ^{16}O, ^{40}Ca, and ^{208}Pb. Using the parameters in 4.1, we resolve the differential equations (4.3–4.7) for the nuclei ^{16}O, and ^{208}Pb. To see how well all three nuclei are modeled, we consider the nuclear charge density. This density is obtained by folding the nuclear charge form factors over the densities we have determined for point like constituents. We use the form factor parameterization found in reference [46][2]. These may then be compared with the experimental data. This has been done

[2] A special thanks to P. Blunden for supplying the form factor folding code.

in the past for models 6 and 7 [40] without the derivative terms. In figure 4.4 we see how models with different μ do at determining the charge density of ^{40}Ca. Notice in particular that the model 4 with $\mu = 1.2$ does considerably better than the RHA model 3. It is interesting to note that model 1 seems to model the charge density near the origin even better than model 4.

In figures 4.5 and 4.6 we see how well the models we favored in nuclear matter do at reproducing the charge densities of the nuclei ^{16}O and ^{208}Pb respectively. These models include all DE terms, and also have different μ values. For ^{16}O we see that models 3 and 4 give essentially the same results. The nonlinear models do slightly worse, although this situation could likely be improved by doing a careful retuning of κ, and λ. Finally, for ^{208}Pb we see that model 3 gives the best results. Model 4 here has developed a spurious local minimum in the charge density, making it highly unrealistic. Note that model 9, which also has $\mu = 1.2$, does not suffer from this effect. The charge density of model 6 is found to be very similar to the charge density found by Fox [40] in his analogous Set J, using the LDA. The main difference is that the DE terms have increased the charge density at the origin away from the experimental curve.

In summary, we emphasize that the main result that appears from the analysis of the DE in a self-consistent calculation seems to be that it effects the parameters of the model in a non-trivial way. On the other hand, the DE terms do not seem to effect the physical predictions of the model very much, as when we refit our parameters the difference from the LDA is very small. Recall however, that the effect of the DE terms for this size of scalar background is known to be small in the first place. In this sense, it is not surprising that the physical quantities are changed by so little. It is more surprising that the requirement of self-consistency causes the parameters g_s, g_v, and m_s to change by so much.

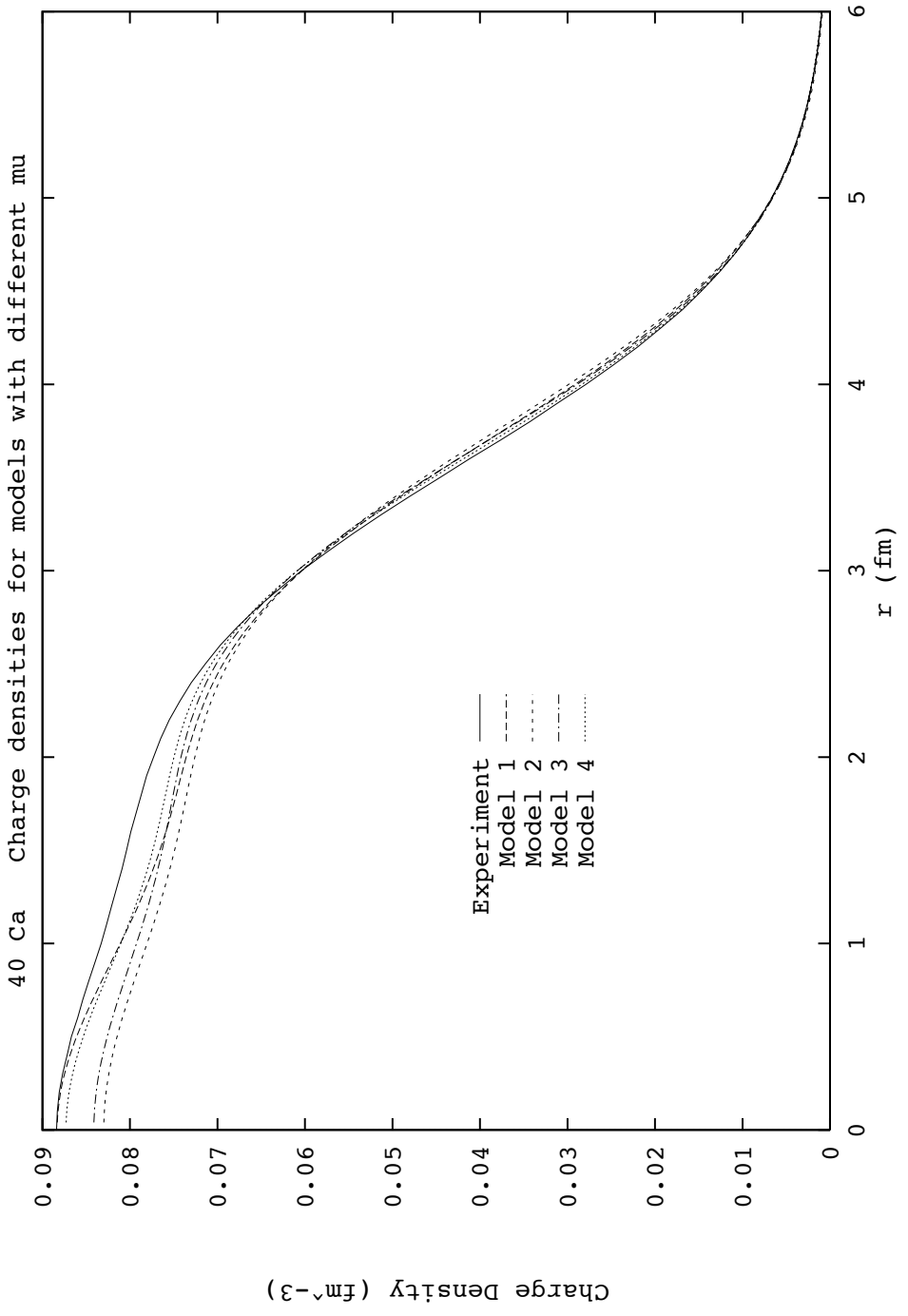

Figure 4.4: μ model comparison with the experimental charge radius for ^{40}Ca.

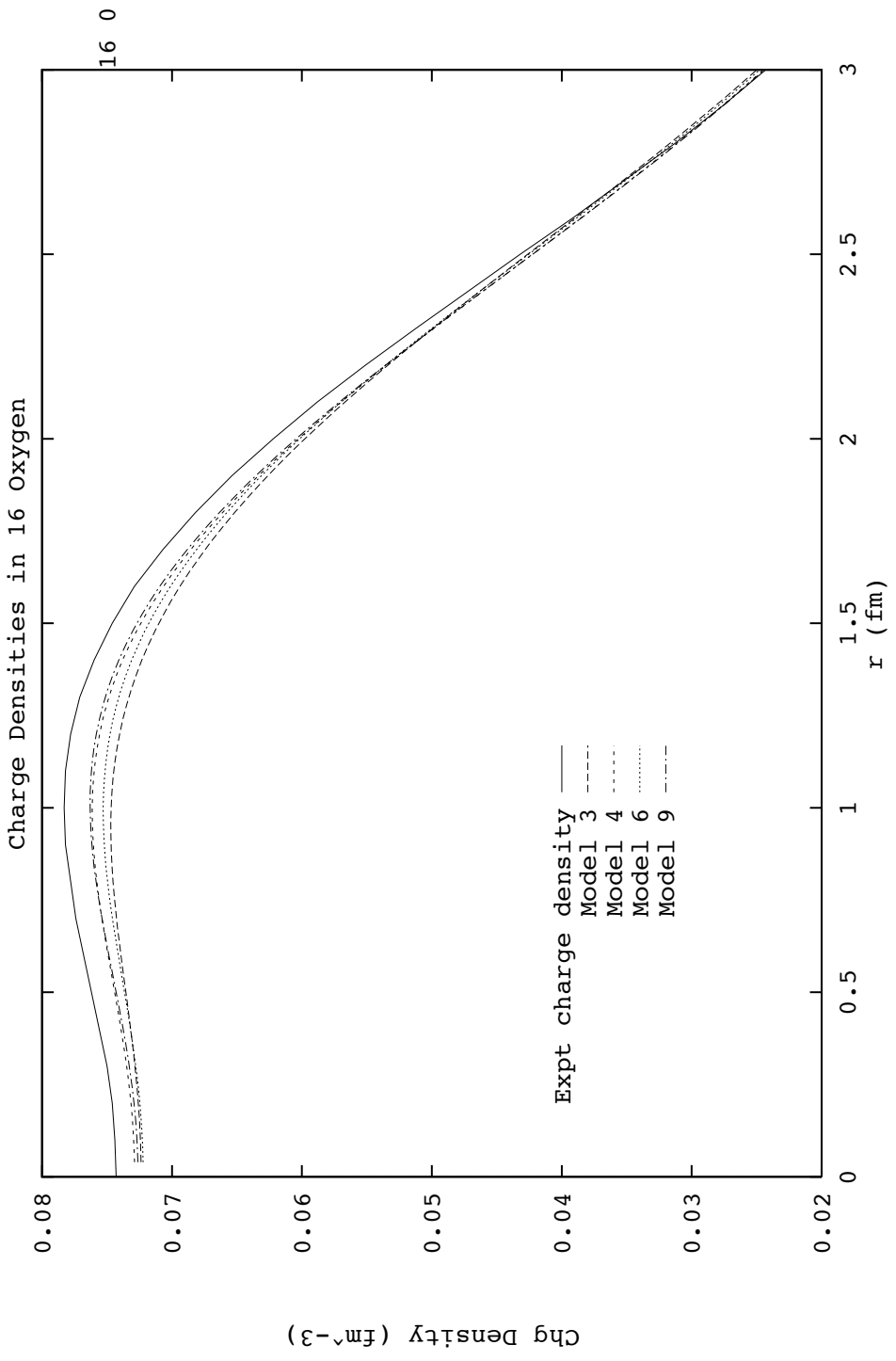

Figure 4.5: Modeling the charge density of ^{16}O.

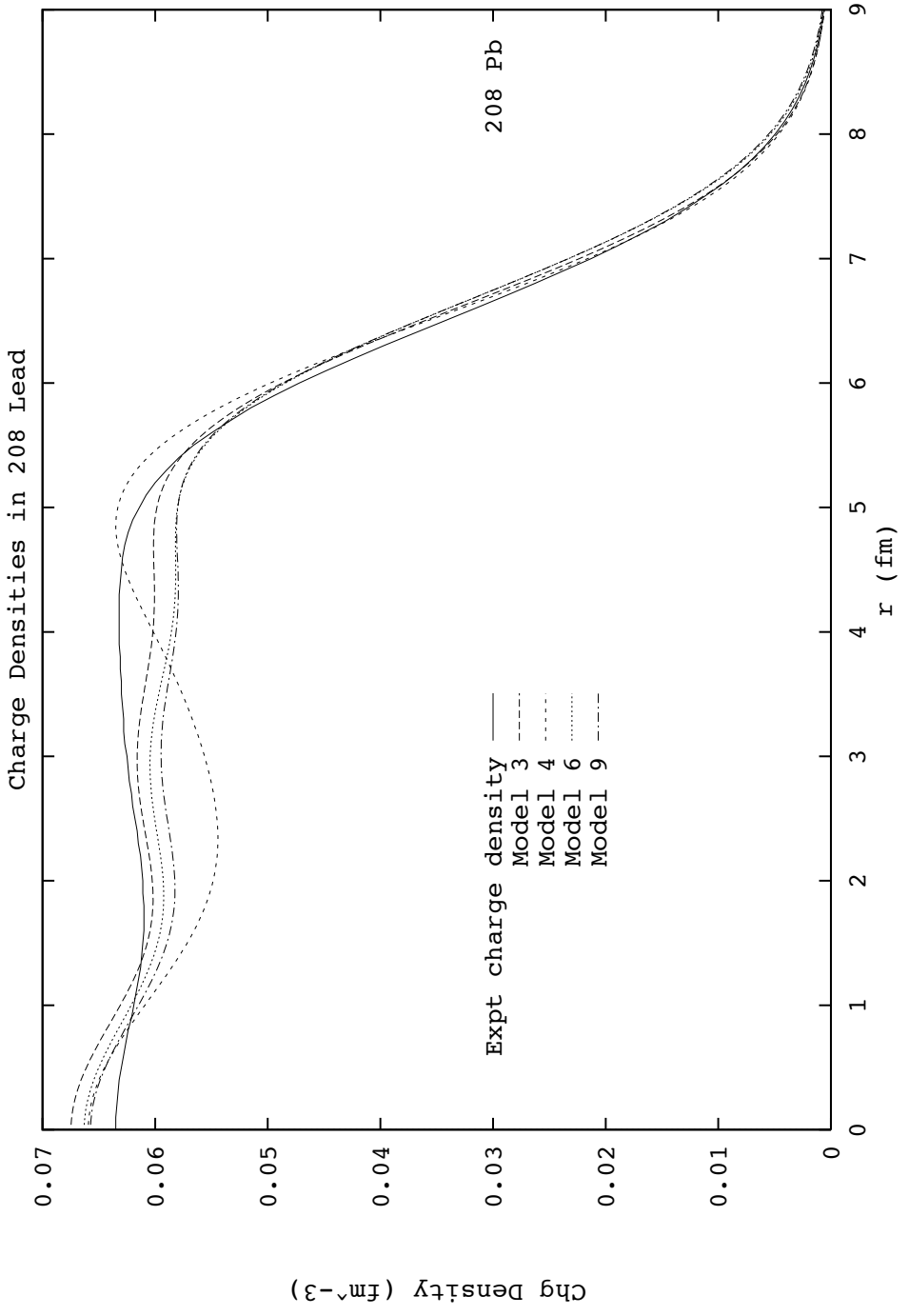

Figure 4.6: Modeling the charge density of ^{208}Pb.

Chapter 5

VACUUM EFFECTS IN A STRONG COUPLING SOLITON MODEL

Here we consider the nontopological soliton model of Bagger and Naculich [1, 47]. They consider solving for the bound states of fermions with a large Yukawa coupling to a scalar field, while including the effects of the one-loop fermion vacuum. There are N flavors of fermions in this model, and the region considered is the large N limit. Physically, this model gives an indication of the relevance of quantum bag formation for Higgs particles in the presence of heavy fermions. The scalar field here generates mass for the fermions through spontaneous symmetry breaking. Currently, we know that the top quark has a mass of 180 ± 12 GeV, and that the mass of the lightest Higgs particle must be greater than 58.4 GeV (95% confidence) [48]. Also, in supersymmetric extensions of the standard model there are predictions of spin-$\frac{1}{2}$ particles (gluinos, neutralinos, and charginos) with masses that may be a fair amount larger than the lightest scalar Higgs particle.

In their model, Bagger and Naculich [1, 47] account for quantum fermionic vacuum fluctuations by using the second order DE of the one-loop effective action. However, we have found that for the size of scalar fields considered in this problem, the DE will not always converge by second order. This convergence depends on the value of the coupling g in the model, becoming worse for larger g as the self-consistent scalar field of the bag shrinks. Although the authors checked the convergence by looking at the relative size of the fourth order terms in the expansion, they did so only for the *energy*. As we found in section 2.4, the energy expansion often hides the true nature

of the convergence that shows up in the dynamical Euler-Lagrange equations. Our purpose therefore, is to reconsider this model and make use of the correction method devised above to be able to account for the fermionic vacuum in an exact manner. The defining characteristics of this model will be left unchanged, with the equations changing only by inclusion of our density correction term (3.46).

5.1 Bagger-Naculich soliton model

The choice of Lagrangian density is [47]

$$\mathcal{L} = \sum_{i=1}^{N} \bar{\psi}_i \left[i\partial\!\!\!/ - \frac{g}{\sqrt{N}}\sigma \right] \psi_i + \tfrac{1}{2}(\partial_\mu \sigma)^2 + \tfrac{1}{2} M_0^2 \sigma^2 - \frac{\lambda}{8N}\sigma^4. \tag{5.1}$$

The utility of the large N parameterization here is to suppress the effect of scalar loops by $1/N$, validating the assumption of a classical scalar field. Note that our notation has been kept consistent at the expense of differing in some cases from that of Bagger and Naculich. To display the method by which the fermions acquire mass, we observe that the scalar field will have a nonzero vacuum expectation value. In terms of the shift from this value, we have $\sigma = \sqrt{N}\upsilon + \phi$. Identifying the fermion mass as $M = g\upsilon$ now makes sense, as the fermion part of the Lagrangian has become

$$\mathcal{L} = \sum_{i=1}^{N} \bar{\psi}_i \left[i\partial\!\!\!/ - g\upsilon - \frac{g}{\sqrt{N}}\phi \right] \psi_i. \tag{5.2}$$

The renormalization and reparametrization of this model is discussed in detail in [47]. The conditions that are applied correspond to fixing υ as the vacuum expectation value, and renormalizing the scalar mass, wave function and coupling g. Also, the inverse fermion propagator for two points is taken to be that of the free field. This renormalization prescription is enforced at the one fermion loop level by the choices:

$$\Gamma^{(1)}_{\phi} = 0, \qquad \Gamma^{(2)}_{\sigma\sigma}\Big|_{p^2=0} = -\mu^2, \qquad \frac{d\Gamma^{(2)}_{\sigma\sigma}}{dp^2}\Big|_{p^2=0} = 1,$$
$$\Gamma^{(3)}_{\sigma\psi\bar{\psi}}\Big|_{p_i=0} = \frac{-g}{\sqrt{N}}, \qquad \Gamma^{(2)}_{\psi\bar{\psi}}(p) = p\!\!\!/ - M. \tag{5.3}$$

These one, two and three 1PI generating functionals are analogous to those in equation (1.21), where the subscript here denotes the form of the interaction term in the Hamiltonian density. This prescription will fix (M, μ, g), as the finite parameters of the model.

To examine their model, Bagger and Naculich consider the simple case of states of N fermions which all appear in the lowest single particle energy state. By rescaling the scalar field to

$$\varphi = \frac{\sigma}{\sqrt{N}}, \tag{5.4}$$

the N dependence in the Lagrangian density now contributes as an overall factor. In the unrenormalized Lagrangian, this would read

$$\mathcal{L} = N\left(\bar{\psi}[i\partial\!\!\!/ - g\varphi]\psi + \tfrac{1}{2}(\partial_\mu\varphi)^2 + \tfrac{1}{2}M_0^2\varphi^2 - \frac{\lambda}{8}\varphi^4\right). \tag{5.5}$$

For consistency with our notation of chapter 4, we take $G(r)$ and $F(r)$ to denote the upper and lower $\kappa = -1$ radial Dirac components of the fermion field ψ, respectively. We find it useful to make further redefinitions so that all variables are dimensionless. This can be accomplished by the following transformations:

$$\begin{array}{lll} \dfrac{g\varphi}{M} \;\to\; \varphi, & \dfrac{4\pi}{M}G^{\,2} \to G^{\,2}, & \dfrac{4\pi}{M}F^{\,2} \to F^{\,2}, \\ rM \;\to\; r, & \dfrac{\mu}{M} \to \mu, & \dfrac{\epsilon_1}{M} \to \epsilon_1. \end{array} \tag{5.6}$$

We may then write the equations for the fermions as

$$\frac{dG}{dr} = \frac{G}{r} + (\epsilon_1 + \varphi)F, \tag{5.7}$$

$$\frac{dF}{dr} = \frac{-F}{r} - (\epsilon_1 - \varphi)G, \tag{5.8}$$

subject to the constraint

$$\int_0^\infty dr(G^2 + F^2) = 1. \tag{5.9}$$

The scalar field satisfies the equation

$$\nabla^{\,2}\varphi = \rho_{nl} \;+\; \rho_{val} \;+\; \eta_1\;\rho_{vac}^{LDA} \;+\; \eta_2\;\rho_{vac}^{DE} \;+\; \eta_3\;\frac{g^2}{Z}\;\Delta\rho_{corr}[\varphi], \tag{5.10}$$

where the source terms are defined to be

$$\begin{aligned}
\rho_{nl} &= \frac{\lambda}{2Z}(\varphi^3 - \varphi), && (5.11)\\
\rho_{val} &= \frac{g^2}{4\pi r^2}(G^2 - F^2), && (5.12)\\
\rho_{vac}^{LDA} &= -\frac{g^2}{4\pi^2}\left(\varphi^3 \ln(\varphi^2) - \varphi^3 + \varphi\right), && (5.13)\\
\rho_{vac}^{DE} &= \frac{g^2}{8\pi^2}\left(\frac{1}{\varphi}\left(\frac{d\varphi}{dr}\right)^2 + \ln(\varphi^2)\nabla^2\varphi\right). && (5.14)
\end{aligned}$$

As written, these equations facilitate examining different levels of approximation:

$$\begin{aligned}
&\text{(i)} \qquad \text{Classical:} \quad \eta_1 = 0, \quad \eta_2 = 0, \quad \eta_3 = 0;\\
&\text{(ii)} \qquad \text{LDA}: \quad \eta_1 = 1, \quad \eta_2 = 0, \quad \eta_3 = 0;\\
&\text{(iii)} \qquad \text{DE}: \quad \eta_1 = 1 \quad \eta_2 = 1 \quad \eta_3 = 0;\\
&\text{(iv)} \qquad \text{Exact}: \quad \eta_1 = 1, \quad \eta_2 = 1, \quad \eta_3 = 1.
\end{aligned} \qquad (5.15)$$

Note that only (i) and (iii) were considered by Bagger and Naculich.

For the numerical solution, it is useful to proceed in the following manner. We begin by rewriting equation (5.10) so that the coefficient in front of φ'' is unity:

$$\begin{aligned}
\nabla^2\varphi &= \frac{\lambda}{2Z}(\varphi^3 - \varphi) + \frac{g^2}{4\pi r^2 Z}(G^2 - F^2) - \eta_1 \ \frac{g^2}{4\pi^2 Z}\left(\varphi^3 \ln(\varphi^2) - \varphi^3 + \varphi\right)\\
&\quad + \eta_2 \ \frac{g^2}{4\pi^2 Z}\ \frac{1}{2\varphi}\left(\frac{d\varphi}{dr}\right)^2 + \eta_3 \ \frac{g^2}{Z}\ \Delta\rho_{corr}[\varphi], \qquad (5.16)
\end{aligned}$$

where

$$Z = 1 - \eta_2 \ \frac{g^2}{8\pi^2}\ln(\varphi^2). \qquad (5.17)$$

It is also useful to be able to treat our equations entirely as a boundary value problem. This can be done by treating ϵ_1 as a field, and also introducing a field χ for the

auxiliary equation (5.9) [49], so that

$$\frac{d\epsilon_1}{dr} = 0, \tag{5.18}$$

$$\frac{d\chi}{dr} = G^2 + F^2. \tag{5.19}$$

The boundary conditions applied here are then

$$\begin{aligned} \left.\frac{d\varphi(r)}{dr}\right|_{r\to 0} &= 0, & \frac{d\varphi(R)}{dr} &= (\mu + \frac{1}{R})(1-\varphi(R)), \\ \left.\frac{F(r)}{rG(r)}\right|_{r\to 0} &= \frac{1}{3}(\varphi(0)-\epsilon_1), & \frac{F(R)}{G(R)} &= -\left(\frac{\varphi(R)-\epsilon_1}{\varphi(R)+\epsilon_1}\right)^{1/2}, \\ \chi(0) &= 0 & \chi(R) &= 1, \end{aligned} \tag{5.20}$$

where R is large compared to the length scale of the problem. For N fermions the energy per fermion (in units of M) is

$$\frac{E}{N} = E_{eff}(\varphi) + \epsilon_1(\varphi), \tag{5.21}$$

$$\begin{aligned} E_{eff}(\varphi) = \frac{1}{g^2}\int d^3x \Bigg[& \frac{1}{2}\, Z\,(\varphi(r)')^2 + \frac{\mu^2}{8}(\varphi^2-1)^2 \\ & + \eta_1 \frac{g^2}{16\pi^2}\left(\frac{1}{2}\,(\varphi^2-1)\,(3\varphi^2-1) - \varphi^4 \ln(\varphi^2)\right)\Bigg]. \end{aligned} \tag{5.22}$$

As we noted above, it was found in [47] that we do not need to correct the second order terms of the DE in this energy expression.

5.2 Addressing the numerical problem

Next we consider a method for solving the equations (5.7), (5.8), (5.9), (5.16), (5.18) and (5.19), subject to the boundary conditions (5.20). For this purpose, the solver COLNEW by Ascher and Bader [50] is used. This version improves upon the original solver COLSYS devised by Ascher, Christiansen and Russell [51] by using an improved solution strategy and a different spline basis. The general purpose of the package is to solve mixed order coupled nonlinear ordinary differential equations. The

program implements a finite element method which approximates the solution with collocation at Gaussian points. The nonlinear equations for the splines are solved using relaxation and Newton's method. This method gives us the advantage of solving the coupled nonlinear equations simultaneously. It enables us to handle cases where large contributions arise from the nonlinear vacuum pieces, in particular large DE contributions. Another important aspect of this program is that it keeps track of the error in the solution at all times. This is accomplished through careful application of adaptive mesh selection [52]. The routine COLSYS has been applied previously to soliton bag models. (see [1, 53]).

As in many nonlinear problems, the ability to obtain a solution in reasonable time hinges on ones ability to provide the solver with a reasonable starting point. Here the initial guess for the solutions to the fields is obtained by specifying a initial scalar field of the form (2.103), with $f = 1$. The initial Dirac spinor fields are then calculated by integrating the coupled equations (5.7 and 5.8) out from the origin and in from infinity to some matching point r_m, with an initial guess for the energy eigenvalue. The matching point is chosen to be close to the zero crossing of the effective potential $(\varphi - \epsilon)$. The solutions are then rescaled to match at r_m, and the energy is adjusted in accordance with that match. The procedure is then repeated with this new energy. When the true energy eigenvalue is reached, the boundary conditions will be simultaneously satisfied and the necessary rescaling factor will approach unity. The solutions obtained from this method can then be normalized by calculating the integral (5.9). The initial auxiliary fields are then specified from this spinor solution. For the cases in (5.15) where $\eta_4 = 0$, providing COLNEW with these initial fields is enough to obtain an exact solution to the nonlinear equations in a timely fashion. We may then calculate all quantities of interest, such as the different contributions to the energy and density expressions.

Unfortunately, in the most interesting of the situations, $\eta_4 \neq 0$, we cannot simply apply the COLNEW routine as given. The reason is that with the inclusion of the cor-

rection our equations are now actually integro-differential equations which COLNEW cannot solve. To facilitate this, the code provided by Ascher and Bader was modified so that the scalar field solution and its derivative can be extracted at intermediate stages of the calculation to evaluate the correction functional (3.46). The calculation now becomes internally iterative, with the density correction treated as a source term that is reevaluated at each new iteration. We found that this could be accomplished with minimum change to the COLNEW code by simply passing more variables to the procedure GSUB (which is provided externally to evaluate the boundary value conditions). This procedure is called at the beginning of each new iteration, and it is a simple manner to make additional calls to extract the current scalar potential solution from the splines and evaluate the correction. However, evaluating the correction in this manner proves to be costly in terms of solution time. In fact the speed of the entire strategy is limited almost entirely by the number of times the correction is evaluated. The evaluation of each partial wave correction (given by (3.46)) takes roughly one minute on a DEC Alpha AXP 3000 Model 300 server. To take this into account, code has been incorporated to only reevaluate the correction if the solution is deemed to have changed by a significant amount.

Another issue we should consider is that the scalar field for which we are evaluating the correction is only a preliminary solution to the dynamical equations. The only real problem with this is that the boundary conditions (5.20) may not be valid with high enough accuracy to satisfy the correction routine. The largest effect here occurs with the condition at $r = 0$. To adapt to this situation we can use the equations (3.22) with $s_1 \neq 0$, and because the higher order derivatives are not too smooth, we set the factors s_3 and s_4 (proportional to the third and fourth derivatives of the scalar field at the origin) to zero. This places a restriction on the minimum value of r at which we can safely apply the correction, but this restriction turns out to be unimportant for determining the solution here.

A final issue we must address is the manner in which the COLNEW routine

attempts to improve its solution at each iteration. This is done by making use of information extracted from the Jacobian of the differential equations and boundary value equations. If the correction is to be the driving factor in the equations, it may be useful to have some information as to how this term contributes to the Jacobian. Unfortunately, this involves evaluating the derivative of the correction term with respect to the functions $\varphi(r)$, and $\varphi'(r)$. As the correction is actually a nonlocal function of φ (recall φ occurs in the differential equation that had to be solved to determine the integrand) this in general is a nontrivial procedure. Several ways in which this information may be included were considered, but no method has been found that gives faster convergence than simply ignoring these contributions to the Jacobian.

We start the $\eta_4 \neq 0$ cycle with the solution obtained from solving the equations at the DE level. To allow the aforementioned method of solution to succeed we use the cutoff parameter Λ to control how much of the correction is included. As mentioned in section 3.4, and shown in figure 3.4, we can use the cutoff to extrapolate toward the full correction for each partial wave. This is done in the following manner. We start by picking a number of partial waves to include, κ_{max}, and cutoffs Λ_κ in such a manner that the solution converges. Then the solution to this step may be used as the starting point of another step with different κ_{max} and Λ_κ. This allows us to test the convergence of the correction calculation in the self-consistent solution. Another applicaton of the cutoffs here is to use them to keep the change in the correction source term small relative to the solution obtained so far. Stepping out in the cutoffs then allows us the full correction to be included while keeping the iterative procedure rapidly convergent. Close track should then be kept of the solution mesh size each time κ_{max} and Λ_κ are changed, so that it does not overflow the routine/machine swap space. The numerical results presented here do not make use of this latter cutoff application.

5.3 Solutions using different levels of approximation.

Having outlined the procedure, we are now in a position to look at the solutions. We will consider the effect of working at different levels of the approximation as indicated in (5.15). The quantities obtained from the solution which are of interest include the wave function solutions (φ, G and F), contributions from different density terms at the point of solution ($\rho_{nl}, \rho_{val}, \rho_{vac}^{LDA}, \rho_{vac}^{DE}, \Delta\rho_{corr}$), and the contributions of different terms in the energy expressions (5.21 and 5.22). Our goal is to quantify the effect of the correction on the solution as the coupling becomes large and the DE breaks down.

We begin by discussing the nature of the solutions obtained for different levels of the approximation. The case $g = 10$, $\mu = 1$ will serve as an example. For this value of g, the effects of the correction are just beginning to show up. This enables us to examine the robustness of our method for a case where the correction should only have a fairly small effect. From this solution we also obtain an idea of the directions in which the scalar potential and energy will shift. For cases (i) and (iii), we repeat below some of the general solution features discussed in [47].

For the Classical approximation (i), LDA (ii), and DE (iii), the scalar field φ and spinor component field G and F self-consistent solutions are shown in figure 5.1. The contributions from the fermions and scalar field to the overall bag energy are summarized in table 5.1.

Approximation (i):

Here the equations are treated at the quasi-classical level (no vacuum terms). This approximation is quite limited as scalar fluctuations are expected to be important for small g, while for large g the fermionic fluctuations are important. For small coupling ($g < 3$), weak shallow bag solutions do exist at this level (see [47] for details). For larger coupling the bag becomes deeper and the scalar field obtains a zero and becomes negative for a finite interval out from $r = 0$. The spinor fields G and F give

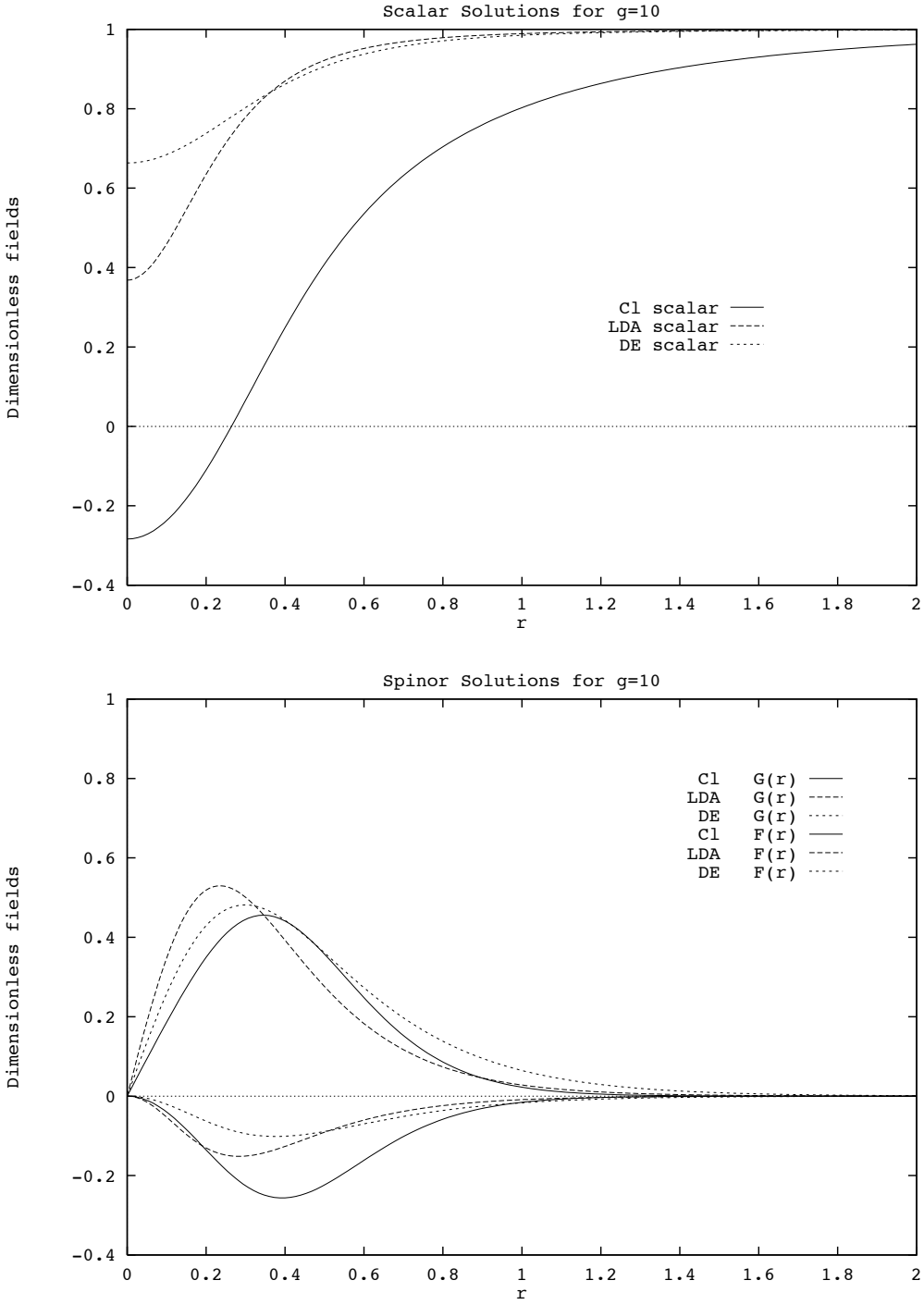

Figure 5.1: Self-consistent solutions of the Bagger-Naculich model for different levels of local approximations to the vacuum densities.

Table 5.1: Contributions to the energy per fermion in the system for the $g = 10$, $\lambda = 1$ self-consistent solutions. Values are expressed in units of the fermion mass M.

Approximation	Energy per fermion			$\phi(r = 0)$
	Fermi level	Scalar field	Total	
Classical	0.3829	0.2373	0.6201	-0.2837
LDA	0.8628	0.0973	0.9601	0.3683
DE	0.9080	0.0594	0.9674	0.6635
Exact ($\kappa = 1$, $\Lambda = 3$)	0.8962	0.0718	0.9680	0.6014
Exact ($\kappa = 1$, $\Lambda = 4$)	0.8950	0.0731	0.9681	0.5948
Exact ($\kappa = 1$, $\Lambda = 5$)	0.8945	0.0737	0.9682	0.5902
Exact ($\kappa = 2$, $\Lambda = 3$)	0.8819	0.0880	0.9699	0.5515
Exact ($\kappa = 3$, $\Lambda = 3$)	0.8698	0.1025	0.9734	0.5212
Exact ($\kappa = 4$, $\Lambda = 3$)	0.8650	0.1085	0.9735	0.5177

concentrated probability for the fermions near the region with the largest slope for the scalar field potential. This behavior can be identified in figure 5.1. The dominant source density term for the scalar potential equation are the valence fermions.

Approximation (ii):

For relatively small couplings, adding in the local density terms has the effect of reducing the depth of the scalar potential, so that a zero no longer appears. The spinor fields are again peaked in the region of the largest scalar potential slope. The energy of the solution state has been dramatically changed from that of the classical approximation. This can be seen in table 5.1. This is the behavior that was noticed by [47]. In their words, the "quantum corrections deflate the bag", meaning that the total energy per fermion in the bag is approaching the free value (M). The largest

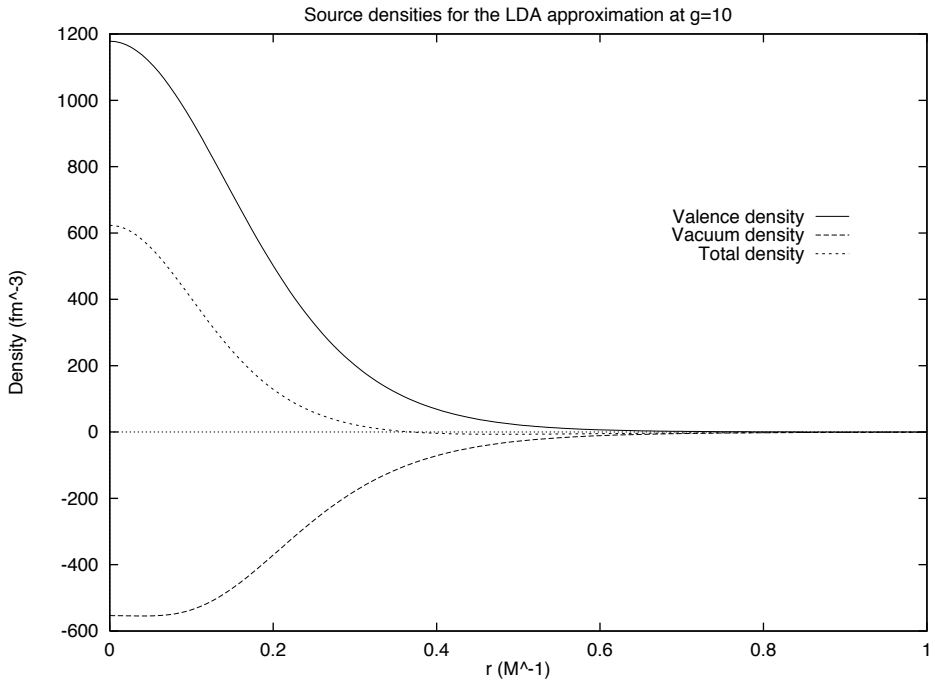

Figure 5.2: The dominant source density terms for the self-consistent LDA solution at $g = 10$.

source density contributions in equation (5.10) are displayed in figure 5.2. Notice that there is a fair amount of cancelation between the valence density and vacuum density terms.

For $g > 10.4$ the LDA approximation is divergent. The reason for this is that solutions which include vacuum terms tend to have a fair amount of cancelation between the vacuum density and density contributions from valence fermions. Looking at the expression for the LDA contribution in (5.13), we see that this function is odd with respect to the scalar field. Increasing the coupling drives the potential deeper, and at some point the solution becomes negative at $r = 0$. At this point the LDA contributions begin to contribute in the opposite direction, driving the solution to more negative depth. At a critical coupling, near $g = 10.4$, the equations no longer support a solution. The reason for introducing the LDA at all is to have an extra

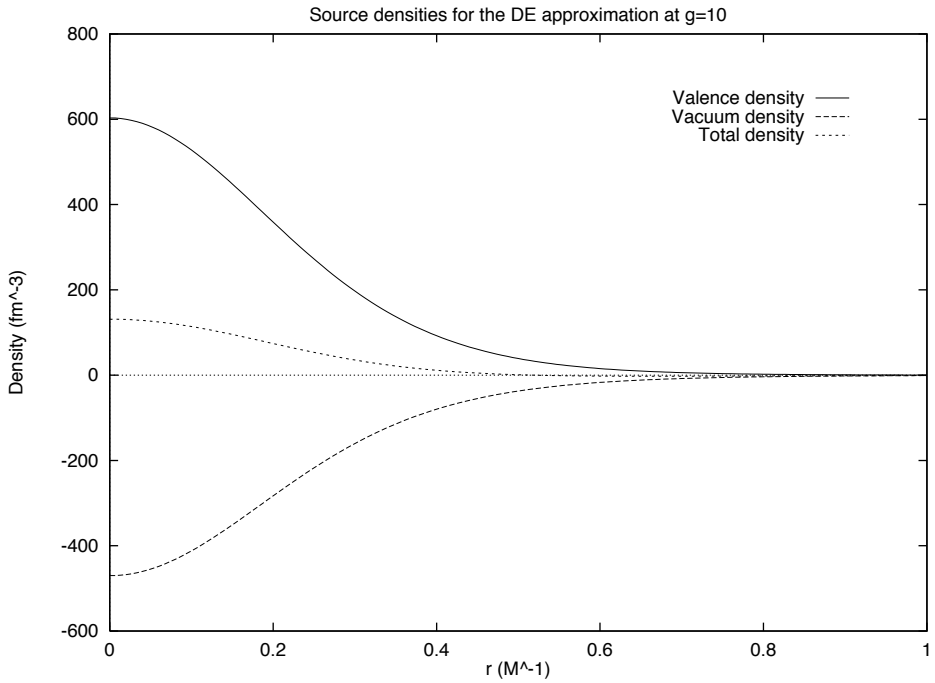

Figure 5.3: The dominant source density terms for the self-consistent DE solution at $g = 10$.

indicator which enables us to consider, for $g < 10.4$, the effect that different terms in the vacuum density have on the solution.

Approximation (iii):

For smaller couplings, the DE acts essentially like the LDA. However, as the coupling is increased we still obtain a solution, as now the derivative terms prevent the vacuum density from changing signs. This allows further cancelation of the vacuum density with the valence fermionic density to occur. For the example we are considering, this cancelation is displayed in figure 5.3. In figure 5.1 we see that the shape of the scalar potential is even shallower than the LDA, and also that the width has decreased. An interesting feature, seen in table 5.1, is that the the energy contributions have changed in such a manner that the overall energy per fermion is relatively unchanged from the LDA result. This is reminiscent of the behavior we observed for

finite nuclei.

Approximation (iv):

We now examine what happens when the density correction term $\kappa = 1$ is included. In figure 5.4 both the scalar and spinor fields are shown. Note that the scalar solutions are given for two values of the cutoff to indicate that a value of $\Lambda = L = 3$ is sufficient for convergence of the correction integral. The energy values for the exact solutions are also included in table 5.1. We notice that despite the fact that the depth of the scalar field has changed, the overall energy is affected very little.

The effect of using the exact vacuum density does not follow the progression of the following three steps but instead favors a deeper potential than in the DE. This behavior is a manifestation of further terms in the derivative expansion having oscillatory convergence. We find that to get the exact correction it is sufficient to use partial waves up to $\kappa = 4$. This can be seen in figure 5.5, where the self-consistent solution is shown for calculations including an increasing number of partial waves. Note that the time for the numerical self-consistent solution grows linearly with κ. By $\kappa = 4$ the series is convergent. Energies for the higher partial wave solutions are shown in table 5.1. We see that the scalar potential is becoming deeper, so that the energy of the scalar field grows and Fermi level drops away from M. However, the total energy is rising, making the bag even more unstable. The exact calculation has reduced the binding energy to only 2.7%, from the 3.3% of the DE.

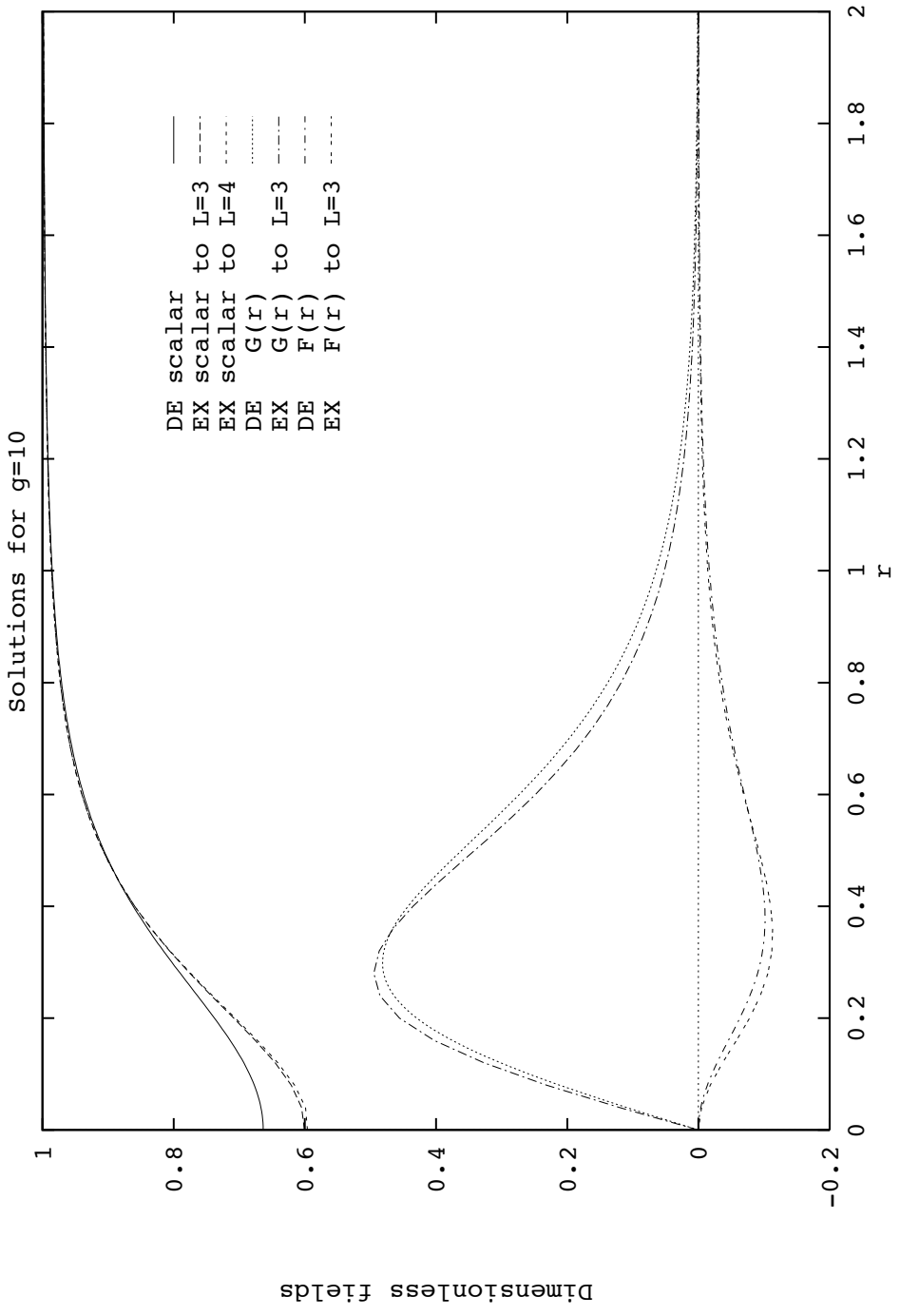

Figure 5.4: Effect of $\kappa = 1$ correction on self-consistent solution at $g = 10$.

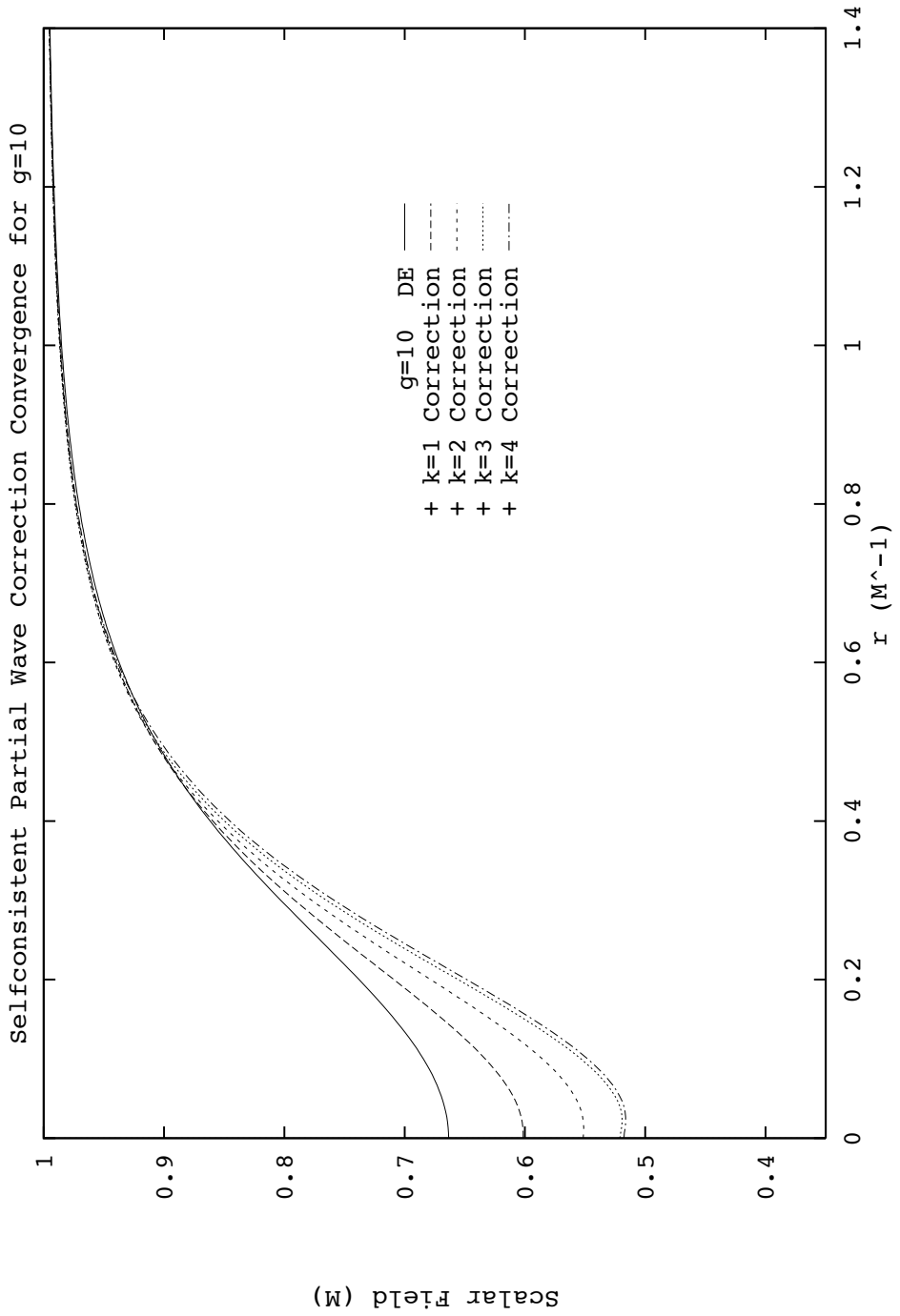

Figure 5.5: Self-consistent solutions with increasing number of terms in the partial wave correction series for $g = 10$.

Table 5.2: Contributions to the energy of the system in the $g = 25$ self-consistent solutions. Values are expressed in units of the fermion mass M.

Approximation	Energy per fermion			$\phi(r = 0)$
	Fermi level	Scalar field	Total	
Classical	0.1345	0.1182	0.2527	-0.4217
LDA	–	–	–	–
DE	0.8764	0.0772	0.9536	0.5307
Exact ($\kappa = 1$, $\Lambda = 3$)	0.8433	0.1143	0.9576	0.3638
Exact ($\kappa = 1$, $\Lambda = 4$)	0.8408	0.1174	0.9582	0.3513
Exact ($\kappa = 2$, $\Lambda = 3$)	0.8118	0.1555	0.9673	0.2865
Exact ($\kappa = 3$, $\Lambda = 3$)	0.7903	0.1866	0.9770	0.2423
Exact ($\kappa = 4$, $\Lambda = 3$)	0.7851	0.1940	0.9792	0.2612

5.4 Large coupling regime

To further examine the breakdown of the DE result, we now consider a case where the coupling is even larger. We take the parameters used by Bagger and Naculich, ($g = 25$, $\mu = 1$). In figure 5.6 we have reproduced the field solutions given by Bagger and Naculich [1]. Note that our normalization for the spinor fields differs from these authors. For physical reasons (a Landau pole, tachyon, and vacuum instability) [47], g must be less than 30 in this model, so that $g = 25$ is close to the upper limit. The numerical results for the solutions here are displayed in table 5.2.

In figure 5.7, we see that the first partial wave correction is much larger for $g = 25$. Also, note that by a cutoff of $\Lambda = L = 3$ the correction is convergent. In table 5.2, we see that, in a similar manner as for $g = 10$, the $g = 25$, $\kappa = 1$ correction has a large effect on the depth of the scalar field, but a much lesser effect on the energy.

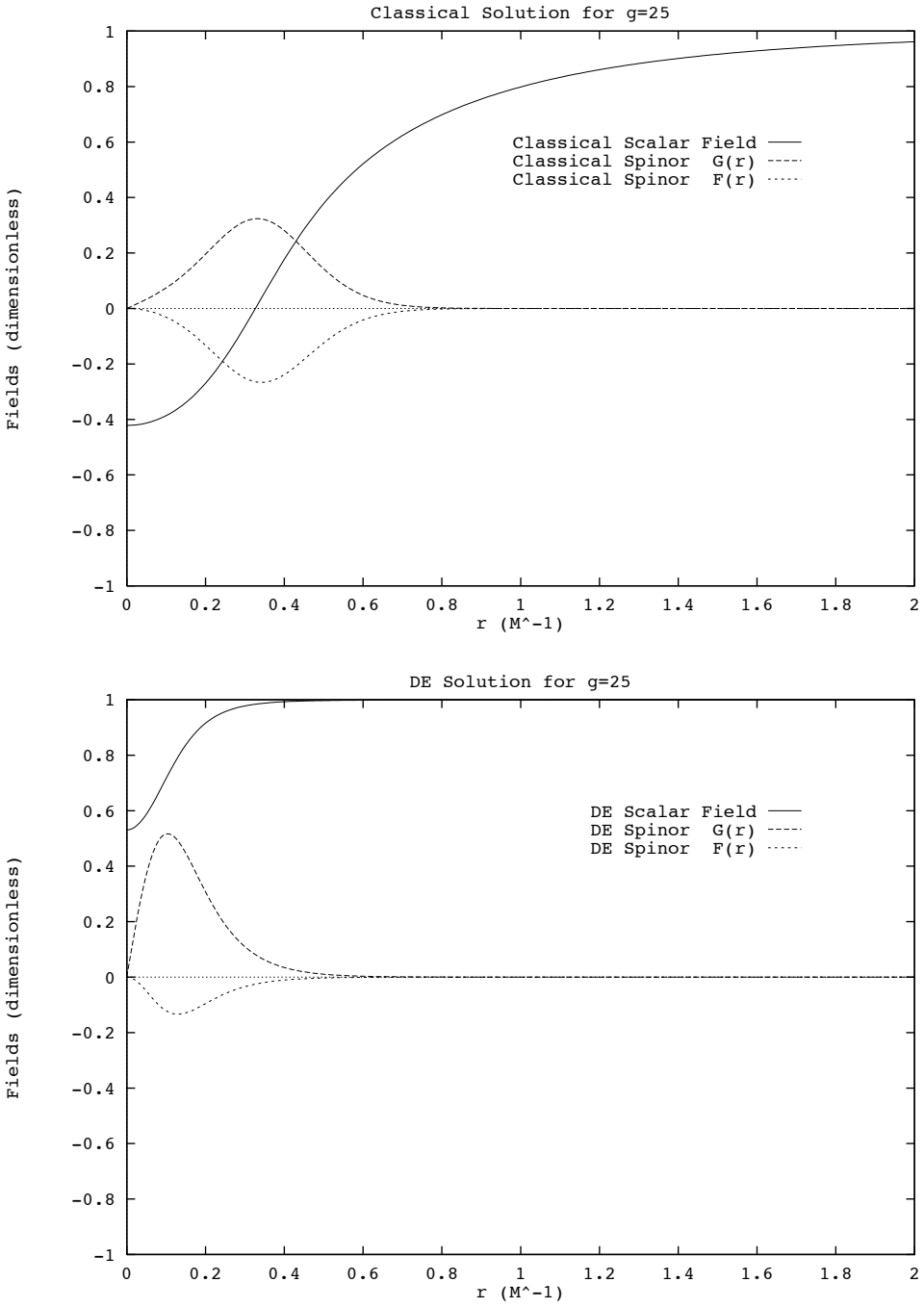

Figure 5.6: Reproduction of the results of Bagger and Naculich [1] at $g = 25$. Fields are shown for the classical and quantum solutions. Note that the normalization choice for our spinor wave functions differs from theirs.

The results for $\kappa = 2, 3$ and 4 are also shown in the table and figure. Notice that the correction is close to convergence for $\kappa = 4$. The effect of higher partial waves for $g = 25$ has yet to be considered[1]. Another thing to note is that when higher partial wave corrections are included the scalar fields develop a small dip very close to the origin. This is a numerical effect that results from the intermediate boundary condition issue discussed in section 5.2. To remove this small numerical feature it would likely be necessary to implement the application of the cutoff that is discussed at the end of that section. In any case this effect will only slightly increase the value of the scalar field at the origin.

In this chapter we have learned that in a case where the correction is large it can substantially affect self-consistent solutions. By being careful with our cutoff dependence, we have managed to obtain acceptable convergence by $\Lambda = 3$. It is also promising to see that the partial wave series of corrections for $g = 10$ converges under the self-consistent calculation by $\kappa = 4$. Also, as only a small number of partial waves are needed, it is possible to obtain the exact solution with the one-loop vacuum polarization in this model.

[1] Work in progress.

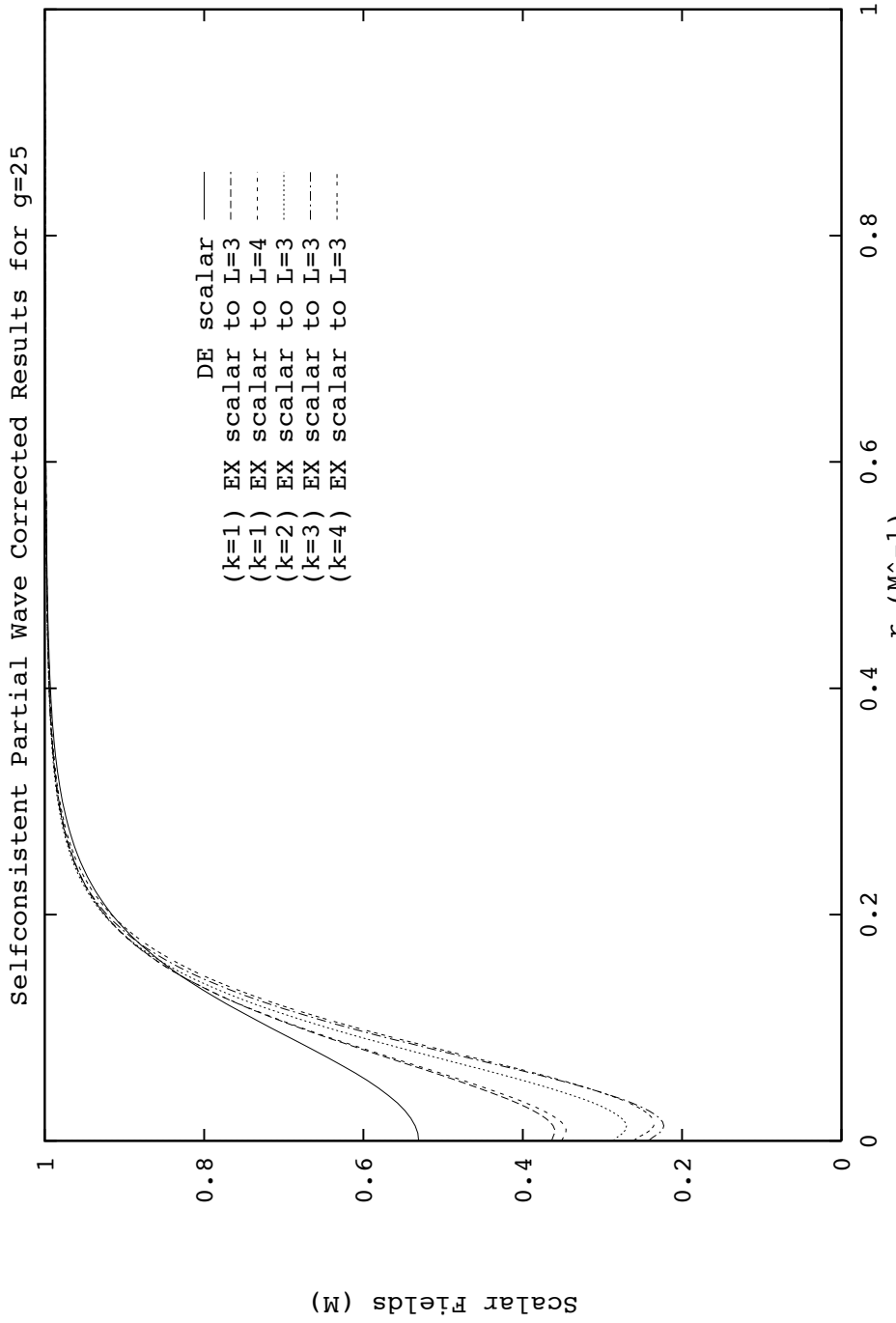

Figure 5.7: Self-consistent solutions with increasing number of terms in the partial wave correction series for $g = 25$.

Chapter 6

CONCLUSIONS

A method has been devised whereby the exact fermionic one-loop vacuum polarization may be calculated for a scalar background field in $3+1$ dimensions. Using the method of derivative expansion to calculate contributions from large loop energies, and high angular momentum partial waves, yields an efficient numerical procedure for determining the exact one-loop result. One benefit of this procedure is that we can determine, in an exact manner, whether the DE is convergent for a particular nontrivial background. More importantly, the procedure can be used to evaluate vacuum polarization effects when local methods, like the DE, are not convergent in parts of phase space. In general, the speed of the calculation is limited by the number of partial waves of the DE that must be corrected, growing linearly in time with κ. The desired numerical accuracy is also influential, as it determines the energy mesh and maximum cutoff that must be used.

The correction procedure devised here can be extended to fermionic loops in different bilinear backgrounds (e.g. vector background fields) in a straightforward manner. A similar procedure could also be used to find the exact bosonic loop density contributions at the one-loop level.

In terms of using the correction in a self-consistent calculation, the work here has been restricted to the case of interacting fermion and scalar fields where there are N flavors of fermions found in the ground state. For this case, we examined the manner in which using the correct one-loop vacuum polarization effects the self-consistent solution. The way in which a more structurally complex self-consistent calculation may be done was also described, but for a case in which the DE converges. The case

considered involved several mean fields, both bosonic and fermionic loops, as well as different valence fermionic levels. For a more general theory, where the DE is not convergent, the correction routine devised here could be used to obtain the correct vacuum results in an analogous manner.

Appendix A

CONVENTIONS

The conventions used in this thesis are as follows. The dimensionality of the applicable spacetime will often be denoted in the form $3+1$ dimensions, meaning 3 spatial dimensions and 1 time dimension. When a generic spacetime is considered, the dimension will be denoted by D. The dimension of the spatial part of a generic spacetime will then be referred to as d, where $d = D - 1$. The spacetime variables will be written in regular mathematical text, such as position x and momentum p. The spatial part of a spacetime variable will be distinguished by an arrow over top, such as $\vec{x}$ and $\vec{p}$. All spacetime indices are denoted by lowercase Greek letters, while Roman letters are used for spatial indices.

The usual notation for a function of a variable is used, such as $\rho(x)$, and functionals are distinguished by using square brackets, such as $\Gamma[\phi]$. We will often suppress some of the function and functional dependencies for the sake of clarity. Operators will generally be identified by capital Roman letters, such as A, and path integral measures will be enclosed in square brackets, such as $[d\phi]$.

When primes are used to denote the derivative of a function or functional this will be explicitly noted in the following text. Also, note that Lorentz invariant contractions are implicit on derivative expressions, such as

$$\partial^2 = \partial_\mu \, \partial^\mu, \qquad (\partial_\mu \sigma)^2 = (\partial_\mu \sigma)(\partial^\mu \sigma). \tag{A.1}$$

The metric tensor here is chosen so that $\mathrm{tr}\, g_{\alpha\beta} = -d+1$, so that in $3+1$ dimensions

the three spatial diagonal elements are negative,

$$g_{\alpha\beta} = g^{\alpha\beta} = \begin{bmatrix} 1 & 0 & 0 & 0 \\ 0 & -1 & 0 & 0 \\ 0 & 0 & -1 & 0 \\ 0 & 0 & 0 & -1 \end{bmatrix}. \tag{A.2}$$

Hence for a particle of mass m with momentum p, $p^2 = m^2$.

Traces that involve at least one continuous variable are denoted by Tr, whereas traces over purely internal spaces are denoted by tr. To keep track of the variables over which a Tr is taken, we use subscripts to list the continuous variables and a superscript ^{int} to remind us if internal traces are also included. All position space traces are integrals over spacetime, whereas momentum space traces are integrals with a normalization factor of $(2\pi)^{-D}$. Two examples are:

$$\mathrm{Tr}_x = \int d^D x, \qquad\qquad \mathrm{Tr}_{\vec{p}} = \int \frac{d^d p}{(2\pi)^d}. \tag{A.3}$$

Superscripts and subscripts are also used on quantities to denote different types of the same basic object. In particular, ρ^s denotes a scalar density, while ρ^s_{vac} denotes the scalar density from fermionic loops.

When a particular representation of gamma matrices is required we use

$$\gamma_0 = \begin{bmatrix} 1 & 0 \\ 0 & -1 \end{bmatrix}, \qquad\qquad \gamma_i = \begin{bmatrix} 0 & \sigma_i \\ -\sigma_i & 0 \end{bmatrix}, \tag{A.4}$$

where $i = 1, 2, 3$, and σ_i are the Pauli spin matrices.

Finally, our notation for Dirac angular momentum states follows that of reference [3], and in particular is simply specified by the separation of variables in the form

$$\frac{G(r)}{r}\mathcal{Y}_{\kappa m}(\theta, \phi), \tag{A.5}$$

and the relation (3.10).

Appendix B

GENERAL EFFECTIVE ACTION DERIVATIVE EXPANSION

A general method for finding the derivative expansion for either bosonic or fermionic loops can be given as follows. This method was devised by Chan [54] to fourth order in the background fields, while an extension of the necessary expressions to sixth order may be found in [25]. To fourth order in our notation the result is

$$\begin{aligned}\Gamma_{vac}[\mho, V] &= i\mathrm{Tr}_x^{int}\,\ln\Big(-P^2+\mho(X)\Big) &\text{(B.1)}\\ &= i\mathrm{Tr}_{x,p}^{int}\Big[\ln(\Theta^{-1})+\frac{p^2}{D}\Theta_\mu^2+\frac{2p^4}{D(D+2)}\Big(2\Theta_\mu^4-(\Theta_\mu\Theta_\nu)^2\\ &\qquad -2(\Theta\Theta_\mu^\mu)^2+(F_{\mu\nu}\Theta^2)^2+4i\Theta F^{\mu\nu}\Theta\Theta_\mu\Theta\Theta_\nu\Big)\Big], &\text{(B.2)}\end{aligned}$$

where

$$\begin{aligned}\Theta^{-1} &= -p^2+\mho(X), \qquad & \Theta_\mu=\mathcal{D}_\mu\Theta,\\ \mathcal{D}_\mu &= P_\mu=i\partial_\mu+\lambda_a V_\mu^a(X), \qquad & F_{\mu\nu}=[\mathcal{D}_\mu,\mathcal{D}_\nu]. \qquad \text{(B.3)}\end{aligned}$$

The subscripted Greek indices on Θ denote covariant derivatives, and $\mathcal{D}_\mu$, and λ_a are generators of a spin-1 gauge group. The background field $\mho(X)$ can have arbitrary internal finite group structure. With this expression we can find the DE, to 4th order in the background field derivatives, for quite a general class of theories that share the one-loop functional form (B.1). We stress here the manner in which the fermionic results can be placed in this form. The key is manipulating the expression for the action as follows:

$$\Gamma_{vac}[\psi] = -\mathrm{Tr}_x^{int}\,\ln\left(\pm\not{P}-\sigma(X)\right) \qquad \text{(B.4)}$$

$$
\begin{aligned}
&= -\frac{1}{2}\mathrm{Tr}_x^{int}\left[\ln(-\not{P}-\sigma(X))+\ln(\not{P}-\sigma(X))\right] \\
&= -\frac{1}{2}\mathrm{Tr}_x^{int}\left[-P^2+\sigma^2(X)+[\not{P},\sigma(X)]\right]. \qquad \text{(B.5)}
\end{aligned}
$$

In (B.4) the sign of the $\not{P}$ term is irrelevant, as the internal spin trace allows only terms that are even in the number of γ matrices to survive. So from the form (B.5), with

$$\mho(X) = \sigma^2(X) + [\not{P}, \sigma(X)], \qquad \text{(B.6)}$$

we may use equation (B.2) for fermionic actions too.

BIBLIOGRAPHY

[1] J. Bagger and S. Naculich, Phys. Rev. Lett. **67**, 2252 (1991).

[2] M. Li, L. Wilets, and R. J. Perry, J. Comput. Phys. **85**, 457 (1989).

[3] B. D. Serot and J. D. Walecka, *Adv. Nucl. Phys.* (Plenum, New York, 1986), Vol. 16, p. 1.

[4] J. F. Donoghue, E. Golowich, and B. R. Holstein, *Dynamics of the Standard Model* (Cambridge University Press, New York, 1992).

[5] L. Wilets, *Nontopological Solitons*, Vol. 24 of *Lecture notes in physics* (World Scientific, Singapore, 1989).

[6] C. Itzykson and J. Zuber, *Quantum Field Theory* (McGraw-Hill, New York, 1980).

[7] F. Mandl and G. Shaw, *Quantum Field Theory* (John Wiley and Sons, New York, 1984).

[8] W. Greiner and J. Reinhardt, *Quantum Electrodynamics* (Springer-Verlag, Berlin Heidelberg, 1992).

[9] L. H. Ryder, *Quantum Field Theory* (Cambridge University Press, New York, 1985).

[10] M. E. Peskin and D. V. Schroeder, *Introduction to Quantum Field Theory* (Addison-Wesley, Reading, Massachusetts, 1995).

[11] A. Fetter and J. Walecka, *Quantum Theory of Many-Particle Systems* (McGraw-Hill, New York, 1971).

[12] J. Preskill, field theory course, Caltech, Fall 1995 (unpublished).

[13] R. Jackiw, Phys. Rev. D **9**, 1686 (1974).

[14] M. Coppens and H. Verschelde, Z. Phys. **C349**, 349 (1993).

[15] B. D. Serot, Rep. Prog. Phys. **55**, 1855 (1992).

[16] J. Bjorken and S. Drell, *Relativistic Quantum Mechanics* (McGraw-Hill, New York, 1964).

[17] R. J. Perry, Phys. Lett. **B214**, 307 (1986).

[18] M. Li, R. J. Perry, and L. Wilets, Phys. Rev. D **36**, 596 (1987).

[19] P. G. Blunden, Phys. Rev. C **41**, 1851 (1989).

[20] D. A. Wasson and S. Koonin, Phys. Rev. D **43**, 3400 (1991).

[21] D. A. Wasson, Nucl. Phys. **A535**, 456 (1991).

[22] R. J. Perry, Nucl. Phys. **A467**, 717 (1987).

[23] M. Li and R. J. Perry, Phys. Rev. D **37**, 1670 (1988).

[24] M. Li, Ph.D. thesis, University of Washington, 1988.

[25] J. Caro and L. L. Salcedo, Phys. Lett. **B309**, 359 (1993).

[26] P. G. Blunden, private communication (unpublished).

[27] L. H. Chan, Phys. Rev. Lett. **54**, 1222 (1985).

[28] R. J. Perry, Phys. Lett. **B182**, 269 (1986).

[29] C. Kim, Phys. Rev. D **51**, 4415 (1995).

[30] I. Aitchison and C. Fraser, Phys. Lett. **B146**, 63 (1984).

[31] F. W. R. MacKenzie and A. Zee, Phys. Rev. Lett. **53**, 2203 (1984).

[32] O. Cheyette, Phys. Rev. Lett. **55**, 2394 (1985).

[33] J. A. Zuk, Phys. Rev. D **32**, 2653 (1985).

[34] R. J. Furnstahl and C. E. Price, Phys. Rev. C **41**, 1792 (1990).

[35] R. J. Furnstahl and C. J. Horowitz, Nucl. Phys. **A485**, 632 (1988).

[36] E. Wichmann and N. Kroll, Phys. Rev. **101**, 843 (1955).

[37] T. Ferree, C. Price, and J. Shepard, Phys. Rev. C **47**, 573 (1993).

[38] W. H. Press *et al.*, *Numerical Recipes* (Cambridge University Press, Cambridge, England, 1992).

[39] D. A. Wasson, Phys. Lett. **B210**, 41 (1988).

[40] W. R. Fox, Nucl. Phys **A495**, 463 (1989).

[41] R. Furnstahl and B. D. Serot, Phys. Rev. C **47**, 2338 (1993).

[42] R. J. Furnstahl, H. Tang, and B. D. Serot, preprint IU/NTC 94-18 (unpublished).

[43] B. D. Serot and H. Tang, Phys. Rev. C **51**, 969 (1995).

[44] H. D. Politzer and M. B. Wise, Phys. Lett. **B273**, 156 (1991).

[45] S. Rudaz, P. Ellis, E. Heide, and M. Prakash, Phys. Lett **B285**, 183 (1992).

[46] Hohler *et al.*, Nucl. Phys. **B114**, 505 (1976).

[47] J. Bagger and S. Naculich, Phys. Rev. D **45**, 1395 (1992).

[48] L. Montanet *et al.*, Phys. Rev. D **50**, 1173 (1994).

[49] L. Dodd and M. Lohe, Phys. Rev. D **32**, 1816 (1985).

[50] G. Bader and U. Ascher, Siam J. Scient. Stat. Comput. (1987).

[51] U. Ascher, J. Christiansen, and R. D. Russell, Math. Comp. **33**, 659 (1979).

[52] R. D. Russell and J. Christiansen, SIAM J. Numer. Anal. **15**, 59 (1978).

[53] T. Koppel and M. Harvey, Phys. Rev. D **31**, 171 (1984).

[54] L. H. Chan, Phys. Rev. Lett. **57**, 1199 (1986).